THE USE OF LIPOPHILIC MOLECULES AS SOLUBILITY PROMOTERS FOR CATALYSIS, SYNTHESIS AND NANOPARTICLE MODIFICATION

A Dissertation

by

CHIH-GANG CHAO

Submitted to the Office of Graduate and Professional Studies of
Texas A&M University
in partial fulfillment of the requirements for the degree of

DOCTOR OF PHILOSOPHY

Chair of Committee,	David E. Bergbreiter
Committee Members,	John A. Gladysz
	Lei Fang
	Melissa A. Grunlan
Head of Department,	Simon W. North

December 2017

Major Subject: Chemistry

ABSTRACT

This dissertation describes the use of lipophilic molecules as solubility promoters for the development of homogeneous recyclable catalysts, the facilitation of efficient purification in organic synthesis, and the preparation of highly soluble nanoparticles in nonpolar solvents. Several polyisobutylene (PIB)-bound metallophthalocyanines (MPcs) were prepared as highly heptane-soluble oils and were used as catalysts. PIB-bound cobalt(II) MPc was synthesized and used as an effective and recyclable catalyst for nitroarene reduction. The result showed that the catalyst was effective and recyclable for at least 10 cycles. The use of a PIB-bound iron(II) MPc for aerobic oxidation of ethyl phenylhydrazinecarboxylate and the use of a PIB-bound chromium(III) MPc for the rearrangement reaction of an epoxide to an aldehyde are also discussed.

Octadecyldimethylchlorosilane was used as a silylation reagent and a purification auxiliary. A procedure using heptane phase selectively soluble octadecyldimethylsilyl groups to facilitate separations and silyl reagent regeneration was developed. Alcohols and alkynes protected by these groups were shown to be phase-selectively soluble in hydrocarbon solvents, allowing these compounds to be purified by a simple liquid/liquid extraction. Applications of using the octadecylsilyl protecting group in a Grignard synthesis and Sonogashira reaction were studied.

Highly heptane-soluble iron-oxide nanoparticles were synthesized using PIB-supported ligands. These PIB-supported ligands were synthesized and grafted to nanoparticles to prepare heptane-soluble PIB-modified magnetic nanoparticles as

magnetically susceptible oils. These magnetic oils were dissolved in poly(α-olefin)s and molten polyethylene to prepare magnetically susceptible polymeric nanocomposites. Using the magnetic oil to remove heptane from water is also discussed. The work was also extended to explore strategies that can solubilize silica nanoparticles in heptane.

DEDICATION

This dissertation is dedicated to my father, mother, and two sisters for their love over the years. This dissertation is also dedicated to my three grandparents, who passed away during my PhD study.

ACKNOWLEDGEMENTS

First of all, I would like to thank my advisor, Dr. David E. Bergbreiter, for his instruction and guidance throughout my Ph.D. study. I have learned a lot from him about chemistry and about how to do research. I also appreciate his support throughout these years and his willingness to help teach me new areas of chemistry.

I also want to thank my committee members, Dr. John A. Gladysz, Dr. Lei Fang, and Dr. Melissa A. Grunlan, for their guidance and support throughout the course of this research. I would also like to thank Dr. Matthew Sheldon for attending my final oral exam as a substitute committee member.

I would like to thank Jill, Dr. Bergbreiter's secretary, for helping to organize things for me. I would also like to thank the group members of the Bergbreiter group for their assistance and support during my studies. I also want to thank Dr. Nilusha Boralugodage (Priyadarshani), Dr. Tatyana Khamatnurova, Dr. Stephanie Skiles, Dr. Jakkrit Suriboot, Dr. Yannan Liang, Mary Layne Harrell, Peerada Samunual, Thomas Malinski, Christopher Watson, Ying-Hua Fu, Ashley Leibham, Raquel Khanoyan, Neil Rosenfeld, and Vladimir Yelkhimov. Particularly, I also want to thank Ashley Leibham and Raquel Khanoyan for working with me as undergraduate researchers.

I want to especially thank my girlfriend, Mary Layne Harrell, who has been always supportive to me. She has helped me tremendously both in research and in life. She also helped me a lot in job searching process and helped me find a good job.

At the end, I would like to thank my family for their supports, especially to my father, mother, and two sisters. Thanks also go to my friends and the department faculty and staff for making my time at Texas A&M University a great experience.

CONTRIBUTORS AND FUNDING SOURCES

Contributors

This work was supervised by a thesis committee consisting of Professor David E. Bergbreiter, Professor John A. Gladysz, and Assistant Professor Lei Fang of the Department of Chemistry and Professor Melissa A. Grunlan of the Department of Biomedical Engineering.

The syntheses of organosilyl compounds in Chapter III was conducted in part by Ashley Leibham, who was an undergraduate researcher mentored by me for two years. The syntheses and the analyses depicted in Chapter IV and V were conducted in part by Assistant Professor Sherzod Madrahimov and Dr. Manyam Praveen Kumar of the Department of Chemistry at Texas A&M at Qatar and Raquel Khanoyan, who was an undergraduate researcher mentored by me for one and a half year.

All other work conducted for the dissertation was completed by the student independently.

Funding Sources

Graduate study was supported by a fellowship from Texas A&M University. This work was made possible in part by National Science Foundation under CHE-1362735, in part by Qatar National Research Fund under NPRP 7-1263-1-230, and in part by the Robert A. Welch Foundation under A-0639.

NOMENCLATURE

ACS	Alkyl-chain-soluble
ATRP	Atom-transfer radical polymerization
BHT	Butylated hydroxytoluene
Boc	*tert*-Butoxycarbonyl
BSA	Bovine serum albumin
CBz	Carbamate
CDTPC	4-Cyano-4-(dodecylsulfanylthiocarbonyl)sulfanyl pentanoic acid
CoMPc	Cobalt phthalocyanine
Cr(OTf)MPc	Chromium triflate phthalocyanine
CWA	Chemical warfare agent
DCM	Dichloromethane
DEAD	Diethyl azodicarboxylate
DMF	Dimethylformamide
DMSO	Dimethyl sulfoxide
DSSCs	Dye sensitized solar cells
E. coli	Escherichia coli
EA	Ethyl acetate
FeMPc	Iron phthalocyanine
HBC	Hexabenzocoronene
hPG	Hyperbranched polyglycerol

HQ	Hydroquinone
ICP-MS	Inductively coupled plasma mass spectrometry
LCST	lower critical solution temperature
MeCN	Acetonitrile
Mmsb-OH	2-Methoxy-4-methylsulfinylbenzyl alcohol
MNPs	Magnetic nanoparticles
MPcs	Metallophthalocyanines
MWNTs	Multi-walled carbon nanotubes
OLEDs	Organic light-emitting diodes
PAHs	Polycyclic aromatic hydrocarbons
PB	Polybutadiene
PDI	Polydispersity index
PEG	Poly(ethylene glycol)
PEGMA	PEG-tethered methacrylate
PEGDME	Polyethylene glycol dimethyl ether
PE	Polyethylene
PEI	Poly(ethyleneimine)
PEMA	Poly(ethyl methacrylate)
PIB	Polyisobutylene
PIP	Polyisoproprene
PMAA	Poly(methacrylic acid)
PNIPAM	Poly(*N*-isopropylacrylamide)

PNIPAM-*c*-PNASI	Poly(*N*-isopropylacrylamide)-*c*-poly(*N*-acryloxysuccinimide)
PS	Polystyrene
PU	Polyurethane
PVA	Poly(vinyl alcohol)
PVP	Poly(vinylpyrrolidone)
P2VP	Poly(2-vinylpyridine)
RAFT	Reversible addition-fragmentation chain-transfer
ROMP	Ring-opening metathesis polymerization
SPPS	Solid-phase peptide synthesis
TBAF	Tetra-*n*-butylammonium fluoride
TBS-OH	*tert*-Butyldimethylsilanol
TEM	Transmission electronic microscope
TGA	Thermal gravimetric analysis
THF	Tetrahydrofuran
XRD	X-ray diffraction

TABLE OF CONTENTS

Page

LIST OF FIGURES

Page

LIST OF TABLES

Page

LIST OF SCHEMES

CHAPTER I

INTRODUCTION

The importance of solubility is one of many properties of compounds that students learn about at the beginning of general chemistry. It is an intrinsic property of a substance that can vary widely in different solvents. Examples of substances with different solubility can be easily seen in our daily life. For example, sugar dissolves in water readily, but sand will never dissolve in water. Although the solubility of one compound in a solvent under a specific condition such as 25 ^{o}C and 1 atm is constant, chemists can chemically modify a compound to change its solubility. The hydroxy groups of sugar can for example be alkylated to form ethers that makes sugar insoluble in water. In fact, a tremendous amount of chemistry has been developed leading to different approaches to modify a molecule, a complex, or a cluster of nanoparticles to adjust their solubility. These efforts allow the solubility of a compound or material to be either increased or decreased. Such solubility difference can lead to materials solubility changing dramatically from insoluble to very soluble or to selectively soluble in a certain class of solvents.

The reasons to change a substance's or material's solubility varies widely depending on the targeted applications. Higher solubility makes it possible to prepare solutions with wider ranges of concentration. This can affect the reaction rates and the results of chemical reactions. Alternatively, a compound with high solubility is easier to process and fabricate in industrial applications. On the other hand, decreasing a compound's solubility can enable separation and isolation of a given substance or

material. This strategy has long been used in organic chemistry to facilitate simpler purification and separation. Chemists have used many methods to improve the solubility of molecules and materials. One of the most common methods is to covalently modify a molecule or a material. This can involve the introduction of either polar or nonpolar groups to make molecules or materials soluble in polar or nonpolar solvents respectively.

A common strategy to increase solubility of molecules or materials in nonpolar solvents is to install aliphatic alkyl chains onto molecules. For example, polycyclic aromatic hydrocarbons (PAHs) such as hexabenzocoronene (HBC) and graphene as shown in Figure 1 have been extensively studied by Müllen as promising materials for nanoelectronics and field-effect transistor devices.[1] Because of their multiple fused benzene rings, these PAHs have very rigid backbones and usually suffer from low solubility in common organic solvents. With the installation of alkyl chains on the benzene rings, the solubility of PAHs in organic solvents can be increased and the increased solubility of these materials allows their liquid phase characterization, solution processing and thin-film fabrication.[2]

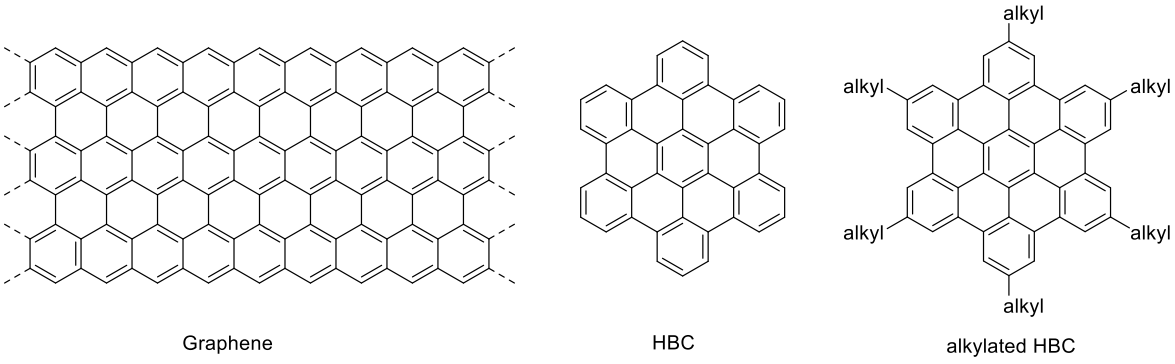

Figure 1. Representative examples of polycyclic aromatic hydrocarbons.

Similar research interest is also seen in the development of organic light-emitting diodes (OLEDs). OLEDs have received a lot of attention for the past few decades because of their energy efficiency, flexible manufacturability, and high color contrast. The organic chromophores that have been used in those devices are usually highly conjugated aromatic molecules. Although these molecules have good light emitting properties, they usually suffer from solubility issues because of their stiff skeletons. Fang and coworkers recently reported a review illustrating several methods to prepare highly conjugated molecules with moderate solubility by installing a number of different molecules onto these highly conjugated molecules to enhance their solubility.[3] For example, his group used quinacridone derivatives to synthesize a highly conjugated ladder polymer **1** (Figure 2). The solubility of **1** in organic solvents was improved with the installation of multiple alkyl chains and the *t*-butoxycarbonyl (Boc) groups, which prevent the formation of hydrogen bonds. After the thermal cleavage of Boc moieties, intermolecular hydrogen bonds were seen to occur formed and the resulting ladder polymer became insoluble and showed high solvent resistance

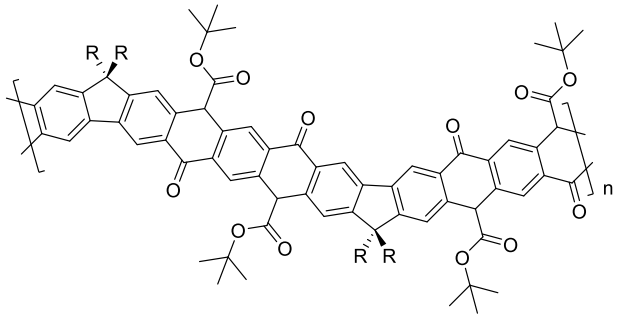

1

Figure 2. Boc-protected poly(quinacridone) **1**.

Solubility engineered into molecules or materials depends not only on the length of the solubilizing groups. Scherf[4] reported the synthesis of two poly(*p*-phenacene)s **2** and **3** shown in Figure 3. **2** has (3,4-dihexyloxy)phenyl units as side chains and **3** has 4-decyloxyphenyl units as side chains. It was found that these two polymers have different solubility even though they have similar chemical formulas. This indicates that the number of alkyl groups acting as solubilizing groups also affects the solubility. During the synthesis of these compounds, both polymer products precipitated from dimethylformamide (DMF) solution because the solubility of the product decreased. It was found that the M_n of **2** was able to reach *ca.* 12,000 Da but the M_n of **3** could only reach *ca.* 4,000 Da before the polymer precipitated. This suggests that **2** was more soluble in DMF because it had di-substituted alkyl groups as side chains instead of mono-substituted alkyl groups like **3**.

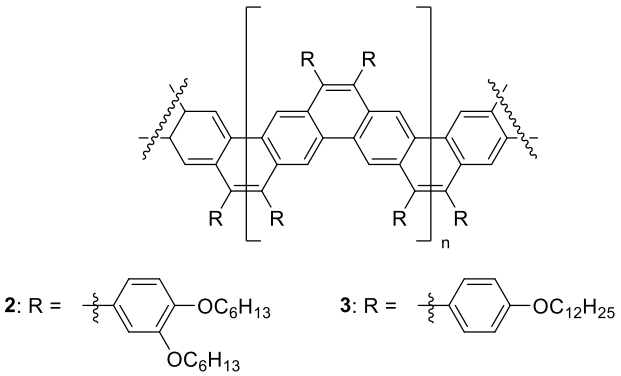

Figure 3. Poly(*p*-phenacene)s **2** and **3** with different solubility due to the different length and number of alkyl groups as side chains.

Nonpolar alkyl chains added to improve organic molecules' solubility have also been used in organic synthesis to facilitate efficient purifications of organic molecules and facile monitoring of organic reactions. Chiba has reported the use of a carbamate (CBz)-type of alkyl-chain-soluble (ACS) support to facilitate a facile synthesis for oligonucleotides without the need of repetitive purification.[5] As shown in Scheme 1(a), the synthesized nucleotide **4**, bearing three octadecyl chains, has high solubility in nonpolar solvents and low solubility in polar solvents. This allows **4** to be precipitated in polar solvents and the by-products to be washed away with polar solvents, leading to highly pure products. The same solubilizing reagent can later be easily cleaved by palladium-catalyzed hydrogenolysis to afford the pure nucleotide **5**. They further demonstrated that another ACS support – 2,4,5-tris(octadecyloxy)benzyl alcohol as shown in Scheme 1(b) – can function similarly as a solubility enhancer for synthesizing the peptide **6** and can double as a colorimetric indicator after the acid-triggered dealkylative coupling and cleavage of the soluble tag from the peptide.[6]

Solubility tags can be also designed to make less polar molecules or materials more soluble in polar solvent. For example, this approach has been used to increase the solubility of some types of peptides in polar solvents. Some amino acids such as valine, leucine, and phenylalanine are relatively hydrophobic and peptides comprising these nonpolar amino acids can have low solubility in water that leads to their self-assembly in aqueous solutions. Solubility tags can then be designed to increase the solubility of those peptides in aqueous solutions. For example, Brik's group has developed a method using allyloxycarbonyl phenylacetamidomethanol to protect cysteine.[7] The cysteine derivative

7 shown in Scheme 2(a) can then undergo solid-phase peptide synthesis (SPPS) to synthesize a peptide with many nonpolar moieties. The allyloxycarbonyl group functions as a soluble tag so the resulting peptide can be solubilized and collected after the cleavage of the peptide from the solid support. Tulla-Puche and Albericio also reported that they have used 2-methoxy-4-methylsulfinylbenzyl alcohol (Mmsb-OH) as a safety-catch linker to bridge a targeting hydrophobic peptide sequence and a six-alanine composed solubilizing tag (Scheme 2(b)).[8] This strategy enhanced the solubility of the solubilizing-tag-attached peptide **8** during SPPS and allowed the selective cleavage of the solubilizing tag under mild conditions.

Scheme 1. Use of ACS support in biosynthesis. (a) Synthesis of **5** using CBz-type of alkyl-chain-soluble (CBz-ACS) support. (b) Synthesis of **6** using 2,4,5-tris(octadecyloxy)benzyl alcohol as an ACS support and a colorimetric indicator.

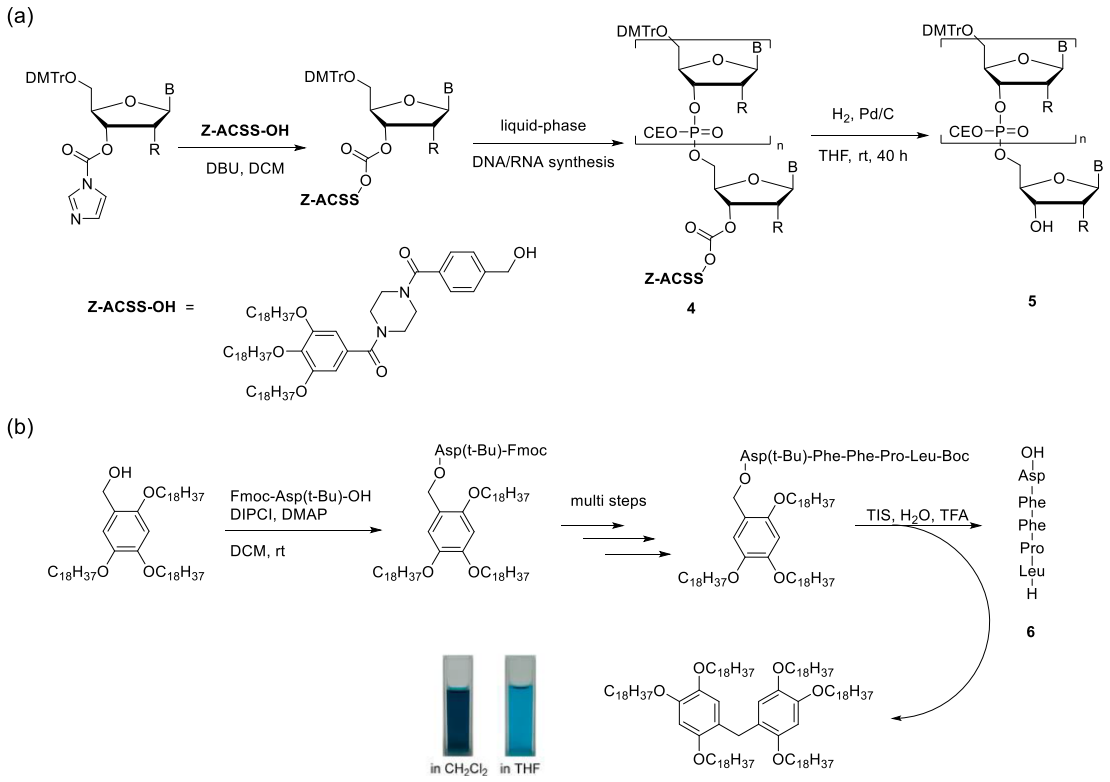

Scheme 2. Syntheses of peptides using solubilizing tags. (a) Schematic synthesis of a peptide using **7** as a solubilizing tag. (b) Schematic synthesis of a peptide using an Ala hexamer as a solubilizing tag and Mmsb as a linker.

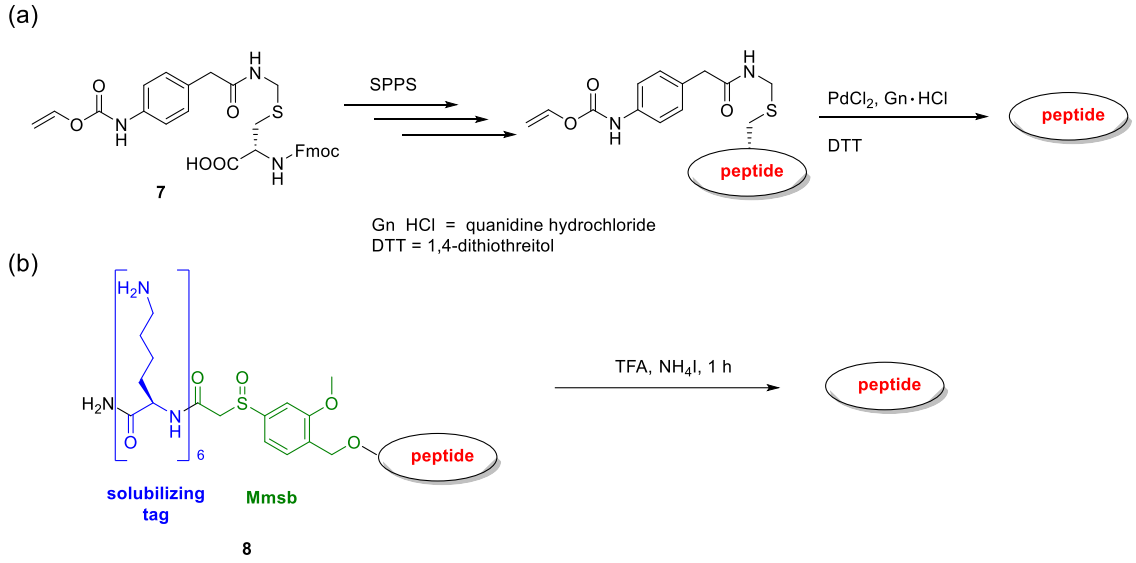

Solubility tags have also been used with nanoparticles, to increase their solubility. Nanoparticles are particles with a size in the range of 1 to 100 nm. Nanoparticles are receiving considerable attention because they possess different properties than bulk materials. Their unique properties have allowed these nanoparticles to be widely used in pharmaceuticals, materials, electronic device, and catalysts. However, the poor solubility of nanoparticles in solvents remain a problem. Moreover, nanoparticles dissolved in solutions are not always stable and they sometimes form an undesirable aggregate. Many researches have worked on attaching surfactants to nanoparticles to stabilize them and improve their solubility in organic solvents.

Molecules containing a long alkyl chain on one end and reactive functional groups on the other end (shown in Figure 4) have been widely used as solubilizing promoters for

nanoparticles in organic solvents. For example, alkyl thiols have been used to stabilize gold nanoparticles by utilizing the strong affinity of thiols to gold nanoparticles. Alkyl thiols can passivate the surface and prevent the agglomeration of these thiol-capped gold nanoparticles. The tailing alkyl chains also increase the solubility of the gold nanoparticles in organic solvents. Fatty acids have also been shown as good solubilizing reagents.[9] Several reviews have reported that oleic acid can be attached to different nanoparticles including a variety of metallic, metal-oxide, and silica nanoparticles. The carboxylic acid group of oleic acid can form a strong bond to the surface of those nanoparticles and the resulting oleic-acid-attached nanoparticles have shown enhanced solubility and stability in nonpolar or weakly polar organic solvents such as hexane, toluene, and tetrahydrofuran (THF). The enhanced solubility is effected by both the long alkyl chain and the V-shape structure of oleic acid because of the double bond at the 9,10 position of the surfactant. Markovich also reported the synthesis of aliphatic alkyl phosphonate-grafted magnetic nanoparticles and found that they had poorer dispersibility in apolar solvents but better biocompatibility compared to oleic acid-grafted magnetic nanoparticles.[10]

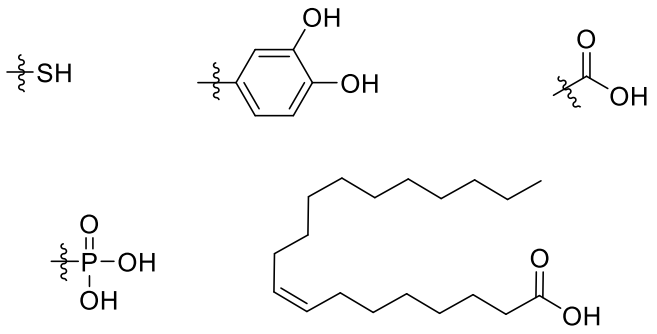

Figure 4. Commonly used solubilizing reagents for nanoparticles.

Polymers can also be grafted onto nanoparticles to solubilize them in different solvents and to mix nanoparticles homogeneously with polymers. With proper design and syntheses, polymers can be prepared with targeted molecular weights, chemical structures, and varying solubility. By attaching polymers to nanoparticles, solubility inherited from these polymers allows these nanoparticles to be soluble in certain solvents and to be used for applications such as medical treatments and material engineering. For example, poly(ethylene glycol) (PEG) can be attached to magnetic nanoparticles to solubilize them in aqueous solutions and these nanoparticles can be applied in physiobiological environments for hyperthermia treatments. Polystyrene (PS)-supported gold nanoparticles can dissolve in dichloromethane (DCM) and THF. The enhanced solubility of these gold nanoparticles in organic solvents can also allow them to be soluble in a PS matrix. Numerous studies have reported different synthetic approaches to prepare polymer-grafted nanoparticles.

In general, there are two strategies to synthesize polymer-grafted nanoparticles. As shown in Scheme 3, the first one is the "grafting-to" method that uses synthesized polymers with reactive end-groups to bind to the surface of nanoparticles. The second method is the "grafting-from" that conducts polymerization from the surface of nanoparticles and generates polymer chains onto nanoparticles. Both methods have their advantages. The "grafting-to" method can be easily used to control the functionality and chemical structure of polymers. On the other hand, the "grafting-from" method can achieve higher grafting density of polymers on nanoparticles.[11] Several reviews have summarized work done using both methods, here a few examples of both methods are

illustrated to describe the concept of solubilizing nanoparticles in different solvent media by polymer modification.

Scheme 3. Schematic illustration of different approaches to prepare polymer supported nanoparticles: grafting-to and grafting-from methods.

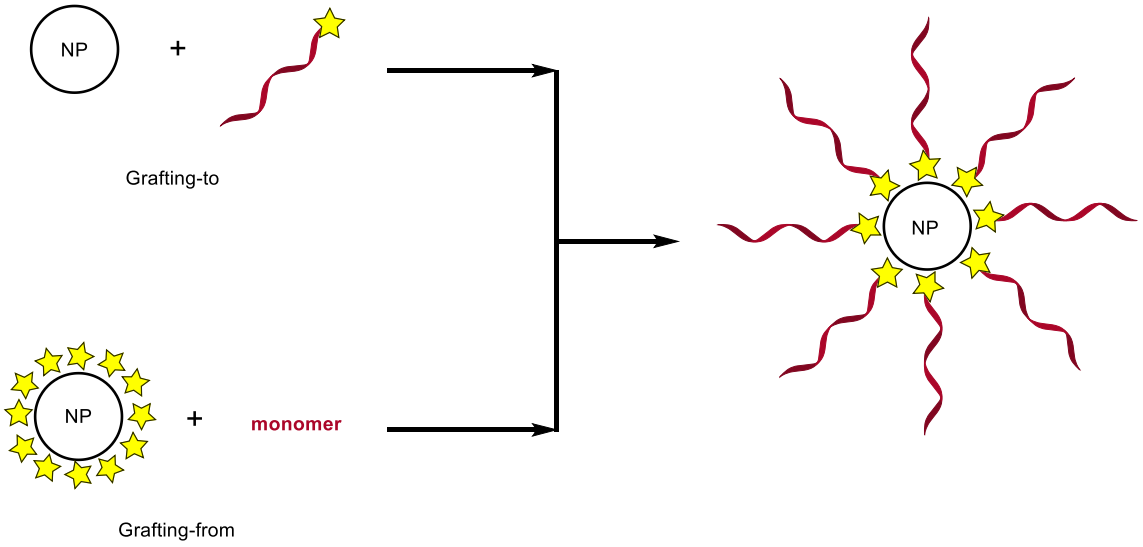

For the "grafting-to" method, a polymer is synthesized and then the reactive functionalities form either covalent or ionic bonds with the functional groups on the nanoparticles to attach the polymer. PEG has been widely used as a polymer support to solubilize nanoparticles in aqueous solutions. Other polar polymer supports such as poly(vinyl alcohol) (PVA), poly(vinylpyrrolidone) (PVP), and poly(ethyleneimine) (PEI) can also function similarly. With proper design, these polymers can either use their original functional groups or post-installed functionalities to attach to nanoparticles. For example, thiol-terminated PEG[12] has been shown to serve as a good ligand for gold nanoparticles and the resulting gold nanoparticles **9** showed high solubility in water and

decreased opsonization in blood, leading to longer circulation time in blood. On the contrary, polymer supports can also solubilize nanoparticles in organic solvents. Thiol-terminated PS has been used to modify the surface of gold nanoparticles to prepare PS-stabilized gold nanoparticles **10** that are soluble in various organic solvents such as toluene, benzene, DCM and THF.[13] PEG can be also grafted to the surface of silica nanoparticles by reacting its hydroxy group with isocyanate groups on silica nanoparticles to form urethane bonds.[14] Compared to pristine silica nanoparticles, these PEG-grafted silica nanoparticles **11** showed greatly improved solubility in the prepolymer of polyurethane (PU). The hybrid PU films prepared from this prepolymer mixture also showed improved transparency and hardness, supporting the improved solubility of **11** in PU.

Recently the use of stimuli-responsive polymers for functionalizing nanoparticles has also received attention. In addition to improving the solubility of functionalized nanoparticles in different solvents, stimuli-responsive polymers also allow these grafted nanoparticles to undergo phase changes under different conditions. One recent paper from Karg's group reported that they synthesized carboxylic acid-terminated poly(*N*-isopropylacrylamide) PNIPAM by reversible addition-fragmentation chain-transfer (RAFT) polymerization and then used the trithiocarbonate group to attach the polymer to gold nanoparticles.[15] The corresponding gold nanoparticles **12** were soluble in water, ethyl acetate (EA), and chloroform. They also found that when the pH was at 2.7, when carboxylic groups were protonated, reduced electrostatic repulsion allowed **12** to phase transfer from water to chloroform upon heating and transfer back to water phase after

cooling. The phase-transfer behavior of **12** as shown in Figure 5 between chloroform and water was reversible for at least eight cycles.

Scheme 4. Syntheses of polymer-supported nanoparticles 9-12 by a "grafting-to" method.

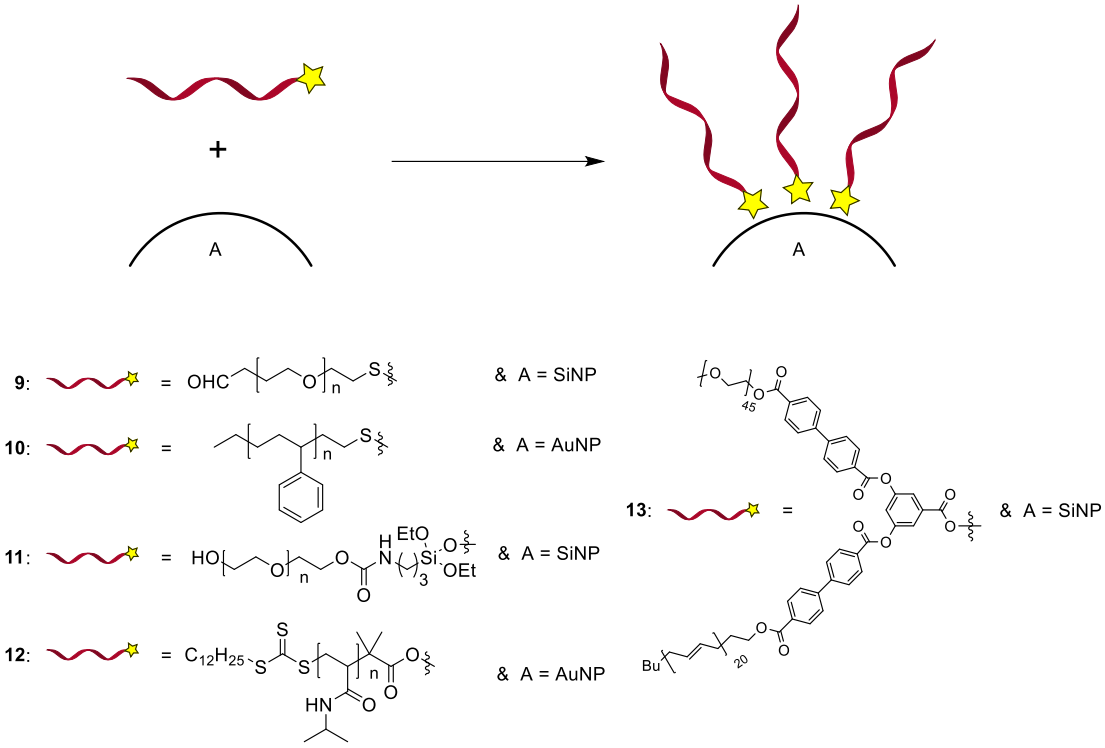

Block copolymers have been also investigated to solubilize nanoparticles. One advantage of using block copolymers is that multiple properties from each block of a block copolymer can be combined and introduced to nanoparticles. Block copolymers also make it possible to solubilize nanoparticles in a broader range of solvents. One interesting example using a block copolymer to improve the solubility of nanoparticles has been reported by Zubarev and coworkers.[16] They synthesized gold nanoparticles modified with a V-shaped polybutadiene (PB)-*b*-PEG block copolymer. The amphiphilicity of this PB-

b-PEG copolymer allowed this PB-*b*-PEG-stabilized gold nanoparticles **13** to be soluble in a wide range of organic solvents including hexane, benzene, DCM, THF, methanol, dimethyl sulfoxide (DMSO), and water.

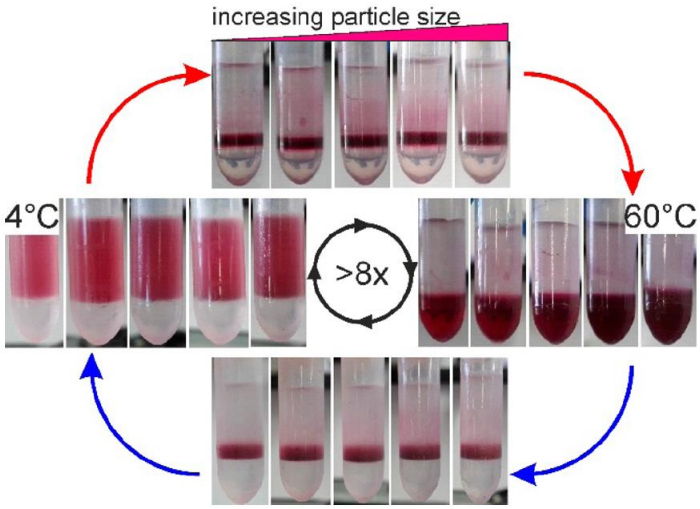

Figure 5. Reversible phase transfer of PNIPAM-supported gold nanoparticles **12** in chloroform and water.

In the "grafting-from" method, a polymer is synthesized from the surface of nanoparticles that first functionalized with initiators for a polymerization. Generally controlled/living polymerizations such as atom-transfer radical polymerization (ATRP), RAFT polymerization, and ring-opening metathesis polymerization (ROMP) are popular methods to prepare polymer-modified nanoparticles. Silanes are commonly used to install initiators on nanoparticles. For example, Jia has reported the use of (11-(2-bromo-2-methyl)propionyloxy)undecyl-trichlorosilane as a coupling reagent to install ATRP initiators on the surface of silica nanoparticles (Scheme 5).[17] These initiators can then

polymerize PEG-tethered methacrylate (PEGMA) to synthesize poly(PEGMA)-attached silica nanoparticles **14**. These nanoparticles **14** fully mixed with polyethylene glycol dimethyl ether (PEGDME) and improved the viscosity of the resulting nanocomposites. The viscous and gel-like nanocomposites showed fair conductivity in an I_2/LiI/PEGMA mixture and can be used as an electrolyte in dye sensitized solar cells (DSSCs).

Scheme 5. Synthesis of poly(PEGMA)-grafted SiNP by ATRP.

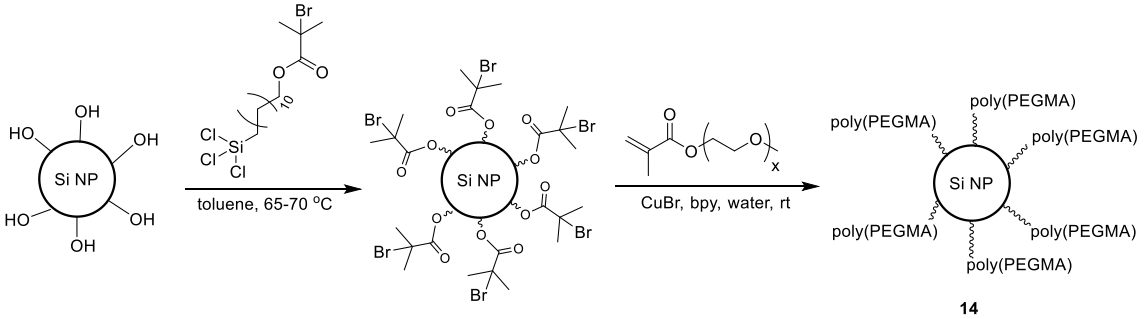

Benicewicz has reported several examples of syntheses of polymer-grafted nanoparticles by RAFT polymerization. He and his coworkers functionalized silica nanoparticles with 4-cyanopentanoic acid dithiobenzoate. He then grafted polymers such as polyisoproprene (PIP),[18] PS-*b*-poly(2-vinylpyridine) (P2VP),[19] and polymethacryate derivatives[20] onto the surface of these nanoparticles by RAFT polymerization. The resulting silica nanoparticles **15-17** shown in Scheme 6 were soluble in a variety of media and can be well dispersed in several polymers. For example, **15** can dissolve in THF and disperse in PIP; **16** can dissolve in in THF and disperse in PS; **17** was soluble in DMSO. Benicewicz and coworkers also synthesized poly(methacrylic acid) (PMAA)-grafted magnetic nanoparticles by RAFT polymerization that were soluble in dimethylformamide

(DMF) and water.[21] These magnetic nanoparticles were further modified with the β-lactam antibiotic penicillin-G to test the resulting nanoparticles' antimicrobial effect to *Escherichia coli* (*E. coli*). After these penicillin-G attached magnetic nanoparticles were added into the *E. coli* cultural solution for incubation at 37 ºC for overnight, it was found that they showed an antimicrobial effect to *E. coli*; in fact, the inhibition of the growth of *E. coli* was enhanced ca. 40% more by these penicillin-G attached magnetic nanoparticles than by free penicillin-G. These magnetic nanoparticles were recyclable for antimicrobial tests and were easily removed after the test by magnetic separation to avoid nanoparticle pollution in the biological environment.

Scheme 6. Syntheses of 15-17 by REAT polymerizations.

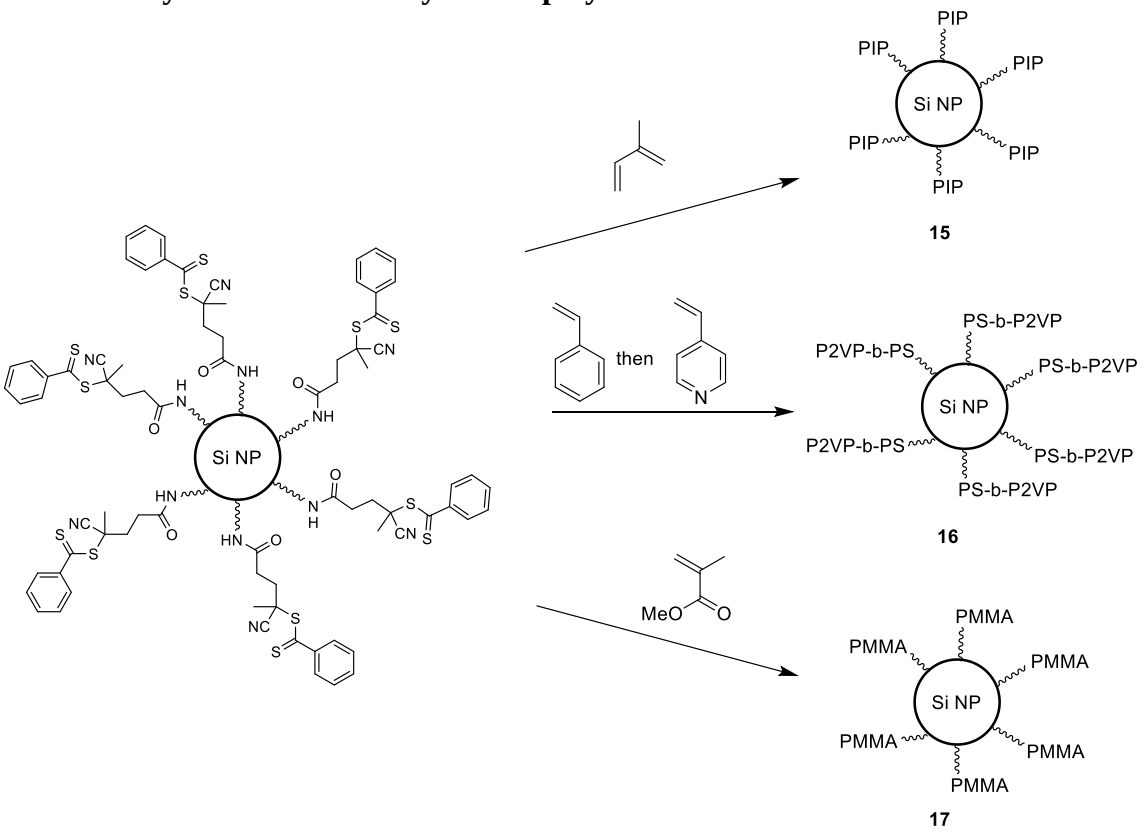

ROMP is also an attractive method to conduct living polymerizations from the surface of nanoparticles. Reiser's group has utilized ROMP to prepare polymer-grafted magnetic nanoparticles that were in turn used as recyclable acylation reagents.[22] After modifying magnetic nanoparticles with norbornenes, acylated *N*-hydroxysuccimide pendant polynorbornene-attached magnetic nanoparticles **18** can be prepared by ruthenium-catalyzed ROMP. These nanoparticles **18** were soluble in a 90% chloroform/methanol mixture and were recyclable for amine acylation. Recently Swager and coworkers also reported the synthesis of triarylmethanol-pendant block copolynorbornene-attached silica nanoparticles **19** as a chemical warfare agent (CWA) responsive material.[23] The hexadecane and tetraethyleneglycol side chains allowed **19** to be soluble in a range of solvents such as toluene, THF, and water. The triarylmethanol groups can react with diethyl chlorophosphate, a mimic for more toxic CWAs, to collapse the polymer chain, leading to a decrease in hydrodynamic volume and porosity of these nanoparticles. This material can be used in soldiers' armors to prevent soldiers from further exposure of CWAs in combat situations.

Other than linear polymers, hyperbranched polymers and dendrimers have also been studied as candidates for solubilizing nanoparticles.[24,25] Their three-dimensional structure enables protection and solubilization of nanoparticles in different solvents. For example, Li and Haag reported the synthesis of hyperbranched polyglycerol (hPG)-coated mesoporous silica nanoparticles as carriers for cancer treatments in a pH-responsive drug delivery system.[26] They found that the hyperbranched polyglycerols allowed these supported silica nanoparticles to become soluble in aqueous solution and also to slow

down the release of a drug model compound, rhodamine B, in a pH 5.5 environment. These polymer-supported nanoparticles have potential to target cancer cells and to release drugs when they are exposed to a similarly acidic environment. Alper and coworkers synthesized polyamidoamine dendrimer-supported magnetic nanoparticles that are soluble in organic solvents such as DCM, THF, benzene, and toluene.[27] These nanoparticles can be phosphonated, complexed with rhodium, and then used as a recyclable catalyst for hydroformylation. Yang and coworkers used similar polyamidoamine dendrimer supported magnetic nanoparticles grafted with Bovine serum albumin (BSA) for chiral separations.[28] In this work, BSA was shown to selectively bind to one enantiomer of a racemic phenylalanine. The free and bound enantiomers of phenylalanine then be separated by magnetic separation.

Scheme 7. Syntheses of 18 and 19 by Ru-catalyzed ROMP.

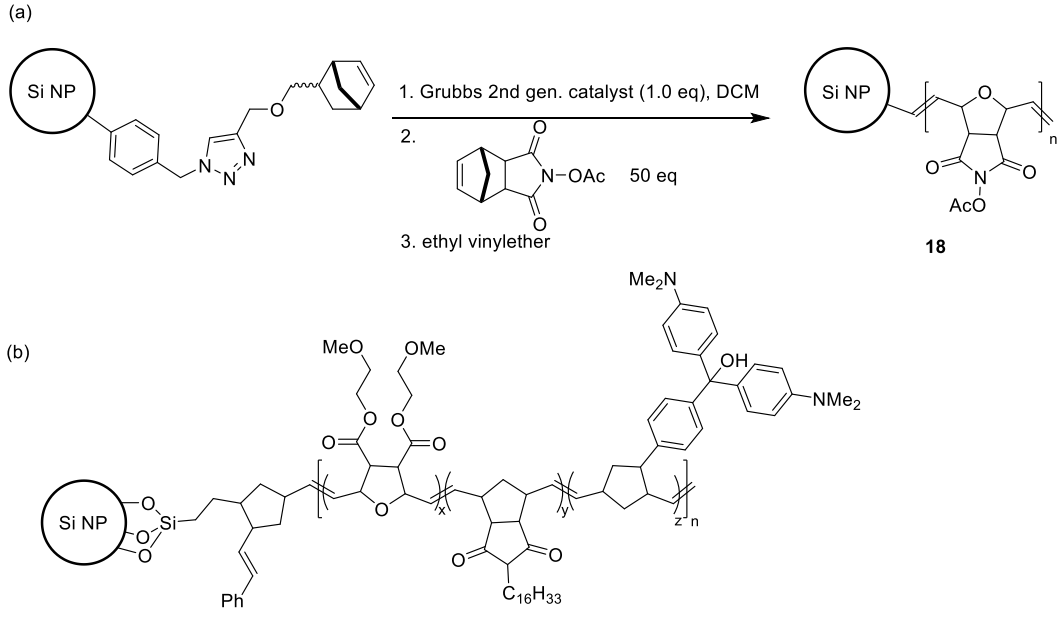

The above examples are representative examples of using solubilizing tags to solubilize organic and inorganic materials. These soluble materials are advantageous for more effective syntheses, better separation, easier solution processing, and well-controlled drug delivery. In addition, polymer supports can also be used to substantially decrease the solubility of one material to enable facile separation of the material. One most influential application of using insoluble polymer supports is SPPS which was briefly discussed earlier. The second most widely used application is for the preparation of recyclable heterogeneous catalysts. Several reviews have summarized the use of insoluble polymer-supports on different catalysts.[29–31] In general, an insoluble polymer is functionalized to attach the catalyst, which renders the catalyst insoluble in common organic solvents. Then a heterogeneous reaction is conducted in the presence of this insoluble polymer-supported catalyst. After the reaction, the catalyst is separated from soluble products/impurities by filtration and then can be reused for subsequent reactions if the catalyst is still reactive. Although using insoluble polymer supports for the development of recyclable catalysts is popular, the supported catalysts usually suffer from the difficulty of liquid-phase characterization and reactivity optimization because of their poor solubility in organic solvents. Therefore, using an alternative method to recycle catalysts in solution phase is desired.

The Bergbreiter group has a long history of functionalizing soluble polymers to prepare polymer-supported catalysts for homogeneous reactions. One advantage of using soluble polymer supports is that the catalysts that are prepared can be used as solutions in organic solvents after modification. This allows for homogeneous reactions to occur and

for catalysts to be easily modified to optimize their reactivity. A second advantage is that soluble polymer supports facilitate simpler separation of the catalyst from products after a catalytic reaction. More specifically, the solubility of the catalyst is changed because of the polymer support and the catalyst can be separated from a reaction mixture by physical phase separation. Many soluble polymer supports such as PEG, PNIPAM, polyethylene (PE), and 4-alkyl-substituted PS have been used in our group to prepare recyclable polymer-supported catalysts (Figure 6). In recent years, our group has primarily focused on using polyisobutylene (PIB) oligomers as solubilizing tools to prepare PIB-functionalized catalysts.

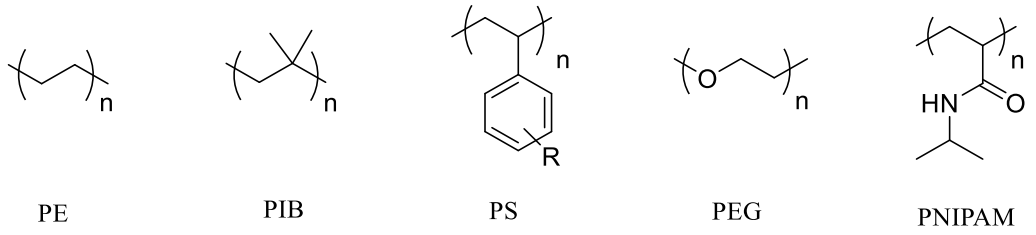

Figure 6. Soluble polymer supports that the Bergbreiter group has used for recyclable catalysts.

PIB oligomers are viscous oils and their derivatives are used as additives in gasoline to improve combustion and as lubricants.[32] Industrially, PIB is synthesized by cationic polymerization of isobutylene and it contains an alkene group at the end of the polymer chain. This alkene group can be functionalized to make ligands that are used to attach PIB onto catalysts. The resulting PIB-supported catalysts are selectively soluble in nonpolar and weakly polar solvent such as hexane, heptane, toluene, DCM, and THF, but

they are not soluble in polar solvents such as DMF, acetonitrile (MeCN), and 90% aqueous ethanol. The high phase selectivity of PIB-attached catalysts in nonpolar hydrocarbon solvents and in modestly polar solvents along with PIB's insolubility in polar organic solvents facilitates liquid/liquid biphasic separation of catalysts and products and recycling of catalysts in a hydrocarbon phase like heptane.

The Bergbreiter group developed two strategies as shown in Scheme 8 to effect biphasic liquid separations and to facilitate homogeneous reactions using polymer-supported catalysts; one is a latent biphasic system and the other one is a thermomorphic system.[33] A latent biphasic system involves the use of two solvents that are initially miscible for a reaction but are separable after the solvent mixture is perturbed. A thermomorphic system involves the use of two solvents that are initially immiscible. These two solvents form a single-phase solution upon heating but change back to two phases after cooling. The two-phase mixture can then be separated by a liquid/liquid extraction assuming they have a sufficient difference in density. Thus, using PIB-supported catalysts together with a proper solvent system enables homogeneous catalytic reactions to occur under monophasic conditions with catalyst isolation, separation from products and recycling as a nonpolar phase after a catalytic reaction forming a polar phase product in complete.

Scheme 8. Solvent systems that facilitate homogeneous reactions and recycling of polymer supported catalysts: The left on is a latent biphasic system and the right one is a thermomorphic system.

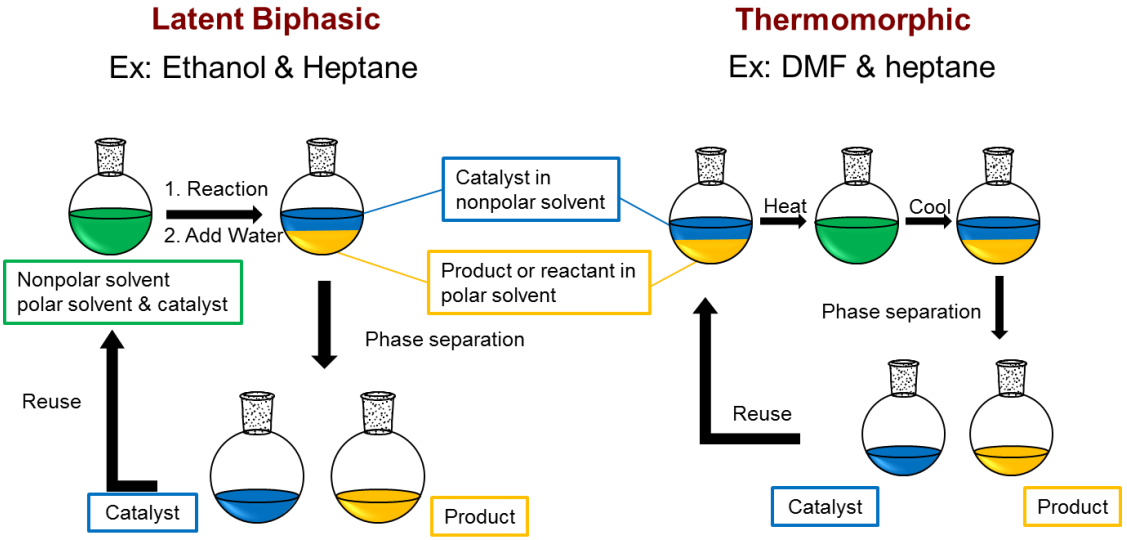

After the first work describing the functionalization of PIB[34] was reported by the Bergbreiter group, numerous PIB-supported catalysts have been prepared and studied for their recyclability. For example, ruthenium-catalyzed metathesis reactions have been widely used as a powerful tool for organic synthesis. However, the high cost of precious metals impedes their wider applications in industry. The Bergbreiter group synthesized PIB-attached Hoveyda-Grubbs catalysts **20** and **21** through attaching PIB either on the methylidene[35] or *N*-heterocyclic carbene ligand (Figure 7a).[36] Compared to the commercially available Hoveyda-Grubbs catalyst, the resulting PIB-attached Ru catalysts are selectively soluble in heptane, as shown in Figure 7b, but not soluble in polar solvents like MeCN and DMF. Both **20** and **21** can catalyze the ring-closing metathesis of 1,6-heptadienes or 1,7-octadienes to their corresponding cyclic olefins (Figure 7c). After the

reactions were completed, both catalysts were recycled. This was accomplished in one of two ways. MeCN could be added to remove cyclic products from the heptane solution and then the catalyst that remained in the heptane layer could be reused by adding fresh reagents. It was also possible to utilize the poor solubility of products in heptane to recycle the catalyst without using any added solvent. In suitable cases, the product would self-separate as a precipitate because of its poor solubility in heptane. Then the heptane solution containing the catalyst could be reused for another run of ring-closing metathesis reaction.

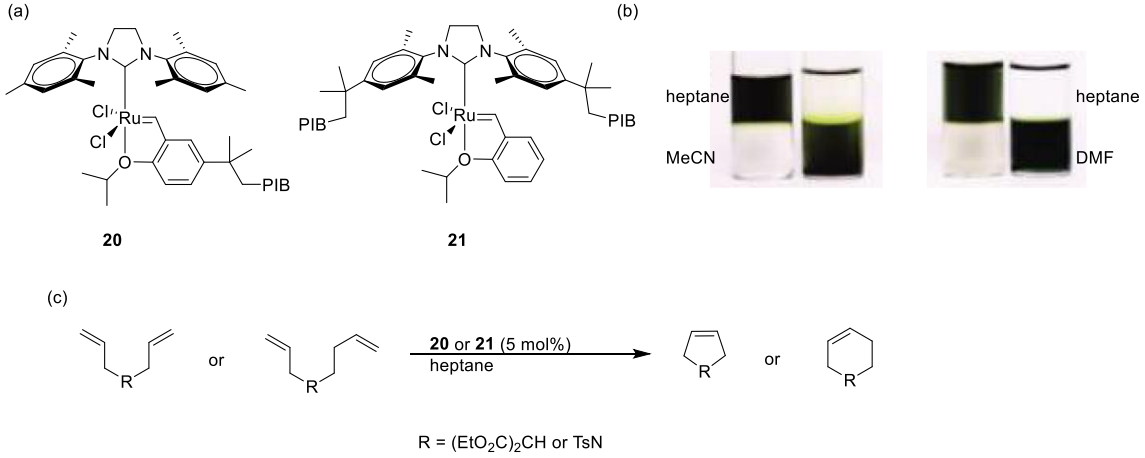

Figure 7. Use of **20** and **21** as recyclable catalysts for ring-closing metathesis reactions. (a) PIB-attached Hoveyda-Grubbs catalyst **20** and **21**. (b) Phase selectivity of **20** and commercially available Hoveyda-Grubbs catalyst in a heptane/MeCN (left) and a heptane/DMF (right) mixture. (c) Ring-closing metathesis of 1,6-heptadienes or 1,7-octadienes were catalyzed by **20** or **21**.

The Bergbreiter group also synthesized PIB-attached tris(bipyridine)ruthenium(II) chloride ([Ru(PIB-bpy)$_3$Cl$_2$]) **22** and used it as a recyclable catalyst for photo-redox reactions.[37] In recent years, light initiated redox reactions using either metal or organic

catalysts have received a lot of attention because of their environmental benignity. Macmillan[38,39] and Yoon[40] have reported several examples illustrating that highly efficient and effective reactions can be done by using iridium and ruthenium complexes or organic dyes as catalysts and visible light as an energy source to initiate organic transformations. However, the recycling of precious metals or organic dyes that are used as catalysts remains an issue. A previous group member Nilusha Priyadarshani prepared **22** and used this ruthenium complex as a catalyst for a photo-induced free radical polymerization of methyl methacrylate.[37] She noted that the PIB groups on **22** dramatically changed the solubility of this ruthenium complex. As shown in Figure 8b, **22** is selectively soluble in heptane but the analogous complex $[Ru(bpy)_3Cl_2]$ that does not contain PIB groups is insoluble in heptane and selectively soluble in DMF. The high solubility of the starting monomer and **22** in heptane together with the insolubility of polymethacrylate derivatives enabled a homogeneous polymerization reaction to be carried out and simple recycling of the catalyst as well as facile isolation of the product. Using ethyl methacrylate as a monomer led to a polymer product that precipitated from heptane after the molecular weight of the polymer grew to *ca.* 40,000 Da. Simple filtration separated the product poly(ethyl methacrylate) (PEMA) from the heptane solution of catalyst **22**. The catalyst **22** that remained in the heptane filtrate was then reused for subsequent polymerizations. An inductively coupled plasma mass spectrometry (ICP-MS) analysis of the synthesized PEMA showed that < 2.0 ppm of Ru was present in the product. In a direct comparison, the ruthenium contamination of a PEMA product using $[Ru(bpy)_3Cl_2]$ as a catalyst was 48

ppm. The catalyst **22** was reused for three cycles and the polydispersity index (PDI) of the synthesized polymers was 1.4.

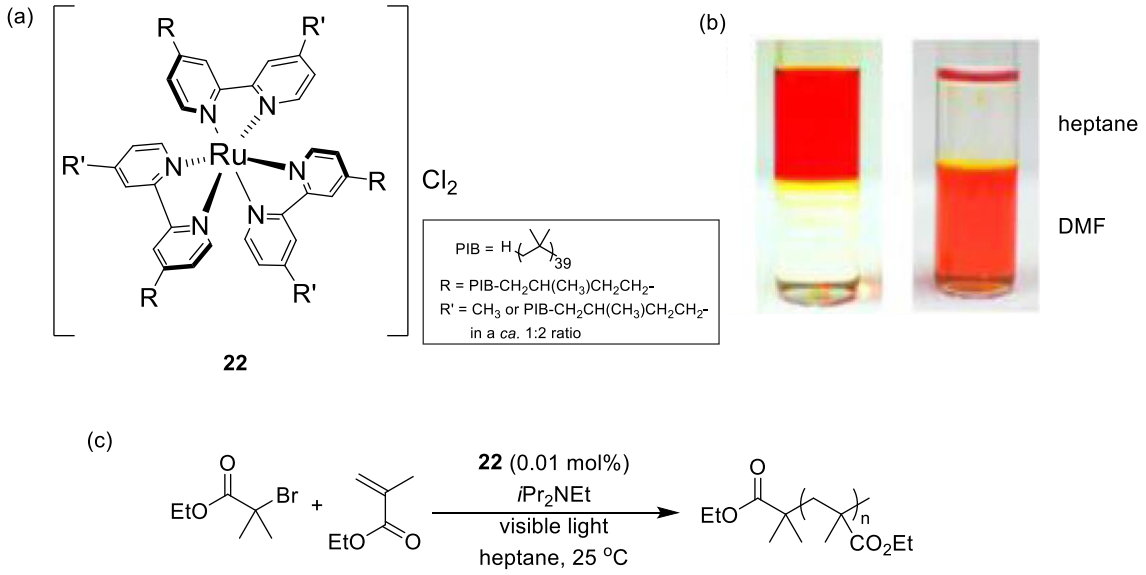

Figure 8. Use of PIB-attached tris(bipyridine)ruthenium(II) chloride **22** as recyclable catalysts for photo-redox reactions. (a) Chemical structure of **22**. (b) Phase selectivity of **22** and $[Ru(bpy)_3Cl_2]$ in a heptane/DMF mixture. (c) A photo-initiated free radical polymerization of ethyl methacrylate using ethyl 2-bromoisobutyrate as an initiator was catalyzed by **22**.

Yannan Liang in our group also demonstrated that the same complex **22** can function as a recyclable catalyst for oxidative C-C bond cleavage of 2,3-diphenylpropanal to synthesize 1,2-diphenylethanone.[41] This catalyst was recycled for five cycles without losing its reactivity. He further studied the synthesis of PIB-attached 10-phenylphenothiazine **23** as a recyclable organocatalyst for visible light-mediated polymerization of methyl methacrylate as shown in Scheme 9.[42] As was the case for **22**, this catalyst **23** was recyclable for at least three cycles and it showed well-controlled

reactivity with light-on and light-off conditions. The examples described above illustrate the use of PIB as solubility promoters for catalysts in nonpolar solvents and how PIB's solubility can be utilized to recycle PIB-supported catalysts as well as to reduce the amount of metal leaching in products.

Scheme 9. Light-mediated radical polymerizations of methyl methacrylate catalyzed by 23.

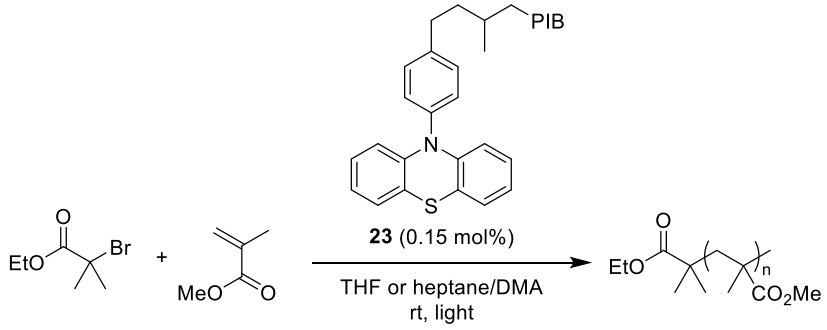

In addition to using polymers as supports for catalysts, another research focus in the Bergbreiter group is to functionalize surfaces with polymers to alter materials properties. For example, Kang-Shyang Liao in our group in conjunction with the Batteas group reported the direct amination of multi-walled carbon nanotubes (MWNTs) with PEI.[43] These PEI-supported MWCTs contained 6-8% of PEI coating and were well-dispersed and stable in polar solvents such as methanol, DMF, and water. He then further developed a layer-by-layer procedure to covalently graft PEI-MWCTs and Gantrez onto oxidized polyethylene as shown in Figure 9a. The amine groups on PEI could under amidation with stearic acid to form octadecyl carboxamide derivatives. The lipophilic octadecyl groups converted the superhydrophilic surface of the PE composite film to a

superhydrophobic one. With the success of functionalizing PE by a layer-by-layer method, Ainsley Allen[44] and Kang-Shyang Liao[45] in our group in conjunction with the Batteas group reported the functionalization of both PE and glass with poly(*N*-isopropylacrylamide)-*c*-poly(*N*-acryloxysuccinimide) (PNIPAM-*c*-PNASI) and aminated silica nanoparticles (Figure 9b). The PNIPAM contained in this composite has lower critical solution temperature (LCST) behavior and the temperature for this material's LCST is known to be perturbed by salts and solubility due to the Hofmeister effect.[46] Droplets containing different salt solutions showed different contact angles after they were deposited on these functionalized PE and glass surfaces. Later studies that prepared similar nanocomposite grafts on a porous frit showed that the resulting supported membranes had water permeability that was temperature dependent. These same membranes had permeability that was sensitive to the identity of salts. For example, an aqueous 0.8 M Na_2SO_4 solution has a flow rate through a modified frit that was 1000-fold slower than a water solution.[44] The impermeability of the frit to Na_2SO_4 decreased when the study was conducted at low temperature where the temperature of the frit was below the Na_2SO_4 induced LCST. These representative examples from our group illustrate the potential of using polymers to solubilize inorganic materials in organic solvents. The properties inherited from the polymers being used allow these functionalized materials to be used for wide applications such as solvent discrimination and self-cleaning.

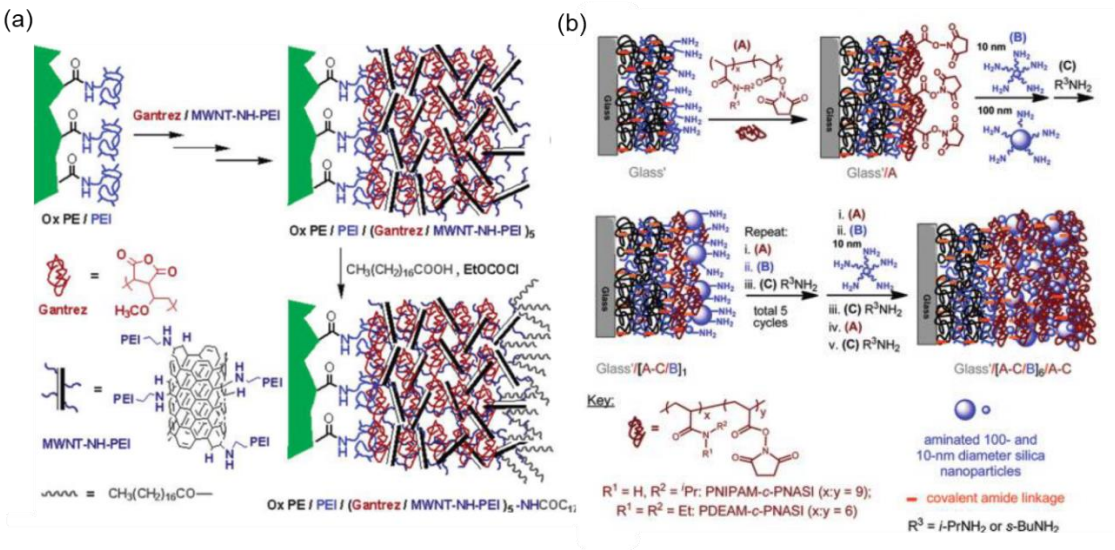

Figure 9. Functionalization of surfaces of inorganic materials by a layer-by-layer approach. (a) Preparation of functionalized PE with layer-by-layered PEI-MWCTs and Gantrez. (b) Preparation of functionalized glass with layer-by-layered PNIPAM-*c*-PNASI and aminated SiNPs.

In the following chapters, I will describe my work where I have used lipophilic molecules such as PIB oligomers and octadecyldimethylchlorosilane as solubility promoters to recycle catalysts, to facilitate purification of organic molecules in organic synthesis, and to functionalize nanoparticles. More specifically, Chapter II will talk about the synthesis of a series of PIB-attached metallophthalocyanines as phase-selective catalysts. Different metals including chromium, iron, and cobalt can be incorporated in these macrocyclic structures. The work using these catalysts for homogeneous reactions such as rearrangement of epoxides to aldehydes, oxidation of hydrazines to hydrazones, and reduction of nitroarenes to aminoarenes as well as their recyclability will be discussed. Chapter III will discuss the work involving the use of octadecyldimethylchlorosilane as a purification auxiliary for organic reactions. This will be further illustrated with the success

of purifying silylated products in Grignard reactions and Sonogashira reactions. Last but not the least, Chapter IV and V will talk about different strategies of functionalizing iron oxide nanoparticles and silica nanoparticles with PIB oligomers. Both “grafting-to” and “grafting-from” methods were used to graft PIB to nanoparticles. These functionalized nanoparticles showed high solubility in organic solvents and can be mixed with nonpolar polymers to prepare polymeric nanocomposites.

CHAPTER II

HIGHLY ORGANIC PHASE SOLUBLE POLYISOBUTYLENE-BOUND METALLOPHTHALOCYANINES AS RECYCLABLE CATALYSTS*

Introduction

Metallophthalocyanines (MPcs) were originally developed as pigments[47] but are now also used as photosensitizers, photodynamic therapy agents, and in molecular electronics.[48,49] MPcs can also be used as catalysts. However, their use in homogeneous catalysis is less common than is the case for porphyrins, a structurally similar type of metal complex.[50–52] MPcs are less commonly used as homogeneous catalysts because MPcs have solubility that is in the range of 10^{-5} to 10^{-7} M in organic solvents,[53] a limitation that renders their use as homogeneous catalysts problematic. Our success in synthesis of polyisobutylene (PIB)-bound MPcs that dissolve in hydrocarbon polymers and the others' report of the activity of several MPcs as heterogeneous catalysts for nitroarene reduction[54,55] suggested to us that PIB-modified MPcs could serve as recyclable homogeneous catalysts and that this hypothesis could be tested by examining their use in nitroarene hydrogenation.

Aromatic amines are important organic compounds due to their use in the syntheses of dyes,[56] pesticides,[57] pharmaceuticals,[58,59] and polymers.[60] Reduction of nitro compounds is one of most widely used routes to this class of compounds. Classically

---

* Reprinted with permission from "Highly Organic Phase Soluble Polyisobutylene-bound Cobalt Phthalocyanines as Recyclable Catalysts for Nitroarene Reduction" by Chao, C.-G.; Bergbreiter, D. E. *Catal. Commun.* **2016**, *77*, 89, Copyright 2016, by Elsevier B.V.

reduction of nitroarenes to form anilines uses hydrogenation with Pd/C.[30] More recently, there has been an increase in interest in homogeneous catalysts that use more earth abundant metals,[61–63] that are recyclable,[64,65] or that use alternatives to hydrogen as the penultimate reductant.[66–69]

Our hypothesis about the solubility and activity of PIB-modified MPcs has shown to be true and we illustrate here that a PIB-bound cobalt phthalocyanine (CoMPc) catalyst can be used as a homogeneous catalyst for nitroarene reduction and that this catalyst can be quantitatively separated from products and recycled. We have also shown the broader use of PIB-bound MPcs as homogeneous catalysts by studying the incorporation of different metals in the MPc complexes. The synthesis of PIB-bound iron phthalocyanine (FeMPc) and the use of this complex for the oxidation of ethyl phenylhydrazinecarboxylate to ethyl phenylazocarboxylate, an alternative reagent in Mitsunobu reaction, is discussed as an example of this broader scope of MPc catalysis.

The Mitsunobu reaction is a widely used synthetic tool in organic synthesis that can convert an alcohol to various functionalities derivative including carboxylic acid, ester, azides, thiols, amines, and thiocyanides with high stereospecificity in the presence of triphenylphosphine and a diethyl azodicarboxylate (DEAD) derivative.[70] However, the need for a stoichiometric amount of DEAD derivatives, their toxicity, and the necessary separation of byproducts, dialkylhydrazinedicarboxylate and triphenylphosphine oxide, makes the Mitsunobu reaction a classical example of non-green chemistry.The recent report that showed that a FeMPc acts as a catalyst for the oxidation of ethyl phenylhydrazinecarboxylate to ethyl phenylazocarboxylate, which can then be used as a

catalyst (10 mol%) for Mitsunobu reactions.[71] The use of molecular oxygen as a penultimate oxidant makes this oxidation process environmentally friendly. If FeMPc were to be recycled, this Mitsunobu protocol would be an even more attractive choice since the use of toxic reagents can be reduced. Therefore, using PIB as a polymer support to recycle FeMPc was studied.

Finally, as part of work to explore the broader utility of soluble MPc catalysts, the synthesis of a PIB-attached MPc incorporating Cr and the use of this complex as a catalyst for a rearrangement reaction of an epoxide of cinnamic alcohol to a corresponding aldehyde is discussed.

Results and Discussion

In our initial studies, we first repeated others' work that used an insoluble CoMPc as a heterogeneous catalyst in ethylene glycol to reduce 4-chloronitrobenzene using hydrazine hydrate as the reducing agent.[72] However, extension of this work using the PIB-supported CoMPc **24**[73] (Figure 10) in this same solvent or in mixtures of polar solvents and heptane failed or led to incomplete reduction of 4-chloronitroarene after 24 h at 80 °C (*vide infra*).

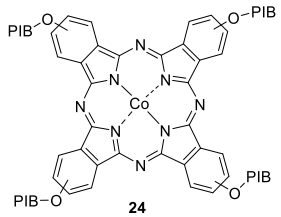

Figure 10. A PIB-bound CoMPc complex **24** that is soluble at 10 wt% in heptane or dichloromethane (CH_2Cl_2) at 25 °C.

We addressed this problem by preparing a CoMPc with PIB groups connected to the phthalocyanine core by electron-withdrawing groups (Scheme 10). Starting with a thiol-ene reaction of vinyl-terminated PIB[74,75] with thioacetic acid, PIB thioacetate **25** was prepared. Hydrolysis of **25** formed the thiol PIB-SH **26**[76] that was allowed to react with 4-nitrophthalonitrile in a nucleophilic aromatic substitution reaction to form the PIB-thiophthalonitrile **27**.[77] Oxidation of **27** with *m*-chloroperbenzoic acid formed the PIB_{1240}-sulfonyl phthalonitrile **28**.[78] Tetracyclization of **28** in the presence of $CoCl_2$ then formed the desired PIB_{1240}-bound MPc **29**.[79] The phthalocyanine **29** so formed is a mixture of species with PIB in different orientations in the four quadrants of the phthalocyanines. As a result, a solution state NMR spectroscopic analysis affords a nondescript ^{1}H NMR spectrum. However, **29** was successfully characterized by inductively coupled plasma mass spectroscopy (ICP-MS) and UV-Visible spectroscopy. ICP-MS analysis of a 1 g sample of **29** showed that it contained 0.0087 g of cobalt. This corresponds to an M_n of 6770 Da that is higher than expected based on a ^{1}H NMR spectroscopic analysis of the M_n of **28**. This analysis of **28** compared the integrated intensity of a known amount of 1,1,2,2-tetrachloroethane internal standard to the integration for the signals for the three aryl protons of **28** at 8.34, 8.29, and 8.07 δ and the two protons in the $–CH_2SO_2$ doublet of doublets of **28** at 3.13 and 2.99 δ of the PIB group and showed that **28** had a degree of polymerization of 22 (a M_n of 1430 Da). This degree of polymerization is higher than that of the starting thioacetate **25** which by a ^{1}H NMR spectroscopic analysis had PIB groups with a degree of polymerization of 20. The difference between **25** and **28** reflects fractionation of the PIB-bound species during the synthesis and purification steps in

Scheme 1. The purification steps leading to isolation of **29** either formed **29** with PIB groups with degree of polymerizations of 26 or formed some **29b** that did not contain Co. If we conservatively assume no further fractionation occurred in forming **29** from **28**, we calculate that **29** is *ca*. 87% metalated.

Scheme 10. Synthesis of 6.

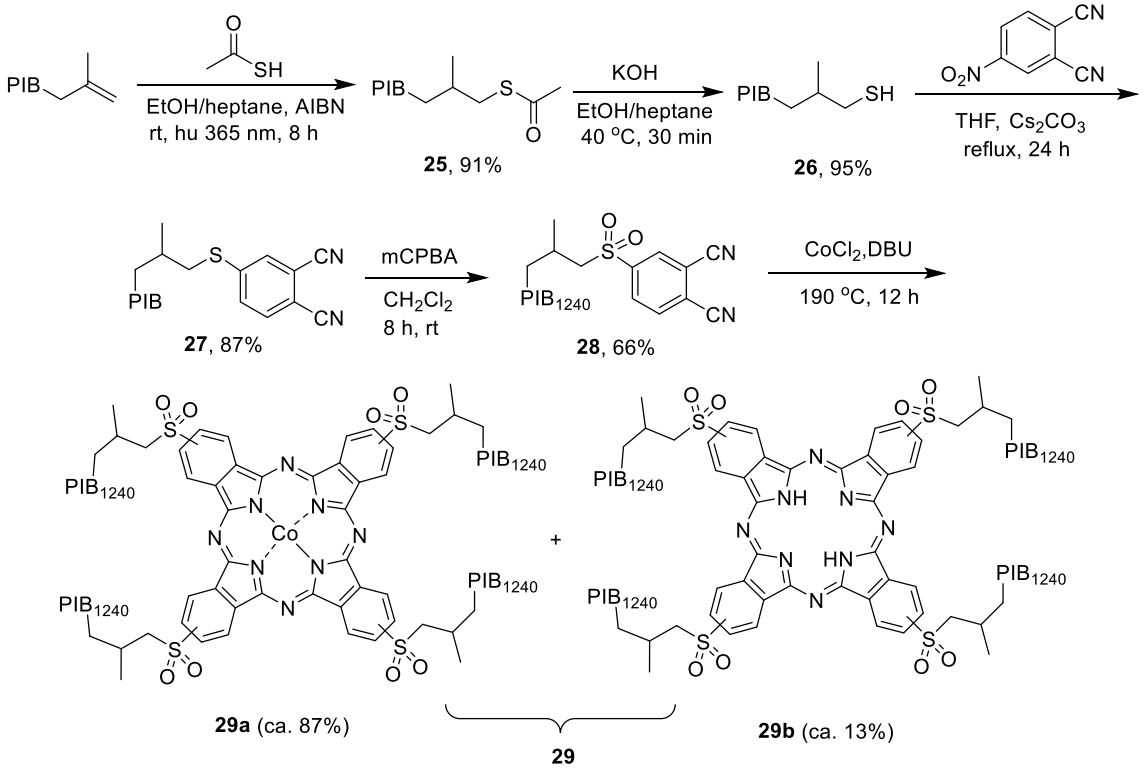

Complex **29** has a λ_{max} at 669 nm that is slightly higher than that reported previously for **24** (λ_{max} = 675 nm) (Figure 11). This peak corresponds to the Q band of the MPc. The shift of the Q band of **29** at 675 to the 669 nm band of **24** is consistent with the introduction of an electron-withdrawing sulfonyl substituent.

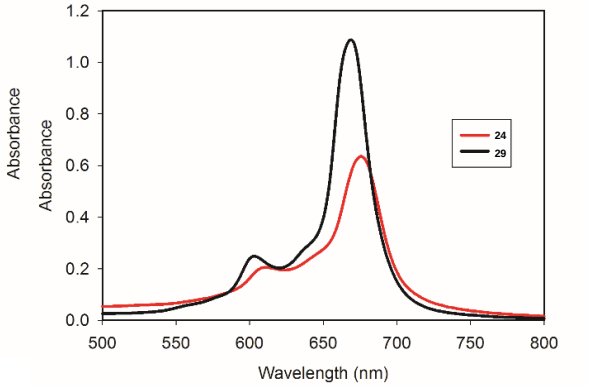

Figure 11. UV-Visible spectrum of complex **24** and **29** in CH_2Cl_2 as concentration is 1.0×10^{-5} M with λ_{max} at 675nm for **24** and 669 nm for **29**.

Gratifyingly, the conversion of 4-chloronitrobenzene to 4-chloroaniline was 100% based on ^{1}H NMR spectroscopy when complex **29** was used as catalyst in the presence of 5 equivalents of hydrazine hydrate instead of **24** (Scheme 11). In these experiments, the reduction was carried out over a period of 24 h at 110 °C using a 1/1 (vol/vol) mixture of a 4.0 x 10^{-4} M heptane solution of **29** and ethylene glycol. Under these reactions conditions, the solution never becomes monophasic but it is rather partially thermomorphic – the volume of the denser phase visually increases and some of **29** dissolves in this phase based on a slight color change of the ethylene glycol rich phase. Fully thermomorphic systems including a 3/1 heptane/ethanol mixture, heptane/glyme (1/1, vol/vol) and heptane/*n*-propanol (1/1, vol/vol) were also examined but reductions in these solvent mixtures only led to 83-95% conversion of the nitroarene to aniline (Table1). Other thermomorphic systems using dimethylformamide (DMF), benzyl alcohol, and glycerol with heptane were even less successful. Control experiments without any catalyst

or with a PIB-bound metal free phthalocyanine **29b** formed no product aniline. Thus, in subsequent studies of the generality and recyclability of **29** in reductions of nitroarenes at 110 ^{o}C, **29** was selected as the catalyst, 5 equivalents of hydrazine hydrate were used as the reducing agent, and 1/1 (vol/vol) mixture of heptane and ethylene glycol was used as the solvent mixture.

Scheme 11. Nitroarene reduction using the heptane-soluble PIB-bound cobalt phthalocyanine catalyst 29.

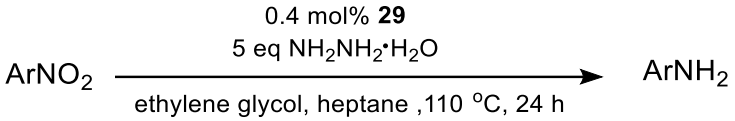

The generality of this reduction and recyclability of these catalysts was tested with varied aryl substituents on nitroarenes as shown in Table 2. 4-Chloro- and 4-bromonitrobenzene gave high isolated yields and complete conversion of the starting nitroarene. Yields of 4-methyl- and 4-*tert*-butylaniline were slightly lower in cycle 1, possibly due to the solubility of these aniline products in the heptane phase. Nitroarenes with electron donating substituents like hydroxy and amino substituents also were quantitatively converted to aniline products affording comparable isolated yields. Reduction of 1-nitronaphthalene was also successful. However, this reduction product is a known carcinogen so repetitive cycles were not performed. Consistent yields cycle-to-cycle were however observed for all the nitroarenes studied, reflecting the high thermal and chemical stability associated with MPcs like **29** and the high phase selective solubility

of **29**. This stability as well as the phase selectivity of **29** due to the PIB support also makes it simple to recycle and to separate the homogeneous catalyst **29** from the aniline products.

Recycling of the cobalt catalyst **29** was accomplished by cooling the reaction mixture to ambient temperature. The less dense heptane-rich phase containing **29** was then physically separated by a gravity separation from the ethylene glycol phase containing the product. The product was isolated from this ethylene glycol phase. Visually no leaching of **29** into the ethylene glycol was seen in any of the 10 recycling experiments with any of the 7-nitroarene substrates in Table 2 with the product phase being a light-yellow color. This qualitative observation of the absence of leaching was confirmed by UV spectroscopic analysis of the product phase for the first cycle for the 4-chloronitrobenzene reduction. While the product phase in these reactions has a yellow color, we were able to use UV-visible spectroscopy to quantitatively assess leaching since **29** has a strong absorbance at 640 nm. From a separate experiment, the extinction coefficient of the 29 in dichloromethane (DCM) was determined as 8.6×10^5 $M^{-1}cm^{-1}$. This extinction coefficient was used to calculate the amount of 29 leached into the ethylene glycol phase after reduction reactions. These experiments showed that the leaching of **29** into the product phase after the first cycle was <0.05% of the charged catalyst **29**. An additional UV experiment was carried using the catalyst isolated from the tenth cycle of a 4-chloronitrobenzene reduction which showed that the recovered catalyst had <0.01% leaching into ethylene glycol.

Table 1. Reduction of 1-chloro-4-nitrobezene to 4-chloroaniline by polyisobutylene-supported phthalocyanines catalysts in the presence of hydrazine monohydrate

Entry	Catalyst	Solvent[a,b]	Temperature (°C)	Equiv of hydrazine	Conversion[c] (%)
1	**24**	Ethanol/heptane	80	2.5	5
2	**24**	Ethylene glycol/ THF	80	2.5	40
3	**24**	Ethylene glycol/ heptane	80	2.5	45
4	**29**	Ethylene glycol/ heptane	110	2.5	75
5	**29**	Ethylene glycol/ heptane	110	5	100
6	**29**	Ethanol/heptane	80	5	59
7	**29**	Ethanol/heptane[d]	80	5	95
8	**29**	Glyme/heptane	85	5	88
9	**29**	*n*-Propanol/ heptane	100	5	83
10	**29**	MeCN/heptane	80	5	45
11	**29**	DMF/heptane	110	5	45[e]
12	**29**	Benzyl alcohol/ heptane	110	5	0
13	**29**	Glycerol/heptane	110	5	66
14	**29b**	Ethylene glycol/ heptane	80	2.5	27
15	-	Ethylene glycol/ heptane	110	5	23
16	CoMPc	Ethylene glycol	80	2.5	100

[a]1 mmol of 1-chloro-4-nitrobezene and 0.4 mol% of catalyst were used in the total amount of 10 mL solvent. [b]All co-solvent system is 1 to 1 volume ratio of each solvent unless otherwise stated. [c]The conversion was determined by ^{1}H NMR spectroscopy. [d]Heptane/ethanol is 3/1 was used, the total volume was 10 mL. [e]*N*,*N*-Dimethyl-4-nitroaniline was the product with 41% isolated yield.

The catalyst-containing heptane phase was reused by simply adding a new batch of nitroarene and hydrazine hydrate in ethylene glycol to the recovered heptane solution of **29**. As shown in Table 2, **29** was able to catalyze at least 10 cycles of reaction with each substrate without significant changes in isolated yield of product.

Table 2. Reduction of nitroarenes to corresponding aminoarenes and recyclability of **29** in ten cycles of nitroarene reduction (Scheme 11)[a, b]

Entry	Nitroarene	Yield in each cycle[c]					
		1	2	3	4	5	6-10[d]
1	4-chloronitrobenzene	74	74	74	73	72	75
2	4-bromonitrobenzene	63	71	73	76	75	71
3	4-nitrotoluene	56	81	79	82	78	80
4	4-*tert*-butylphenylnitrobenzene	68	84	77	81	82	86
5	4-nitrobenzoic acid	70	72	70	75	74	79
6	4-nitrophenol	50	69	69	68	68	65
7	4-nitroaniline	46	69	72	71	65	74
8	1-nitronaphthalene	75	-	-	-	-	-

[a]1 mmol of nitroarene, 4×10^{-3} mmol of **29**, and 5 mmol of hydrazine hydrate were dissolved in 5 mL of ethylene glycol and 5 mL of *n*-heptane and this mixture was stirred at 110 °C under a nitrogen atmosphere for 24 h. [b]After the nitroarene had been completely reduced (as determined by ^{1}H NMR spectroscopy), the reaction mixture was cooled and the bottom product-containing layer was removed. Fresh nitroarene, hydrazine hydrate, and ethylene glycol were added to the flask for a subsequent cycle. [c]The yields reported are isolated yields of products that were pure by ^{1}H and ^{13}C NMR spectroscopy. The product anilines were obtained by extracting the arylamine product from the ethylene glycol phase using ethyl acetate and further purified using column chromatography. [d]The yields for cycles 6-10 are an average yield for each of these five cycles based on the total isolated yield for a combination of the product from the ethylene glycol phases for cycles 6-10.

To confirm that the catalyst **29** had unchanged activity through these ten cycles, we carried out kinetic studies following the conversion versus time for reductions of 4-chloronitrobenzene and 4-nitrobenzoic acid as substrates in a cycle 11 and compared this plot to a similar conversion versus time plot for cycle 1 (Figure 12). In these experiments, we first carried out a reaction using a known amount of **29** in heptane and ethylene glycol and a substrate nitroarene, following the conversion of the nitroarene versus time by ^{1}H NMR spectroscopy. Then, after the tenth cycle, we isolated the PIB-bound catalyst **29** from the heptane-rich solution. The same amount of this catalyst **29** as was used in the reaction with fresh catalyst was then used in an eleventh cycle and the conversion versus time was compared to the plot obtained with fresh catalyst. As shown in Figure 12, the conversion versus time between the first and the eleventh cycle are unchanged for both substrates, indicating that the catalyst activity had not changed during these ten cycles and separations. This is consistent with lack of change in isolated yields of products in Table 1 and with the expected stability of the MPc catalysts.

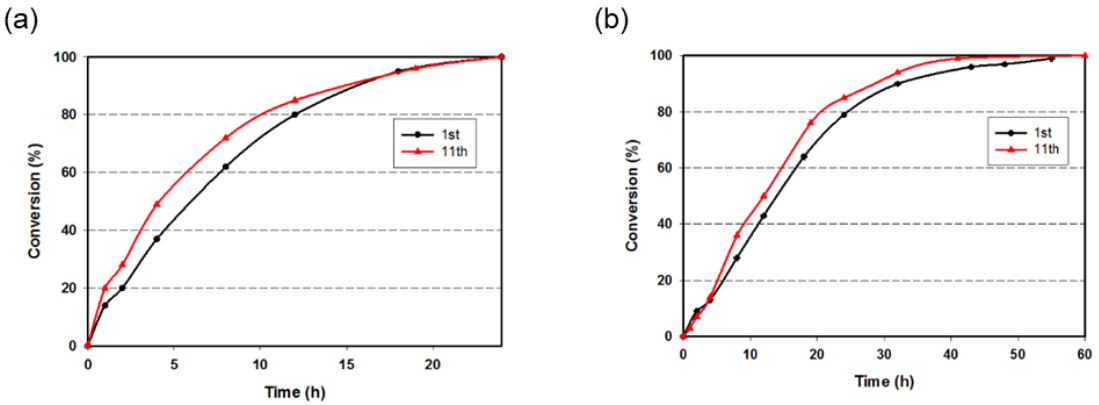

Figure 12. Conversion versus reaction time profile for the first and eleventh cycle for nitroarene reductions catalyzed by **29** with two different nitroarenes: (a) 4-chloronitrobenzene and (b) 4-nitrobenzoic acid.

Finally, we examined the spectrum of **29** by UV-Visible spectroscopy looking both at fresh **29** and at **29** that was isolated after eleven cycles of reduction and separation. As shown in Figure 13, there is no obvious change in the visible spectrum of **29** after eleven cycles of 4-chloronitrobenzene reduction and separation.

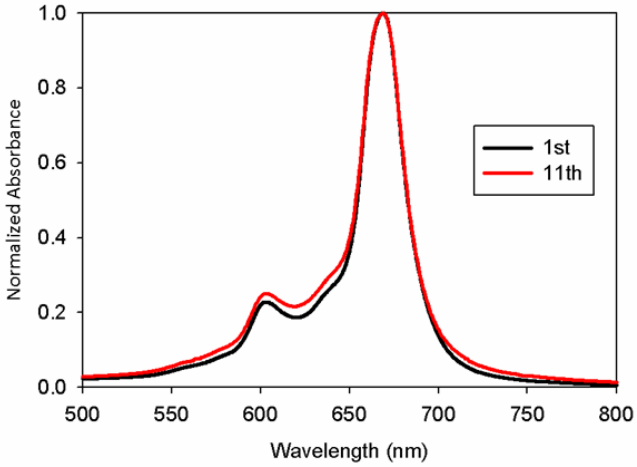

Figure 13. UV-Vis spectrum of a heptane solution of **29** before and after eleven cycles of 4-chloronitrobenzene reduction.

We have also synthesized an iron-incorporated PIB-sulfonyl attached phthalocyanine **30** by a tetracyclization reaction of **28** in the presence of iron dichloride as shown in Scheme 12. We then tested whether the complex **30** could catalyze aerobic oxidation of ethyl phenylhydrazinecarboxylate (Scheme 13). Gratifyingly, as shown in Table 3, ethyl phenylhydrazinecarboxylate was fully converted to ethyl phenylazocarboxylate after 24 h when 10 mol% of **30** was used with tetrahydrofuran (THF) as solvent.

Scheme 12. Synthesis of 30.

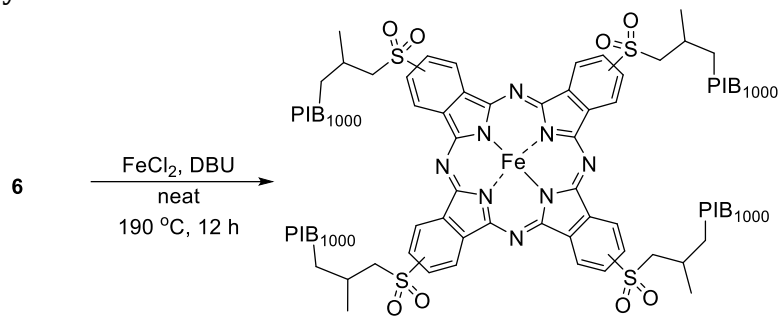

The recyclability of the catalyst was then studied. After the reaction, the solvent was removed under reduced pressure followed by the addition of heptane and 90% aqueous ethanol to extract the product into the aqueous ethanol phase. The heptane phase containing **30** was then isolated by a liquid/liquid separation and then concentrated to give a dark blue oil. THF and ethyl phenylhydrazinecarboxylate were then added to carry out the next cycle. This process was repeated three additional times and the conversion for each cycle was reported in Table 3. As shown in entry 1, the oxidation reactions had quantitative conversion for the first three cycles. However, the conversion dropped noticeably to 45% for the fourth cycle and then to 13% for the fifth cycle. The decrease of conversion in the later cycles was not investigated further. However, it could be due to oxidation of iron(II) to iron (III).

Scheme 13. Aerobic oxidation of ethyl phenylhydrazinecarboxylate to ethyl phenylazocarboxylate catalyzed by 30.

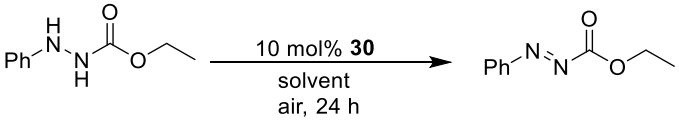

To make the oxidation more sustainable, a latent biphasic solvent mixture, heptane and ethanol, was next studied as a solvent system for the reaction.[33] After the reaction, water was added to perturb the solution and to form a biphasic mixture. The heptane layer containing **30** was isolated by a liquid/liquid gravity separation. Then ethanol and ethyl phenylhydrazinecarboxylate were added to the heptane solution to carry out the second cycle of the reaction. Recyclability of **30** in this heptane/ethanol latent biphasic system was studied by carrying out three additional cycles. As shown in Table 3 entry 2, the conversions of the first two cycles were quantitative within 24 h but the conversion dropped to 71% in the third cycle and then to 19% in the fourth cycle. Two methods were tried to prevent the degradation of **30** which was faster in a heptane/ethanol mixture than in THF. These two methods added either hydroquinone (HQ) as an anti-oxidant or butylated hydroxytoluene (BHT) as a radical trap. However, the conversions dropped even faster in each cycle using these methods.

Table 3. Aerobic oxidation of ethyl phenylhydrazinecarboxylate to ethyl phenylazocarboxylate catalyzed by **30**[a]

Entry	Solvent	Additive	Conversion in each cycle[b]				
			1	2	3	4	5
1	THF	-	100	100	100	45	13
2	Ethanol/heptane	-	100	100	71	19	-
3	Ethanol/hexane	10% HQ	90	16	22	13	11
4	Ethanol/hexane	5% BHT	95	53	23	13	2

[a]0.1 mmol of ethyl phenylhydrazinecarboxylate and 10 mol% of catalyst were dissolved in 5mL of solvent and stirred for 24 h. [b]The conversion was determined by ^{1}H NMR spectroscopy.

Another catalyst, PIB-supported chromium triflate phthalocyanine Cr(OTf)MPc **34**, was prepared as shown in Scheme 14. Alcohol-terminated PIB_{1000} **31** was synthesized by hydroboration and oxidation of vinyl-terminated PIB_{1000}. Then, 4-nitrophthalonitrile was allowed to react with **31** via a nucleophilic aromatic substitution reaction to form PIB-attached phthalonitrile **32**. After tetracyclization of **32** in the presence of chromium trichloride, the chromium chloride-incorporated PIB-attached phthalocyanine **33** was obtained. The chloride ligand on **33** was then changed to a triflate by doing a ligand exchange reaction with silver triflate to form a dark green oil PIB-supported Cr(OTf)MPc **34**.

Scheme 14. Synthesis of 34.

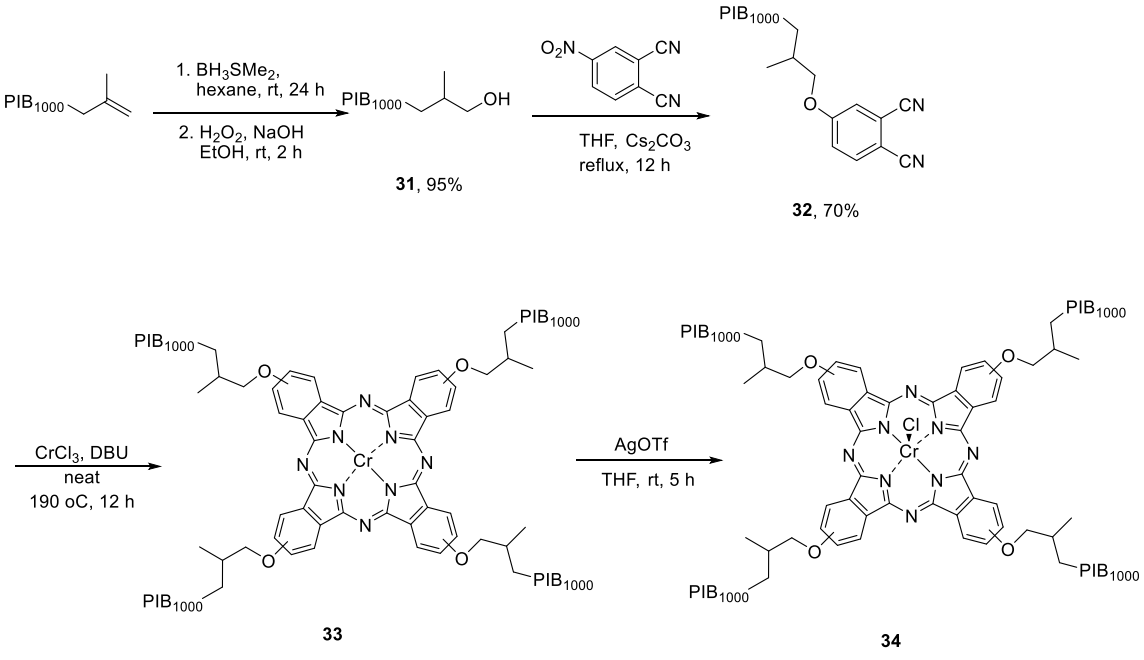

The catalyst **34** was then tested as a catalyst for the rearrangement reaction of an epoxide of a protected cinnamic alcohol **35** to the corresponding aldehyde **36**. Initially, 1,2-dichloroethane was used as solvent to dissolve **35** in the presence of 5 mol% of **33**. The conversion was quantitative as shown in Table 4 (entry 1) based on a ^{1}H NMR spectroscopic analysis after the mixture was allowed to stir for 12 h.

Scheme 15. Rearrangement reaction of 35 to 36 catalyzed by 34

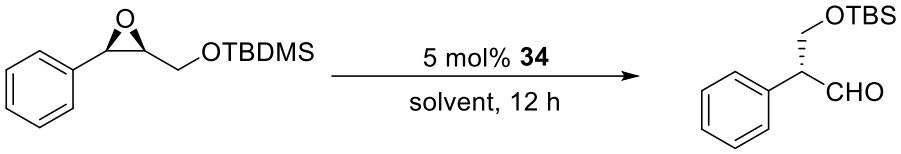

35 **36**

Table 4. Rearrangement reaction of 35 to 36 catalyzed by 34.[a]

Entry	Solvent[b]	Conversion (%) in each cycle[c]	
		1	2
1	Heptane	13	-
2	1,2-dichloroethane	100	53
3	1,2-dichloroethane/heptane	100	50
4	DMF/heptane	0	-
5	MeCN/heptane	14	-
6	Ethanol/heptane	0	-

[a]0.3 mmol of reactant and 5 mol% of catalyst were dissolved in 5 mL of solvent and stirred for 12 h. [b]All co-solvent systems used a 1 to 1 volume ratio of each solvent. [c]The conversion was determined by ^{1}H NMR spectroscopy.

Although the reaction was successful in 1,2-dichloroethane, we wanted to seek alternative solvents because of 1,2-dichloroethane has high toxicity. As shown in Table 4 entry 2, poor conversion to the aldehyde was obtained in heptane. The low polarity of heptane was thought to be responsible for this low conversion. Therefore, a mixture of heptane and a polar solvent was then tested. However, the conversion of the reaction did not improve. 1,2-dichloroethane as a solvent seems to be essential for the reaction; in fact, when a 1/1 (vol/vol) mixture of heptane and 1,2-dichloroethane was used as the solvent, the reaction also showed full conversion. The recyclability of the catalyst using 1,2-dichloroethane as a solvent was then briefly studied. After the reaction, heptane and 90% aqueous ethanol were added to the mixture after 1,2-dichloroethane was removed under reduced pressure. The catalyst was then recovered from the heptane layer by a liquid/liquid separation and then dried under vacuum. Fresh epoxide and 1,2-dichloroethane were added to the catalyst to repeat the reaction. After 12 h, it was found that the conversion in this second cycle dropped to 53% and the color of the catalyst changed from bright green to dark green. Further optimization of the reaction was not attempted due to the catalyst's instability and the difficulty of recycling attempts.

Conclusions

In summary, several highly heptane and organic solvent soluble PIB-supported MPc were synthesized as homogeneous catalysts. A PIB-sulfonyl-supported CoMPc was shown to be an effective and recyclable catalyst for reduction of nitroarenes using hydrazine hydrate as a reducing reagent under semi-thermomorphic conditions at 110 ˚C.

While a variety of solvents yielded product, the use of an equivolume mixture of ethylene glycol and heptane as solvents was optimal. The isolated yields of the reduced aniline products were consistently good for ten cycles with a variety of electron-donating and electron-withdrawing substituents on the starting nitroarene. Because of the PIB-induced phase selective solubility of the PIB-supported CoMPc, the catalyst can be recycled at least 10 times. Kinetic studies show the catalyst has unchanged reactivity and UV-visible spectroscopy shows no change in catalyst structure, results consistent with the expected thermal and kinetic stability of MPc catalysts. A PIB-sulfonyl-supported FeMPc was also shown to be an effective catalyst for the aerobic oxidation of ethyl phenylhydrazinecarboxylate to ethyl phenylazocarboxylate. The catalyst was recyclable at least for three cycles with THF as the solvent but the conversion of the reaction dropped substantially- after the third cycles. A PIB-supported Cr(OTf)MPc was also able to catalyze the rearrangement reaction of an epoxide to the corresponding aldehyde but this catalyst was not recyclable. We believe the solubility introduced into these MPcs by PIB groups can be employed to make other PIB-bound MPcs similarly useful in homogeneously catalyzed processes where a similar biphasic liquid/liquid separation can facilitate both catalyst/product separation and recycling polymer-supported catalysts.

CHAPTER III

HYDROCARBON SOLUBLE RECYCLABLE SILYLATION REAGENTS AND PURIFICATION AUXILIARIES*

Introduction

Chlorosilanes are widely used in organic synthesis as protecting groups.[80] For example, trialkylsilylchlorides are used to form silyl ethers to protect alcohols, and trimethylsilyl groups are used to monoprotect one C-H of ethyne in cross-coupling chemistry. These organosilicon reagents are particularly useful because their installation and removal can be performed with high chemoselectivity under mild conditions. However, when a silyl group is removed, often with a fluoride reagent, it is typically discarded. Here, we show how techniques we developed for the separation and recycling of phase selectively soluble homogeneous catalysts can be adapted to recycle protecting groups. We also show that these same protecting groups can serve as phase handles in a simple extractive purification method for silyl-protected alcohols and alkynes, a strategy that has precedent in liquid/liquid separations that employ fluorous silyl groups.[81] The liquid phase extraction illustrated in this work provides an potential alternative to the solid phase extraction supports our group has explored previously that are also widely available in various forms commercially.[82]

---

* Reprinted with permission from "Hydrocarbon Soluble Recyclable Silylation Reagents and Purification Auxiliaries" by Chao, C. -G.; Leibham, A. M.; Bergbreiter, D. E. *Org. Lett.* **2016**, *18*, 1214, Copyright 2016, by American Chemical Society

The chemistry described here focuses on one sort of liquid phase supported extraction scheme that uses recyclable, separable silylating agents and successfully shows the potential of heptane soluble silyl groups in recycling as well as purification. In initiating this research, we noted that surprisingly few studies have been carried out to explore how to recycle organosilyl species by regenerating chlorosilanes. We further noted that the studies that have been reported also have various issues. Lickiss showed that *tert*-butyldimethylsilanol (TBS-OH) could be recycled and converted to *tert*-butyldimethylchlorosilane. However, in this chemistry, the volatility of the hemihydrate of TBS-OH leads to losses of product during distillation.[83] Darling and coworkers described cross-linked polystyrene supported chlorosilanes that could be used as protecting groups in solid-phase synthesis and regenerated by treatment with BCl_3. However, the heterogeneity of the support resulted in low loading of the silicon reagent, difficult characterization, and modest efficiency in subsequent silylation chemistry.[84] Our experience with hydrocarbon soluble catalyst ligands and others' work with hydrocarbon phase tags that employ octadecyl groups suggested alternative biphasic schemes for separating and recycling silicon reagents might be useful alternatives.[5,6,33,85–89]

Our group has a longstanding interest in phase selectively soluble polymer-supported catalysts.[33] We have shown that it is possible to prepare catalysts or ligands that effect homogeneous reactions and a separation without affecting reactivity by anchoring catalysts or ligands onto soluble polymers.[90] In this strategy, separations are most often effected after completion of the reaction, using a biphasic liquid/liquid separation where the soluble polymer supported species is by design selectively soluble in a phase that does

not contain the product. Alternatively, separations can be carried out using an extractive workup. These methods have been used by us and others to recycle precious metal catalysts and in synthesis.[33,91–94] Here we show how a similar strategy can address the issue of recycling organosilicon species and as a strategy in purification of intermediates.

Results and Discussion

Our initial studies showed the feasibility of using a hydrocarbon phase anchored silylating agent – octadecyldimethylchlorosilane (**37**) - as an analog of trimethylchlorosilane. This silylating agent is commercially available both as an *n*-octadecyldimethylchlorosilane and as a structurally isomeric compound with isomeric octadecyl groups because it is used to make silylated silica gel used in reverse phase chromatography.[95,96] After synthesizing silyl ethers of a variety of alcohols, we showed that the products of silylation that either had an *n*-octadecyl group or that contained a mixture of octadecyl isomers are soluble in alkanes like hexane and heptane, but poorly soluble in common polar organic solvents like dimethylformamide (DMF), 90% aqueous ethanol, and acetonitrile (MeCN). We further showed that this phase selective solubility can be used to assist in the extractive purification of compounds containing this protecting group and to subsequently separate and recycle a spent organosilyl species.

To study the separability of silyl ethers of **37** and the recyclability of octadecylsilyl groups of **37**, we first prepared silyl ethers from a series of primary alcohols. As shown in Scheme 16, alcohols with side chains of various sizes reacted with **37** under mild conditions to give the corresponding silyl ethers with excellent yields. Notably, these

products could be purified by a simple liquid/liquid separation using heptane and 90% aqueous ethanol due to the phase-selective solubility of the products in heptane. In these cases, the products could be isolated by removal of the heptane under reduced pressure. After the ethers were synthesized, we next quantitatively determined the phase selective solubility of silyl ethers in a thermomorphic system of DMF and cyclohexane, which is biphasic at room temperature but forms a monophasic solution on heating. We then analyzed the leaching of the silyl ethers into the polar phase of this thermomorphic system using ^{1}H NMR spectroscopy. Using methoxy(octadecyldimethyl)silane (**38a**), ethoxy(octadecyldimethyl)silane (**38b**), and butoxy(octadecyldimethyl)silane (**38c**) as examples, we found that **38a** showed 3.8% leaching, **38b** showed 2.1% leaching, and **38c** showed 2.0% leaching into the DMF phase of a cyclohexane/DMF thermomorphic system. Similar results were seen in ^{1}H NMR experiments using **38c** in cyclooctane/DMF, hexane/DMF, heptane/DMF, and cyclooctane/90% aqueous ethanol where 2.2%, 4.6%, 3.2%, and 0.7% leaching of **38c** into the polar phase was seen. These results show that **37** is effective at forming products that are reasonably phase selectively soluble in nonpolar solvents and suggests that **37** can be used as a purification auxiliary.

Scheme 16. The synthesis of silyl ethers 38a-e.

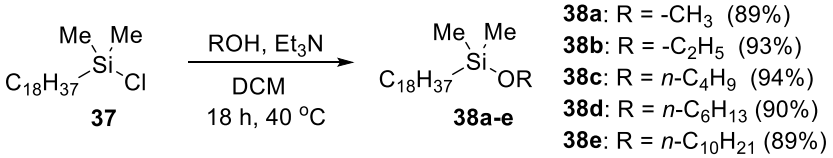

Next, we examined ways to reform the alcohol and to recycle the octadecyldimethylsilyl group (Scheme 17). In this case, we used **38e** as an example, cleaving the silyl ether using tetra-*n*-butylammonium fluoride (TBAF) in a heptane/THF solution. The octadecyldimethylsilyl groups were recovered as a mixture of the silanol and silyl ether **(39)** in 94% yields. The decanol (**40**) yield was lower as some decanol was lost during the extractions that were used to remove the TBAF residues. The octadecyldimethylsilyl residue mixture **39** could be further purified to form **39b**, but the mixture of **39a** and **39b** was typically used directly in recycling experiments.

Scheme 17. TBAF cleavage of 38e to form 39 and decanol.

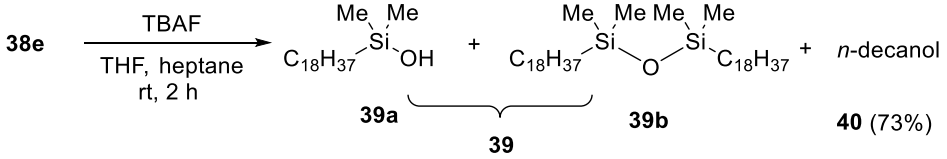

There are a number of reactions that could in principle regenerate **37** from **39**. Some, like Sommer's route using chlorine gas are likely experimentally inconvenient.[97,98] Other procedures including chlorination with acetyl chloride,[99,100] thionyl chloride,[101] oxalyl chloride,[102] phosphorous pentachloride,[103] and concentrated hydrochloric acid[104] are better choices. In our case, we found that **37** can be regenerated quantitatively from **39** by allowing **39** to react with thionyl chloride in the presence of a catalytic amount of DMF (Scheme 18). With these results in hand, a procedure for the cleavage of organosilyl protecting groups and regeneration of **37** was established as shown in Figure 14.

Scheme 18. Regeneration of 37 from 39.

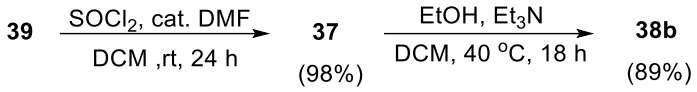

These recyclable hydrocarbon-soluble silylating reagents can also be used in other types of reactions. For example, regenerable **37** can be used to phase tag the alkoxide product of a Grignard reaction. This is shown in Scheme 19 where 10-undecenal was allowed to react with methylmagnesium bromide. Addition of **37** to the alkoxide product solution formed (dodec-11-en-2-yloxy)(octadecyldimethyl)silane (**41**) which after a workup using heptane afforded a 91% yield of **41**. A subsequent fluoride deprotection and liquid/liquid separation procedure afforded dodec-11-en-2-ol (**42**) in 75% yield that was pure by ^{1}H and ^{13}C NMR spectroscopy. This same strategy was used to form an 83% yield of (1-(4-methoxyphenyl)ethoxy)(octadecyldimethyl)silane (**43**) when **37** was added to the product of reaction of methylmagnesium bromide and 4-methoxybenzaldehyde.

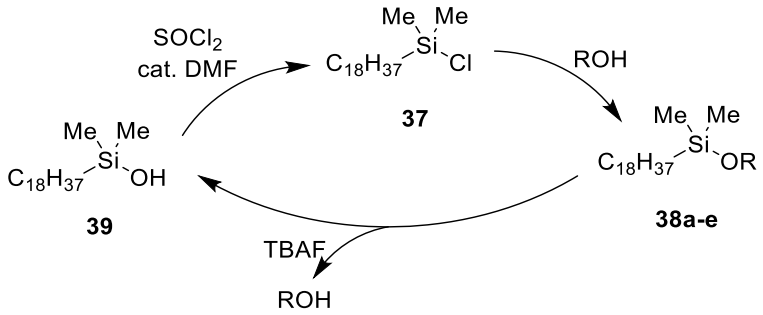

Figure 14. Recycling of **37** after a protection/deprotection sequence.

Scheme 19. The use of 1 to trap intermediates in Grignard reactions.

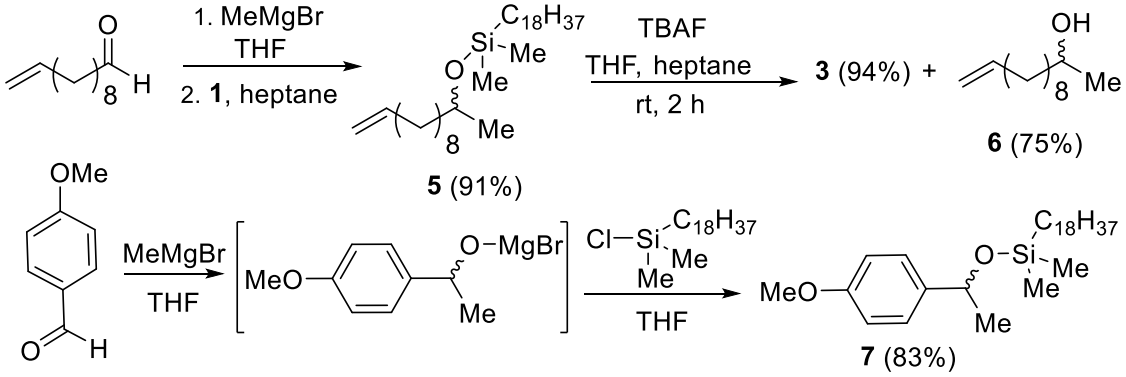

The Sonogashira reaction is a widely used catalytic reaction that leads to alkynes via a palladium-catalyzed cross coupling reaction.[105] A common variant of this procedure uses trimethylsilyl-protected ethyne as a reagent to form terminal alkyne products.[106,107] In these cases, the protected alkyne coupling products are purified by column chromatography to separate them from catalyst residues. To illustrate the broader potential of **37**, we have shown that **37** can replace trimethylsilyl groups in these sorts of Sonogashira coupling reactions, providing both a recyclable silyl protecting groups and a simpler way to isolate the intermediate protected alkyne product.

As shown in Scheme 20, the reaction of **37** with sodium acetylide[108,109] formed octadecyldimethylsilylacetylene (**44**) which could then be coupled with 4-iodoacetophenone to obtain 4-((dimethyl(octadecyl)silyl)ethynylacetophenone (**45**). While a trimethylsilyl analog of **45** previously had to be purified by column chromatography,[110,111] **45** was purified by simple liquid/liquid extraction. The result shows that **44** is a potential replacement for $Me_3SiC{\equiv}CH$ and a purification handle for the intermediate product. In this example, 4-ethynylacetophenone (**46**) was obtained in 95%

yield after cleavage of the silyl group. The starting **37** was then regenerated from **39**. We also showed that regenerated **37** could be used in other chemistry, specifically in a reaction with ethanol to afford a 92% yield of **38b**. The product **38b** formed from regenerated **37** was identical to that formed from fresh **37** and contained no Sonogashira coupling products.

Scheme 20. The use of 37 in a Sonogashira reaction followed by regeneration and reuse of 37.

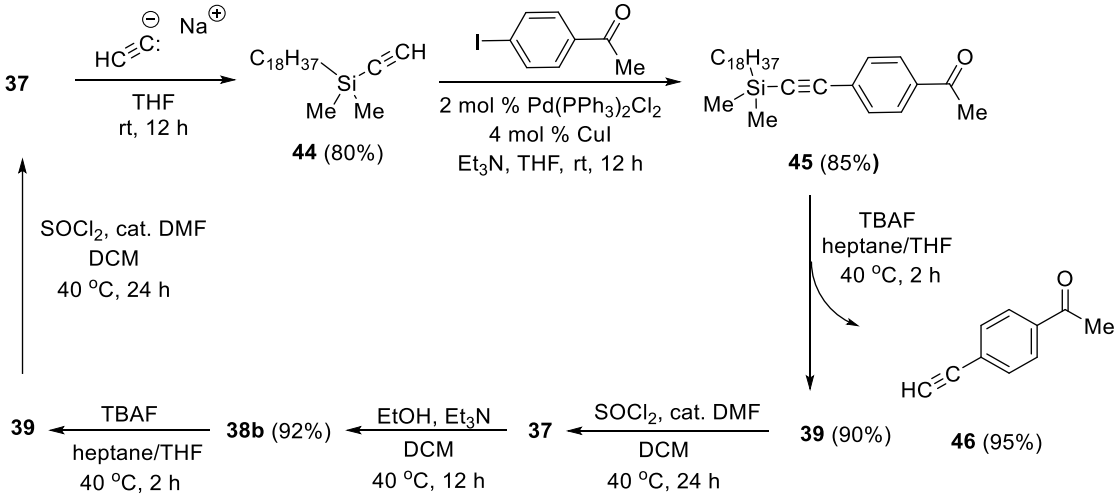

While we were successful in using **37** as a phase anchor as shown in the examples above, **37** has limitations. If the substrate that is appended to **37** has a molar mass comparable to **37** and is significantly polar, leaching levels will exceed 10%. This is illustrated visually in Figure 15 with an octadecyldimethylsilyl-protected derivative of the azo dye **47**. This silylated dye is soluble in a hot homogeneous thermomorphic solvent mixture, but cooling produced a biphasic mixture with significant amount of the dye derivative in the polar phase. Separate experiments with the alcohol precursor of **47** show

it is predominantly in the polar phase of this thermomorphic mixture. We believe this is because the azo dye portion of **47** is both polar and has a mass that is approximately the same as the silyl phase anchor and the hydrophobic groups in **37**.

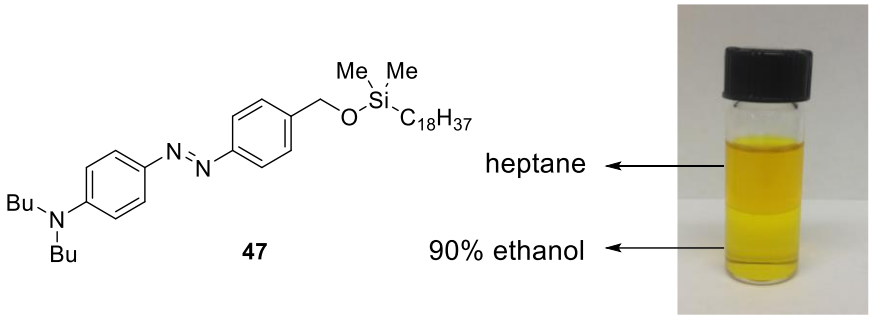

47

Figure 15. Phase selectivity of **47** at 25 °C in a thermomorphic 1/1 (vol/vol) mixture of heptane and 90% aqueous ethanol.

We also tried to synthesized PIB-supported dimethylchloroslane **48** via a hydrosilylation reaction as shown in Scheme 21. A vinyl-terminated PIB was allowed to react with dimethylchlorosilane in the presence of chloroplatinic acid as a catalyst at 80 ^{o}C for 48 h. The product should have better phase selectivity in nonpolar solvents and has the potential for silylation reactions.

Scheme 21. Synthesis of PIB-supported dimethylchlorosilane 48.

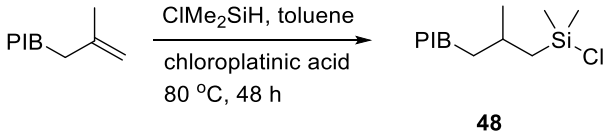

48

Conclusions

In summary, this work shows that hydrocarbon phase anchored silyl protecting groups can serve both as regenerable protecting groups and as purification handles. Using commercially available and inexpensive octadecyldimethylsilylchloride **37**, we showed that a variety of silyl ethers are >95% phase selectively soluble in the heptane phase of a heptane/DMF mixture when alcohols are converted into silyl ethers using **37**. We further show that the octadecyldimethylsilyl products formed in the deprotection can be used to reform **37**. Other experiments show that **37** can be used directly to silylate alkoxides produced in reactions to form silyl ether products that facilitate purification and separation of the products. The broader utility of **37** is shown by the successful use of an ethyne derivative of **37** in a Sonogashira coupling reaction. While our experiments mostly used a well-defined *n*-octadecyldimethylsilylchloride reagent, we also showed that a less expensive commercially available silyl chloride containing octadecyl silyl isomers is similarly effective. We anticipate that in future work we can design more phase selectively soluble silylating agents to ameliorate the modest losses due to leaching of silylated intermediates seen here and to address issues that may come up with protection of more polar or larger polar substrates. We also expect that adaptations of this strategy will be generally useful in recycling stoichiometric protecting groups and reagents.

CHAPTER IV

POLYISOBUTYLENE OLIGOMERS AS TOOLS FOR IRON OXIDE NANOPARTICLE SOLUBILIZATION[*]

Introduction

The development of reliable synthetic routes to nanomaterials and their use continues to be an area of interest because of the usefulness of nanoparticles in widely different areas of chemistry.[112–118] Developing ways to stabilize, disperse, and solubilize nanoparticles also remains an important goal. The most progress in this latter effort has been in developing methodology to form solutions or dispersions of nanoparticles for use in polar milieu by modifying the nanoparticle/solution interface.[119] Often this has been accomplished using polymers that are either grafted to or grafted from the nanoparticle surface.[25,120,121] This chemistry can be used to prepare dispersions of magnetic nanoparticles (MNPs) that are reasonably stable. However, in most cases, an external magnetic field or centrifugation can be used to separate the modified MNPs. Methods to make nanoparticles including MNPs dissolve or form stable dispersions in very nonpolar solvents or materials have also received attention. While in most cases these efforts form dispersions where the concentration of nanoparticles is <10 wt%,[122–124] ferrofluids can have 15% or greater concentrations of modified nanoparticles.[125] In this paper, we explore the use of functionalized polyisobutylene (PIB) oligomers to make solutions of modified

---

[*] Reprinted with permission from "Polyisobutylene Oligomers as Tools for Iron-Oxide Nanoparticle Solubilization" by Chao, C. -G.; Manyam, P. K.; Riaz, N.; Khanoyan, R. T.; Madrahimov, S. T.; Bergbreiter, D. E. *Macromolecules* **2017**, *50*, 1494, Copyright 2017, by American Chemical Society

magnetic nanoparticles in saturated hydrocarbon solvents. These PIB-modified MNPs effectively form solutions in weakly polar solvents like toluene and tetrahydrofuran (THF). These PIB-modified MNPs do not dissolve or form stable dispersions in polar solvents where PIB is insoluble. In the experiments below, we show that this ability to modify magnetic nanoparticle solubility is dependent on the nature of the terminal functional group on the polyisobutylene oligomer and show that catechol terminal groups are especially effective in forming these stable dispersions.

We have a long history of using polymers to manipulate solubility of homogeneous catalysts and metal complexes.[37,126,127] While this work has mainly been focused on developing greener ways to effect catalysis, we have also shown that the same ligands that are used to make catalysts soluble and recyclable in nonpolar solvents like heptane can be used to make other typically insoluble materials highly heptane soluble. This is most evident in our studies of PIB-modified metallophthalocyanines work discussed in Chapter II of this dissertation.[73] In that case, we found that we could prepare phthalocyanines with PIB substituents and that the resulting materials were viscous blue-green oils. These metallophthalocyanines with covalently attached PIB ligands were miscible with heptane at all concentrations and soluble at *ca.* 20 wt% even at -20 °C. Those results suggested to us that terminally functionalized PIB oligomers could similarly be used to disperse nanoparticles in nonpolar or weakly polar solvents.

Iron oxide MNPs are common types of nanoparticles with applications in medicine,[128,129] as tracking agents,[130,131] as reinforcement agents in plastics,[132,133] and as tools for separations.[134] There are numerous methods available to synthesize MNPs using

as examples hydrothermal, thermal decomposition, coprecipitation, and polyol synthesis methods.[112,116] These various methods result in MNPs with different shapes and sizes. It is also known that MNPs have a strong tendency to aggregate and that groups like surface modification can stabilize MNPs by introducing either electrostatic or steric repulsion to their surface. Hydrophobic surfactants can also impart varying stability and some organic solvent solubility to MNPs. For example, oleic acid functionalized MNPs are more effective at stabilizing and solubilizing MNPs than stearic acid.[135,136] Polyolefins containing succinic anhydride end groups have also been used to make stable colloidal suspensions or solutions of magnetite that contain up to 5 wt% magnetite.[122–124,133] The work below explores the utility of modified polyisobutylene oligomers to modify MNP solubility by studying the effectiveness of various types terminal functional groups on PIB in solubilizing bare MNPs in alkanes. These results also compare PIB-bound functional groups to their saturated fatty acid derived alternatives. These comparisons show that using PIB-bound functional groups as ligands instead of stearic acid derivatives leads to PIB-grafted magnetic nanoparticles that have much higher solubility in weakly polar solvents. We show that by using appropriate PIB ligands we can prepare magnetic oils that contain up to 32 wt% MNPs and that such oils dissolve in alkanes or weakly polar organic solvents to form solutions of MNPs that are stable to centrifugation, magnetic separation, and external reagents.

Results and Discussion

In the work below, we prepared MNPs by a literature procedure and then modified these MNPs with PIB groups, collecting modified MNPs using one of three procedures (Scheme 22). As depicted in Scheme 22, the magnetic decantation method A uses an external magnet to magnetically separate soluble PIB-modified MNPs from less soluble MNPs which were then repeatedly washed with solvent. Centrifugation is an alternative way to isolate highly soluble PIB-modified MNPs. A third method C was used for larger scale syntheses and combined a filtration step with a magnetic separation and is discussed below.

Scheme 22. Procedures for Isolation of PIB-Modified Magnetic Nanoparticles

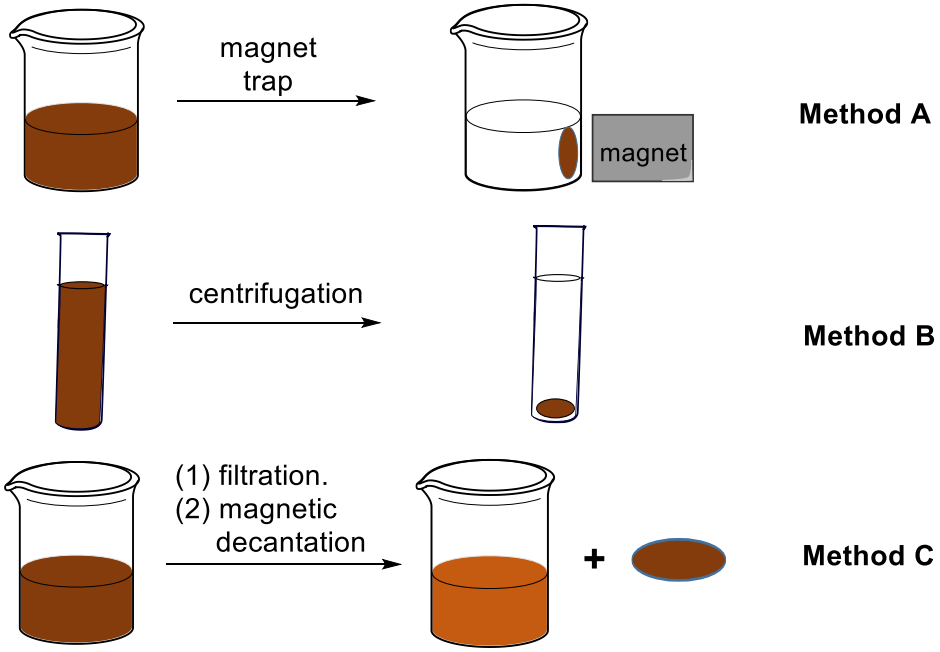

The starting iron oxide nanoparticles were prepared using a coprecipitation method following a protocol initially developed by Nadia Riaz, a visiting scholar in our group. A 300-mL aqueous solution of 50 mmol of $FeSO_4$ and 100 mmol of $FeCl_3$ was added to 30 mL of a 30% aqueous ammonium hydroxide solution to form a black Fe_3O_4 nanoparticle precipitate. Figure 16 shows the X-ray diffraction (XRD) pattern of the resulting product. Six peaks were identified and matched with characteristic peaks corresponding to (220), (311), (400), (422), (511) and (440) crystal planes of Fe_3O_4 nanoparticles in the literature.[137] The Fe_3O_4 nanoparticles so formed have round shapes and an average 9 nm diameter as identified by a transmission electronic microscope (TEM) image (cf. Figure 19a, *vide infra*).

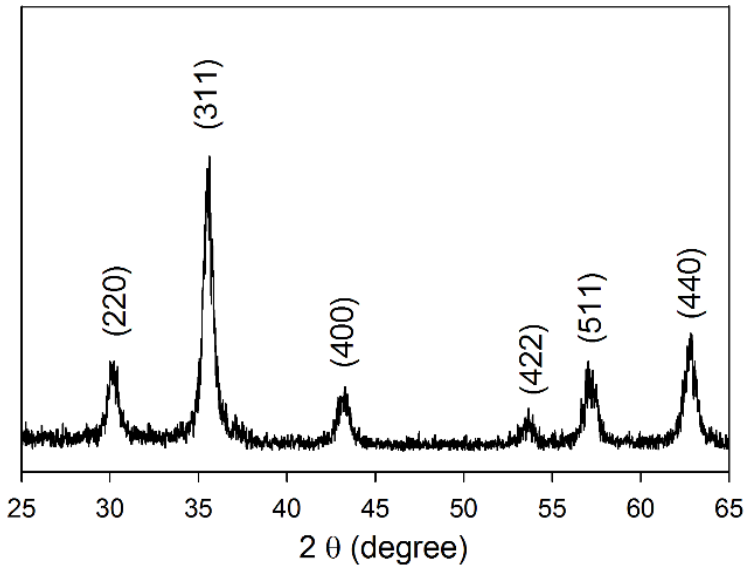

Figure 16. XRD patterns of the ungrafted Fe_3O_4 nanoparticles that were synthesized by the coprecipitation method.

To study grafting of terminally functionalized PIBs onto MNPs, a series of PIB-bound ligands denoted as a PIB-X were prepared using known chemistry or variations on known chemistry as shown in Scheme 23. The syntheses of these functionalized PIB oligomers are described in detail in the supporting information. The PIB-X derivatives **25, 26, 31, 49-56** were characterized by ^{1}H, ^{13}C, and, where appropriate, by ^{31}P NMR spectroscopy and were prepared from commercially available alkene terminated PIB_{1000} (M_n = 1000 Da) and PIB_{2300} (M_n = 2300 Da). These PIB-bound ligands with different M_n values are denoted as PIB_{1000}-X and PIB_{2300}-X in the later discussion.

Scheme 23. Synthesis of 25, 26, 31, 49-56[a]

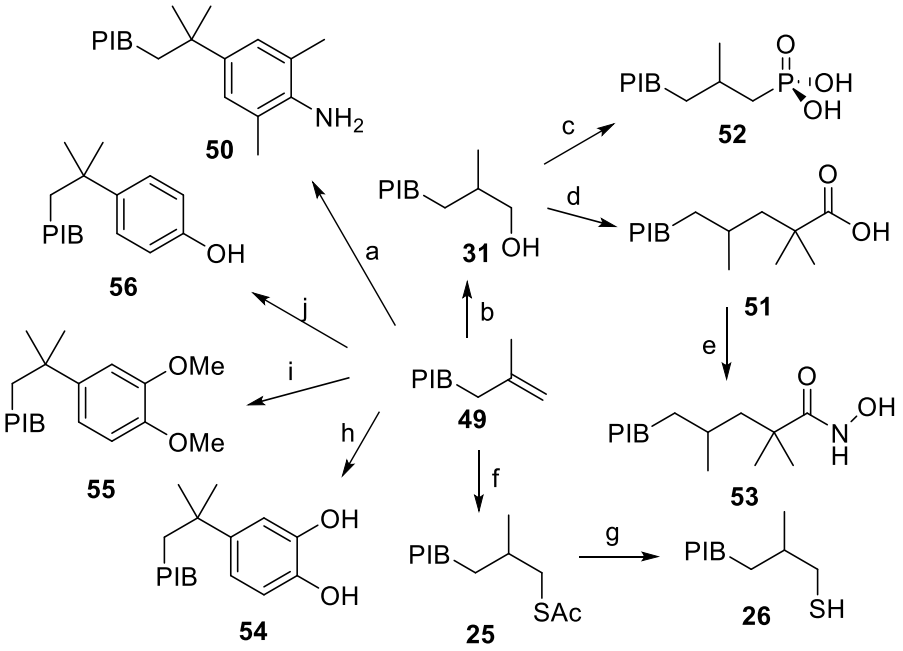

[a]Reaction conditions: (a) 2,6-Dimethylaniline, $AlCl_3$; (b) (i) BH_3-SMe_2, hexane, then (ii) NaOH, H_2O_2, EtOH; (c) (i) I_2, PPh_3, imidazole, (ii) $P(OEt)_3$, (iii) $(CH_3)_3SiBr$, then (iv) MeOH, heptane; (d) I_2, PPh_3, imidazole, (ii) $(CH_3)_2CHCO_2C(CH_3)_3$, LDA, then (iii) H_2SO_4, CH_2Cl_2; (e) (i) 1,1'-carbonyldiimidazole, CH_2Cl_2, (ii) $PhCH_2ONH_2$, MeOH, CH_2Cl_2, then (iii) H_2, Pd/C, THF; (f) CH_3COSH, AIBN, *hν*; (g) KOH, EtOH/heptane; (h) catechol, H_2SO_4, CH_2Cl_2; (i) veratrole, H_2SO_4; (j) phenol, H_2SO_4, CH_2Cl_2

Our initial explorations of MNP modification using the PIB derivatives **25, 26, 31, 49-56** involved reaction of 4.0 mg of the MNP with 0.04 mmol of a PIB-X derivative in an alkane solvent like cyclohexane (Scheme 24). In these experiments, the MNPs were suspended in cyclohexane using sonication. Then 0.1 mL of 3% ammonium hydroxide was added. Initial studies showed this facilitated reactions of PIB-X derivatives with MNPs. We assessed the binding ability of terminally functionalized PIB oligomers **25, 26, 31, 49-56** to MNPs by monitoring the extent of magnetic nanoparticles (MNP) solubilization by periodically measuring the optical density of the reaction solutions over a 4 h period of sonication. In this analysis, samples were taken from the reaction mixture and subjected to centrifugation at 3200 rpm for 15 min. This removed poorly soluble particles from the solution. We then measured the optical density of the supernatant phase at 380 nm.

Scheme 24. Synthesis of Soluble Fe_3O_4 Nanoparticles Using Different Functionalized Polyisobutylene Ligands 25, 26, 31, 49-56[a]

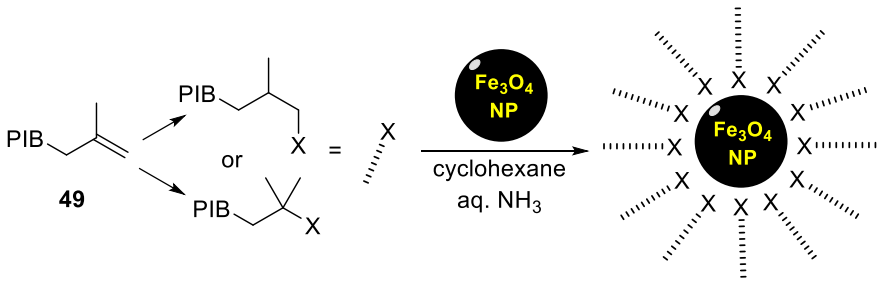

[a]X = 2,6-dimethylaniline (**50**), hydroxyl (**31**), thioacetate (**25**), thiol (**26**), carboxylic acid (**51**), phosphonic acid (**52**), hydroxamic acid (**53**), catechol (**54**), veratrol (**55**), phenol (**56**).

Our experiments initially used PIB-X derivatives that our group had prepared previously.[34] These PIB-X derivatives included the starting material PIB **49**, PIB-2,6-

dimethylaniline (**50)**, PIB-OH (**31)**, PIB-thioacetate (**25**), PIB-SH (**26**) and PIB-carboxylic acid (PIB-CO_2H) (**51**). The extent of solubilization of MNPs achieved in these studies with these functionalized PIB derivatives is shown in Figure 17a and 17b for PIB_{1000} and PIB_{2300}, respectively. These studies used an excess of a series of PIB-X derivatives with the same amounts of MNP in the same alkane solvent. The comparisons of PIB_{1000} and PIB_{2300} shown used equivalent amounts of these functionalized polymers. As shown in Figure 2, PIB alkene **49** showed weak binding to MNPs and little MNP solubilization as expected. Oligomers **50** and **31** were better at MNP solubilization than the commercially available **49**. Oligomer **25** was relatively ineffective at solubilizing MNPs. While PIB_{2300}-thioacetate effected some solubilization of MNPs, the PIB_{1000}-thioacetate was less effective than a PIB_{1000}-thiol **26** whose relatively good binding to MNPs resembles that reported in literature using thiol terminated polystyrene to stabilize and solubilize nanoparticles.[13,121] The carboxylic acid-terminated oligomer **51** was one of the better ligands in these initial experiments as shown in Figure 17. This is consistent with earlier work that has used succinic acid terminated polyisobutylene as a ligand.[124]

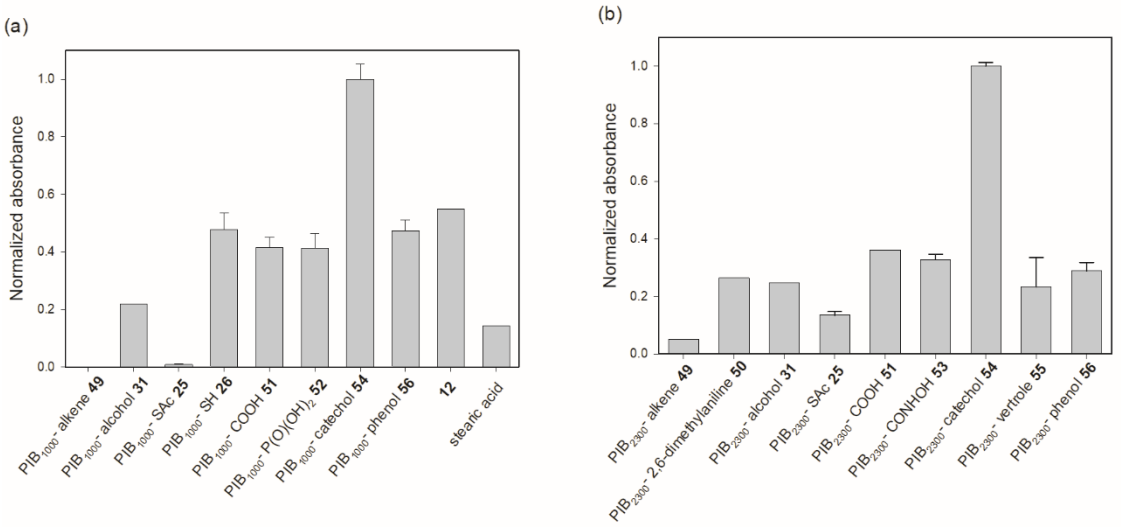

Figure 17. The comparison of UV-Visible spectroscopic absorbance of the supernatant. (a) PIB_{1000}-bound ligands and low molecular weight analogs. (b) PIB_{2300}-bound ligands.

In subsequent experiments, we prepared PIB oligomers with phosphonic acid (**52**), hydroxamic acid (**53**), catechol (**54**), veratrole (**55**), and phenol (**56**) end groups. These groups are all known to be good ligands for metals including iron. The results of these studies too are shown in Figure 17. These results show that catechol terminal groups are superior at effecting MNP solubilization in these experiments.

As noted above, prior studies have used fatty acids and fatty acid derivatives to modify and solubilize MNPs in hydrocarbons. To show if PIB is more effective at solubilizing MNPs, we compared the extent of solubilization of MNP by excess **51** to the solubilization of MNPs by excess stearic acid. The result as shown in Figure 17 was that the PIB derivative was roughly twice as effective in these solubilization experiments that used excess hydrophobic ligands. We also prepared a low molecular catechol-terminated stearic acid derivative **57** and compared it to the catechol-terminated PIB derivative **54**.

Again, the PIB bound species afforded a *ca*. 2-fold greater MNP solubilization than a smaller hydrophobic group. We ascribe this increased solubilization with PIB derivatives to the larger alkyl group of PIB ligands versus the smaller alkyl groups of stearic acid and **57**. Finally, we compared PIB_{1000} oligomers with PIB_{2300} oligomers. Those studies showed only modest differences in the extent of solubilization of MNPs with excess PIB-X. However, while PIB_{1000} and PIB_{2300} oligomers were comparable on a molar basis in solubilizing MNPs, subsequent work showed that PIB_{1000}-catechol could produce higher concentrations of MNP nanoparticles in heptane than PIB_{2300}-catechol.

Our original hypothesis was that the phase selective solubility of PIB derivatives could allow us to make MNPs highly soluble in alkanes and other weakly polar solvents. To see if we could achieve this goal, we quantitatively determined how much MNP we could dissolve in heptane using both PIB_{1000}- and PIB_{2300}-catechol. These studies included optimizing the concentration of soluble modified MNPs using different PIB-catechol/MNP weight ratios as well as determining the polymer loading in the resulting materials as shown in Table 5.

Table 5. TGA Studies of the Effects of Changing the Weight Ratio of MNP/PIB-Catechol on the MNP Loading of a Heptane Soluble PIB-Grafted MNP[a]

Entry	PIB-Catechol (M_n)	MNP/PIB-catechol (g/g)	Separation Method	Starting MNP Solubilized (%)	PIB in the Magnetic Oil or Insoluble Solids (%)	
					oil	solid
1	1000	1.0 : 1.0	A	32	71.9	11.3
2	1000	0.50 : 1.0	A	20	86.8	9.5
3	1000	0.25 : 1.0	A	46	89.4	8.8
4	1000	0.10 : 1.0	A	56	87.6	8.7
5	1000	0.50 : 1.0	B	40	80.5	7.2
6	1000	0.33 : 1.0	B	35	83.1	8.0
7	2300	0.43 : 1.0	A	36	77.6	9.1
8	2300	0.22 : 1.0	A	28	87.2	10.3
9	2300	0.11 : 1.0	A	34	93.3	9.6
10	2300	0.04 : 1.0	A	52	92.2	7.6
11	2300	0.43 : 1.0	B	35	79.5	12.6

[a]Method A used a magnet and repeated washings to differentiate soluble vs. insoluble PIB-modified MNPs. Method B used repeated centrifugations to differentiate soluble vs. insoluble PIB-modified MNPs. The oil phase was the material isolated after removing cyclohexane from the combined cyclohexane supernatant phases isolated using either method A or B. The insoluble solid was residual material that never dissolved. While it did form a suspension in cyclohexane, the suspensions were not stable in the presence of a magnet or upon centrifugation at ambient temperature.

These experiments aimed at optimizing the concentration of solubilized MNPs used 0.2-1.0 g of MNP with 1 mmol of oligomer **54** (i.e. 1.0 g of PIB_{1000}-catechol or 2.3 g of PIB_{2300}-catechol) in 25 mL of cyclohexane. Sonication was carried out for 75 min followed by 12 h of stirring at 40 ^{o}C. The MNPs that dissolved or formed a stable solution

were then isolated in one of two ways. Method A trapped less soluble MNPs with a magnet (a 6.3 cm^3 cube, surface gauss: 5129 G).

While it was difficult to visually see that some less soluble material was separated by the magnet because of the dark color of the mixture, decantation led to a solution and a recovered solid. More alkane was added to the recovered solid. Sonication again formed a suspension that was again treated with a magnet. A second decantation led to a slightly less colored supernatant. Some solid still remained. This process was repeated as many times as necessary until the supernatant after treatment with a magnet was free of MNPs based on its clarity. The supernatant phases from each cycle were then combined and the alkane was removed at reduced pressure to obtain a dark brown-black viscous oil that was magnetically responsive suggesting it contained MNPs. The final insoluble solids that no longer yielded any soluble material on treatment with an alkane solvent were recovered and were dried at reduced pressure. These two fractions of PIB-modified MNPs differ in that the magnetic oil that is soluble has a higher loading of PIB (cf. Table 5). The insoluble magnetic solids typically contained only 10% of less by weight of PIB. While these MNPs with lower PIB loadings can be dispersed in solvents using ultrasound, their lower solubility and greater magnetic susceptibility leads them to form separable precipitates either in the presence of a strong magnetic field or during centrifugation. The modified MNPs in the soluble magnetic oil have a much higher loading for PIB groups (typically >80 wt%) and are completely soluble in the alkane. This solubility leads to a weaker attraction of the supernatant solution to the magnet due to lower concentration of MNPs (cf. the discussion associated with Figure 24, *vide infra*). Thus, we were able to trap the

lightly grafted MNPs using a magnet while pouring away the dilute solutions to successfully separate the insoluble particles with the lower ca. 10 wt% PIB loading from the highly soluble particles (ca. 80 wt% PIB loading).

This insoluble magnetic solid and the heptane soluble magnetic oil isolated from the combined supernatant phases visually had different appearances. The oil was dark brown and the solid was black. Another difference was that while both materials can be dispersed in alkanes and other nonpolar solvents, the dispersions of the insoluble magnetic solid were not stable. Dispersions of the insoluble solids in alkanes were not stable to centrifugation or an external magnetic field. The dispersions formed from the magnetic oil however behave like solutions and are visually stable for extended time (*vide infra*) and stable to centrifugation and are stable to the application of an external magnet.

We also used a second method – Method B – to separate solubilized MNPs (the magnetic oil) from insoluble MNPs. This method used the same synthetic protocol used above but separated soluble MNPs from less soluble MNPs by centrifugation. In this case, the modified MNPs were dispersed in 30 mL of heptane and centrifuged at 4000 rpm for 10 min. After decanting the supernatant, the mixture was dispersed in a second 30 mL portion of heptane and centrifuged again. This procedure was repeated until the supernatant layer was clear. Typically, this produced seven supernatant phases which were combined and concentrated to provide the highly soluble magnetic oil fraction. The insoluble solid fraction could be suspended in an alkane solvent with sonication like the insoluble fraction isolated using method A. The insoluble solids isolated in method B like those isolated in method A did not form stable suspensions and were always separable

from solvent by centrifugation. The total amounts of PIB-modified nanoparticles isolated in methods A and B were generally comparable.

These experiments provided us with 22 samples of magnetic oil or insoluble solids. We analyzed each of these samples by thermal gravimetric analysis (TGA). Under these analysis conditions, the PIB catechol ligands quantitatively decompose. Thus, the residual solid in these analyses was iron oxide and we could use these experiments to determine the loading of MNP in the soluble magnetic oil and in the insoluble magnetic solid. The results of these TGA analyses are summarized in Table 5. While we did not carry out similar studies with all the other PIB-X derivatives, we did examine PIB_{1000}-phenol-modified MNPs by TGA. As expected based on the results in Figure 17, PIB_{1000}-phenol was a poorer ligand as solubilizing MNPs than PIB_{1000}-catechol. This TGA curves is shown in Figure 18. Mass balances showed that >90% of the amount of the original starting magnetic nanoparticle was typically accounted for in these TGA analyses of the highly soluble oil phase and the insoluble solid phase fractions.

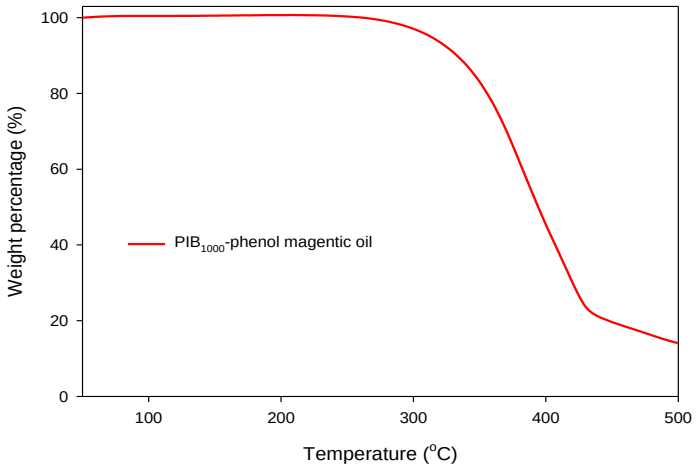

Figure 18. TGA analysis of the PIB_{1000}-phenol-modified magnetic oil.

When an equal mass of PIB_{1000}-catechol and MNP were used in the grafting reaction and Method A was used for separation, the amount of polymer in the insoluble magnetic solids was ~11% by weight (Table 5, entry 1). When less PIB_{1000}-catechol was used in the reaction (Table 5, entry 2-4), the amount of polymer bound to the insoluble solids decreased slightly. The soluble magnetic oils generally had high loadings of the PIB graft. While there was some variation depending on the starting weight ratio of PIB-catechol/MNP and method used, the PIB loading on the soluble oil was always >70% by weight. By using roughly equivalent amounts of MNP and PIB-catechol (i.e. a 1:1 g/mmol ratio), 20-30% of the soluble magnetic oil was MNP. As much as 56% of the starting MNP nanoparticles could be solubilized with PIB-catechol by using more PIB-catechol. However, the concentration of MNP in the soluble material then dropped to *ca.* 10% by weight in these cases. The procedures used to solubilize these MNP proved to be robust and have been repeated both by Raquel Khanoyan, an undergraduate researcher in our

group and by Dr. Manyam Praveen Kumar and Professor Sherzod Madrahimov at Texas A&M Qatar.

The size and the shape of the modified MNPs were analyzed by TEM. Particles size distribution of resolved particles in these images (Figure 19) were carried out using ImageJ software and are shown in histograms in Figure 20. The particle size analyses for ungrafted MNPs showed these particles had an average diameter of 11.1 ± 2.4 nm (after counting over 78 nanoparticles). However, most particles were agglomerated as is apparent in the micrograph of his material. In contrast, the PIB-catechol modified magnetic solid that was partially modified with PIB groups appeared to have a better dispersion of MNPs (Figure 19b). In this case, analysis of 109 nanoparticles using the same ImageJ software led to an estimate for the average particle diameter of 10.7 ± 2.7 nm. We believe the agglomerated particles that were still observed result from the relatively low loading of PIB ligands on these poorly soluble modified particles. Figure 19c and 19d show that the nanoparticles of PIB_{2300}-catechol bound magnetic oil were better dispersed. In these cases, particle size analysis of 155 nanoparticles showed an average particle diameter of 10.3 ± 3.0 nm. While there is still some aggregation of MNPs in Figure 19d, we believe this aggregation reflects the sample preparation process. Indeed, an even better dispersion is seen in a TEM analysis of a solution of the soluble PIB-modified MNPs in a 1758 Da nonvolatile poly(α-olefin) oil (Figure 26a, *vide infra*).

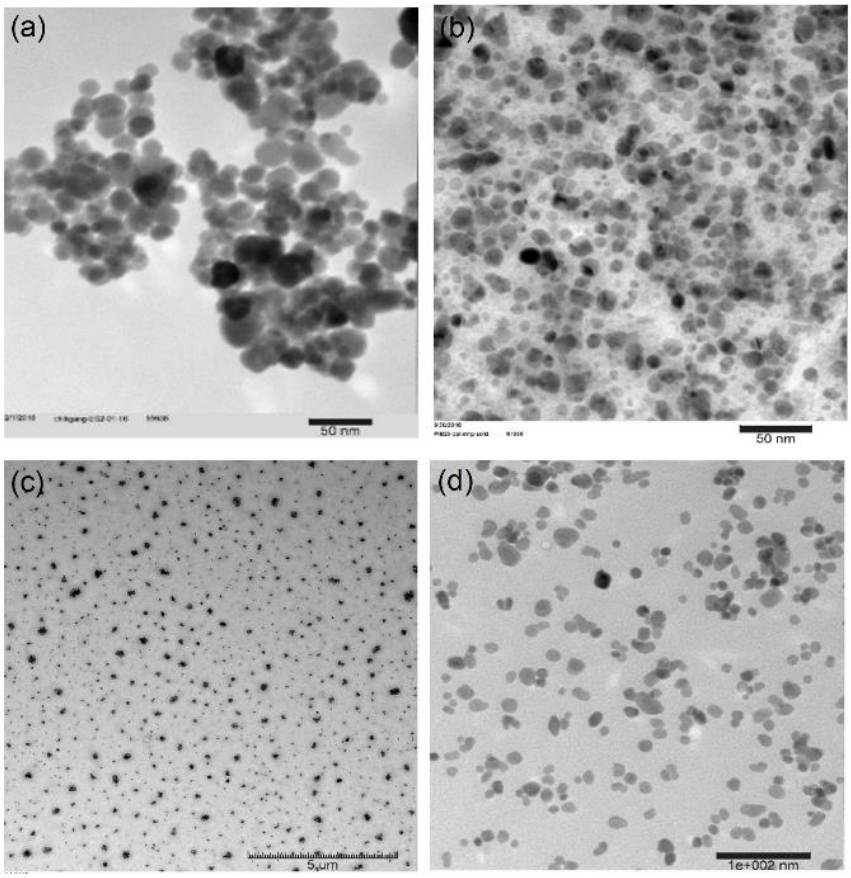

Figure 19. TEM images of as synthesized iron-oxide nanoparticles. (a) Unfunctionalized MNPs under 250K magnification. (b) PIB_{2300}-catechol bound magnetic solid under 250K magnification. (c) PIB_{2300}-catechol bound magnetic oil under 15K magnification. (d) PIB_{2300}-catechol bound magnetic oil under 200K magnification**.**

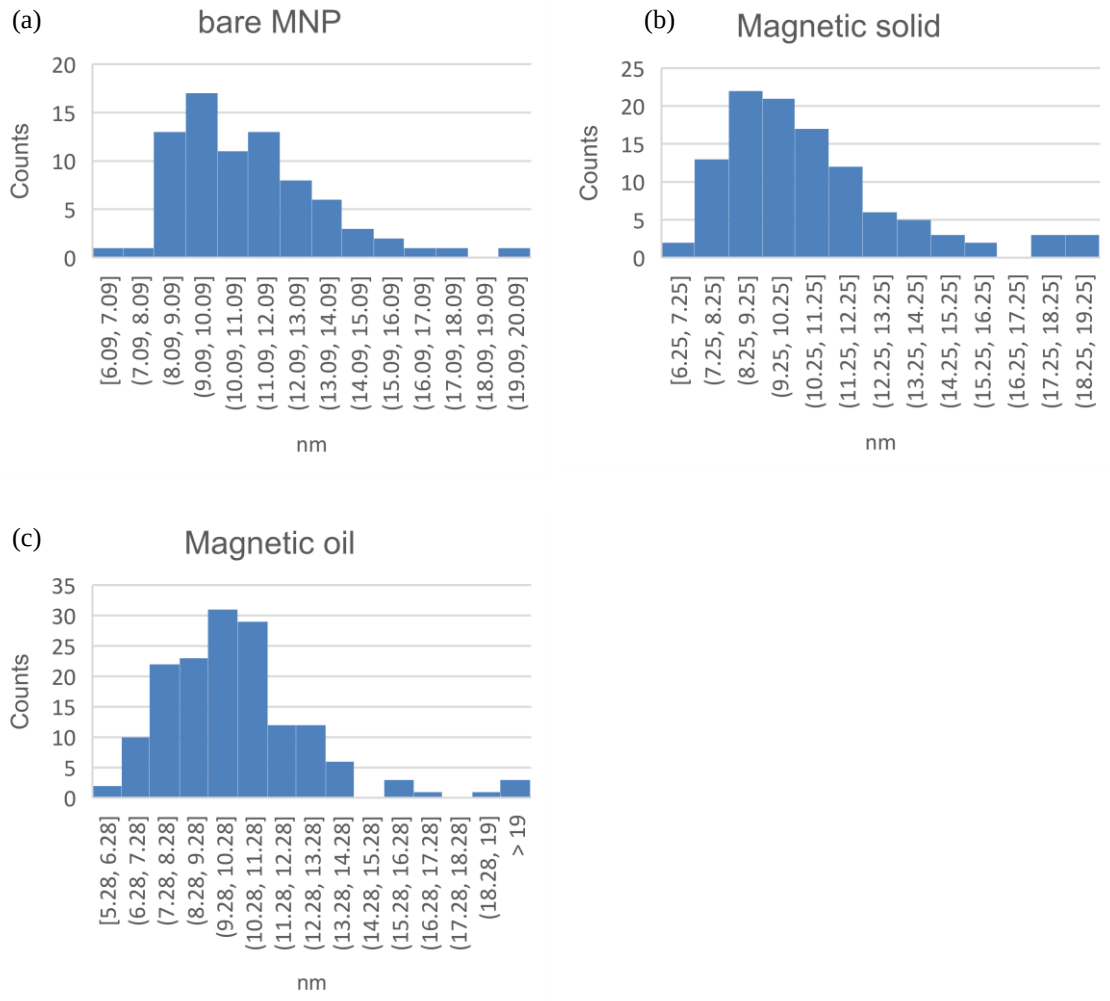

Figure 20. Particle size distribution diagrams. (a) Bare MNP showed 11.1 ± 2.4 nm diameter after 78 particles were counted. (b) The magnetic solid showed 10.7 ± 2.7 nm diameter after 109 particles were counted. (c) The magnetic oil showed 10.3 ± 3.0 nm diameter after 155 particles were counted.

While the magnetic separation and centrifugation methods used to prepare samples in Table 5 worked, these methods only afforded 0.5 – 1.0 g of the soluble magnetic oils. They were not very efficient for synthesis of larger amounts of PIB modified MNPs. Thus, we modified these methods so as to carry out multigram syntheses of modified MNPs.

These larger scale reactions used 10 g of starting MNPs and 10 g of PIB_{1000}-catechol or 5 g of starting MNPs and 11.5 g of PIB_{2300}-catechol in 250 mL of cyclohexane. Aliquots of these larger scale reactions were analyzed periodically over 48 h of sonication. As shown by the UV-Visible spectroscopy data in Figure 21, these larger scale reactions were completed within 24 h. After the completion of the reaction (24 h), the reaction mixtures were allowed to stand for an additional 24 h. During this period, a small amount of solid settled out. This solid was separated by filtration through filter paper. This filtration was carried out a second or third time if necessary until no black solid was observed on the filter paper. While this process removed most of the insoluble solid, some additional sediment was seen after the second 24 h standing. That small amount of sediment that formed after this second 24 h period was trapped with a neodymium magnet (a 6.3 cm^3-cube, surface gauss: 4716 G). The solution that was decanted from this solid did not form any further precipitate after standing for 2 months. This solution of soluble MNPs was then concentrated under reduced pressure affording *ca*. 15 g of a viscous magnetic oil. This modified procedure simplified the procedure for obtaining larger amounts of the desired heptane-soluble magnetic oil.

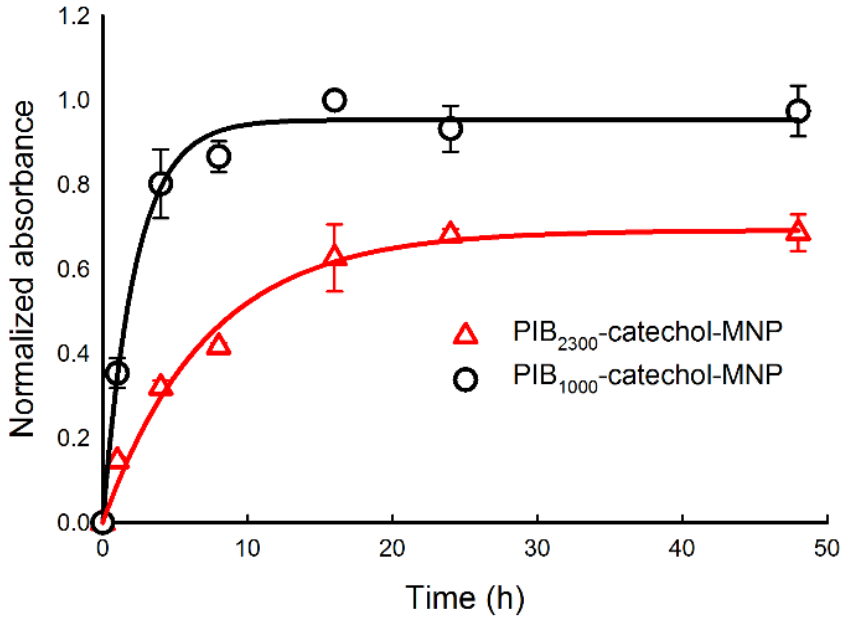

Figure 21. Plot of absorbance of the reaction mixture versus time when 10.0 g of PIB_{1000}-catechol with 10.0 g of MNPs and 11.5 g of PIB_{2300}-catechol and 5.0 g of MNPs were used for the grafting reaction.

The product of this larger scale synthesis was analyzed by TGA using the same procedures used to analyze the various samples in Table 5. The results are shown in Figure 22. Here we show TGA analyses of PIB_{2300}-alkene, PIB_{2300}-catechol, PIB_{1000}-modified magnetic oil, PIB_{1000}-catechol modified magnetic solids, PIB_{2300}-modified magnetic oil, and PIB_{2300}-catechol modified magnetic solids. These results show that the PIB_{1000}-modified magnetic oil obtained from this larger scale synthesis contained 32 wt% of magnetic nanoparticles and PIB_{2300}-modified magnetic oil contained 26 wt% of magnetic nanoparticles. In the case of the PIB_{2300}–catechol modified MNP and the starting PIB_{2300}-catechol, the TGA analysis suggested that there was some residual heptane solvent that volatized at *ca.* 150 °C. The MNP contents of these two materials are comparable to the

MNP content of the magnetic oils prepared in Table 5. The insoluble PIB_{1000}-catechol modified magnetic solid and PIB_{2300}-catechol modified magnetic solids collected were also similar in composition to samples prepared with similar weight ratios of MNP/PIB-catechol in Table 5.

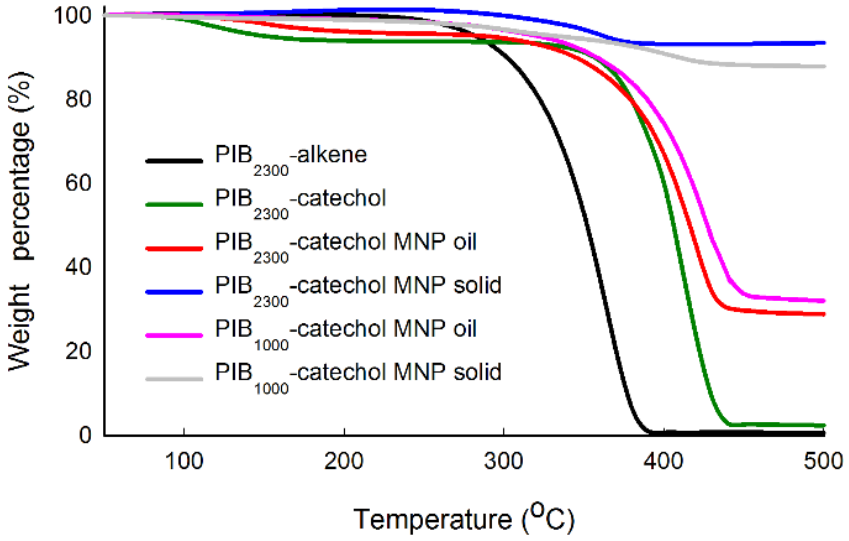

Figure 22. TGA comparison of PIB_{2300}-alkene, PIB_{2300}-catechol, PIB_{1000}-modified magnetic materials and PIB_{2300}-modified magnetic materials.

Portions of the magnetic oil prepared in this larger scale synthesis were used to test the stability of the PIB-modified MNPs. In these experiments, 3 mg of the magnetic oil was dissolved in 10 mL of cyclohexane. The resulting solution was allowed to stir with either water or with a basic or acidic aqueous solution. The optical density of the cyclohexane phase was monitored periodically and the results are shown in Figure 23. In the case of water, the MNP solution was stable over a period of at least 2 months (Figure 23a). The solution was also stable when it was stirred with a 1.0 M NaOH aqueous

solution. Samples of the cyclohexane phase showed no loss of optical density (Figure 23b). We dissolved 0.5 mmol of catechol in 5 mL of 1.0 M NaOH aqueous solution and stirred this solution with the cyclohexane solution of PIB_{2300}-catechol modified MNPs. Again, no change in optical density was seen over 1 week (Figure 23c). However, the cyclohexane solution of PIB_{2300}-catechol modified nanoparticles did decompose slightly over 2 weeks of stirring with 1 M aqueous HCl (Figure 23d). In this case, there was a *ca.* 30% decrease in optical density suggesting that either the PIB ligands were detached from the MNPs or that the MNPs decomposed in the presence of a strong acid.

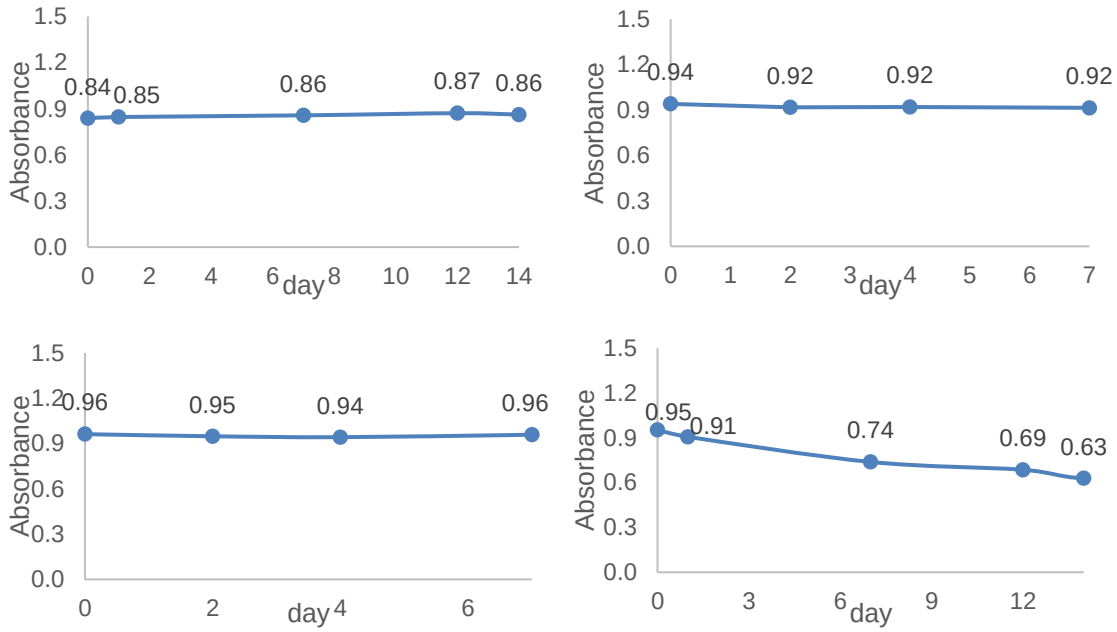

Figure 23. The UV-Visible spectroscopic absorbance of the heptane solution over time. (a) PIB_{2300}-catechol modified magnetic oil in heptane solution was allowed to stir with 10 mL of DI water. (b) PIB_{2300}-catechol modified magnetic oil in heptane solution was allowed to stir with 10 mL of 1M NaOH solution. (c) PIB_{2300}-catechol modified magnetic oil in heptane solution was allowed to stir with 10 mL of 50 mM of catechol in NaOH solution. (d) PIB_{2300}-catechol modified magnetic oil in heptane solution was allowed to stir with 10 mL of 1M HCl solution.

The magnetic oils isolated in multigram scale syntheses of PIB_{1000}-catechol modified MNPs were highly soluble in a variety of solvents. We tested this in various ways. For example, when an equal mass of the PIB_{1000}-catechol modified MNPs oil was mixed with an equal mass of heptane, we obtained a viscous solution. This dissolution process readily proceeds with simple stirring. No sonication is required. The resulting >50 wt% solution of PIB-modified MNP and heptane could be further diluted. We also explored the solubility of these PIB_{1000}-catechol modified MNPs in other organic solvents. We investigated this by making solutions of PIB_{1000}-catechol modified magnetic oil with several common organic solvents at a concentration of 100 mg/mL. The results that are summarized in Table 6 and in Figure 24 show that the magnetic oil is soluble in nonpolar and weakly polar solvents. Two other solvents – dichloromethane and 1,2-dichloroethane – initially dissolved the PIB_{1000}-modified MNPs. However, in these cases, some precipitate did form upon standing. The PIB_{1000}-modified MNPs were, as expected, insoluble in polar organic solvents. Similar results were obtained with the PIB_{2300}-modified MNPs. These studies suggest that the solubility of the magnetic oil is determined mainly by the intrinsic solubility of PIB.

Table 6. Solubility Test of the Magnetic Oil in Common Organic Solvents

Solvent	Solubility[a]	Solvent	Solubility
Hexane	Yes	THF	Yes
Heptane	Yes	Acetonitrile	No
Xylene	Yes	Ethanol	No
Toluene	Yes	Methanol	No
Cyclohexane	Yes	Ethyl acetate	No
Chloroform	Yes	Acetone	No

[a]A sample of 500 mg of PIB_{1000}-catechol bound magnetic oil was stirred with 5 mL of solvent and the resulting mixture's solubility was visually assayed.

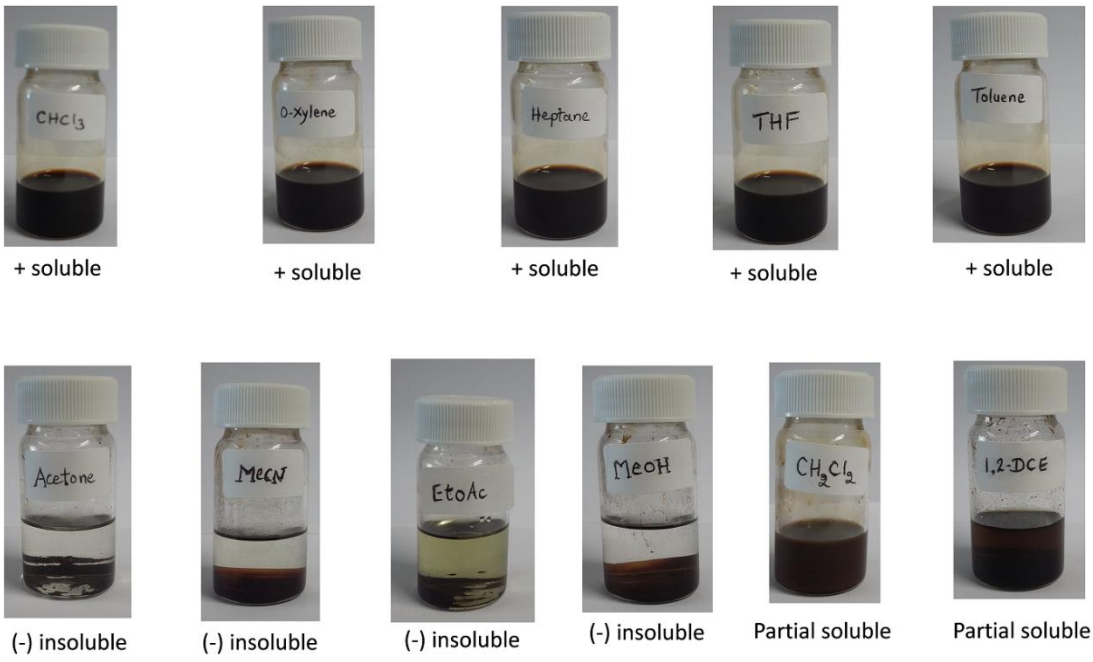

Figure 24. Solubility of the PIB_{1000}-catechol modified magnetic oil in organic solvents.

Our observation that the magnetic oils contained some hydrocarbon solvent even after extended exposure to vacuum suggested that the PIB grafts on these MNPs tenaciously entrain hydrocarbons. This led us to briefly explore the potential of these magnetic oils as agents for hydrocarbon sequestration.[138] Studies with a series of solutions with different weight percentages of the magnetic oil in heptane were used to visually measure the attraction of each of these solutions towards an external magnet. With as little as 1% by weight of the PIB_{2300}-catechol modified MNP dissolved in heptane, the heptane phase in its entirety was very strongly attracted toward the magnet when the magnet was placed at the side of the vial containing a biphasic mixture of the MNP in heptane and water (Figure 25). The same effect was seen for heptane solutions containing higher loadings of the PIB_{2300}-catechol modified MNPs. Even when the PIB_{2300}-catechol modified MNP content was 0.5 wt%, the effect was still noticeable though the separation was no longer as effective in this latter case. Notably, the external magnet effected the entire solution – the magnet does not separate the PIB-catechol modified MNPs from heptane over a 100-fold range of the concentration of the PIB_{2300}-catechol modified MNP in heptane. This process could be repeated multiple times over the course of several weeks. Other MNPs like the PIB-CO_2H modified MNPs had a similar effect.

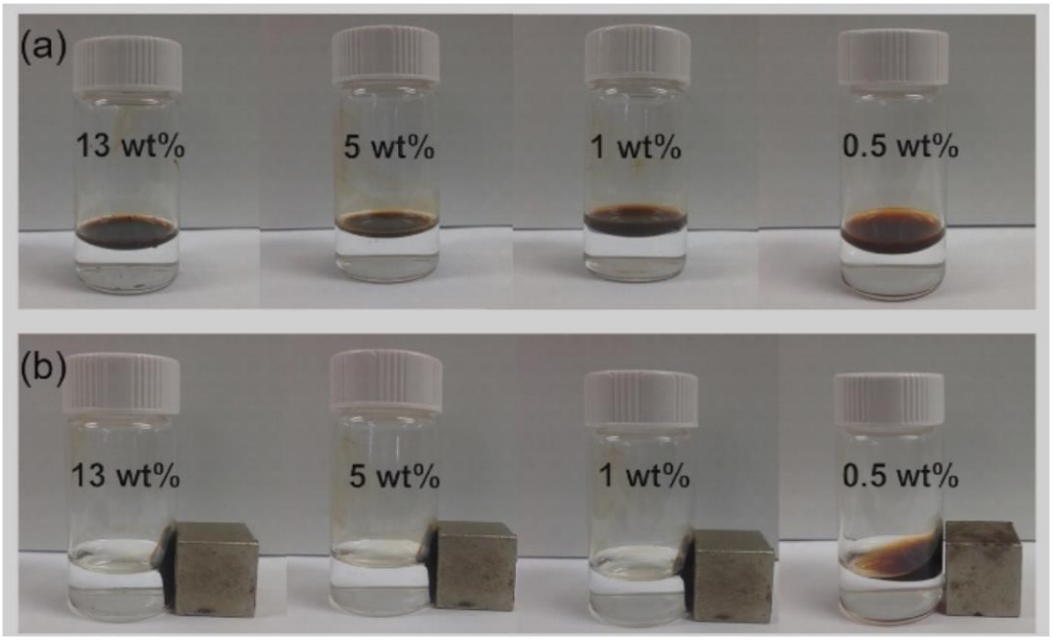

Figure 25. The removal of heptane from heptane/water mixture. (a) Mixtures of PIB_{2300}-catechol magnetic oil in heptane and water. (b) The magnetic heptane layer was trapped by a magnetic force.

The high solubility of the magnetic oil in heptane led us to explore the potential of dissolving this viscous PIB-modified MNP magnetic oil in polyolefins. We found that a mixture of the magnetic oil in a polyethylene oligomer[139] (M_n = 400 Da) in a weight ratio 1 to 10 formed a homogeneous solution with gentle swirling at 90 ºC. Cooling this solution led to a brownish wax. After cryogenic grinding, a magnetically susceptible dark brown polyethylene powder was obtained. Poly(α-olefin) oligomers (PAOs),[140,141] that are commercially available lubricants from ExxonMobile, have also been used as substitutes for heptane in other work in our group.[142] They too are good solvents for this viscous PIB-modified MNP magnetic oil. With heating and swirling, both PAO 10 (M_n = 687 Da) and PAO 40 (M_n = 1758 Da) formed dark brown viscous solutions. This was in contrast to

efforts to mix either unmodified MNPs or the heptane insoluble magnetic solid with PAOs. In these cases, a similar mixture containing 1 g of MNP or the insoluble magnetic solid with MNPs that have ca. 10% PIB loading did not form a solution. A precipitate of the MNP was present in the mixture even after 1 h of heating and stirring at 100 ^{o}C.

This visually homogeneous viscous PIB-modified MNP magnetic oil/PAO solution was further analyzed by TEM. In this case, a solution of the viscous PIB-modified MNP magnetic oil in PAO 40 (M_n = 1758 Da) was analyzed. As shown in Figure 26a, the MNPs were well dispersed. Using ImageJ software, the particles had an average diameter of 10.7 ± 3.3 nm (after counting over 115 nanoparticles) (Figure 27a). The dispersion of MNPs in this case can also be compared to the dispersion of MNPs in heptane in Figure 19d. The more uniform dispersion of MNPs in this nonvolatile PAO 40 polymer solvent we believe results from PAO being a nonvolatile medium that minimizes aggregation of MNPs on the grid while the solvent evaporated during the preparation of TEM sample. We also examined the poorly soluble magnetic solid in PAO 40. This image shown in Figure 26b was also analyzed using ImageJ software and the particles had an average diameter of 10.9 ± 3.0 nm (after counting over 74 nanoparticles) (Figure 27b). In this case, apparent aggregation was seen in the TEM image with the visually observed insolubility of MNPs with sufficient PIB solubilizing groups in both heptane and this PAO solvent.

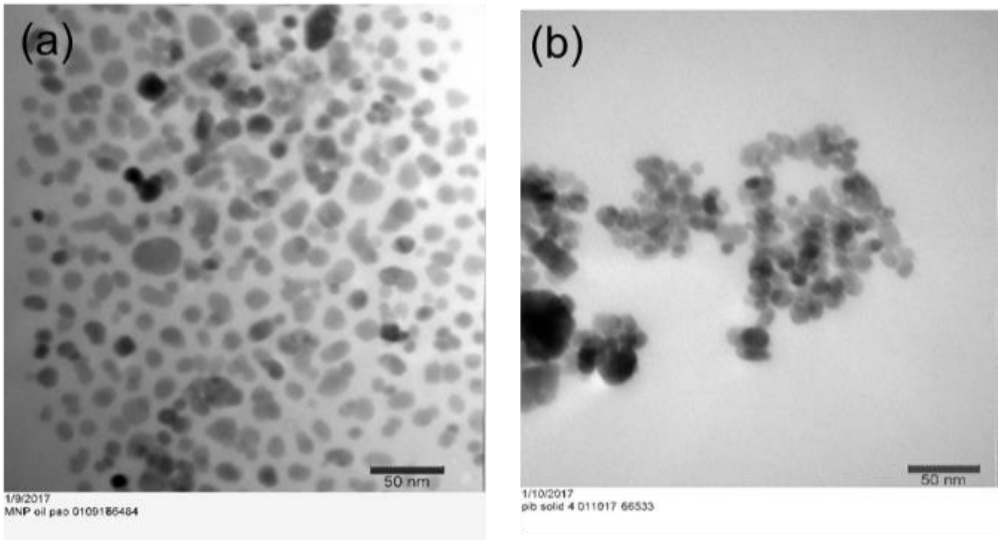

Figure 26. TEM images of magnetic nanocomposites with PAO 40. (a) A mixture of 10 wt% of magnetic oil in PAO 40. (b) A mixture of 10 wt% of magnetic solid in PAO 40.

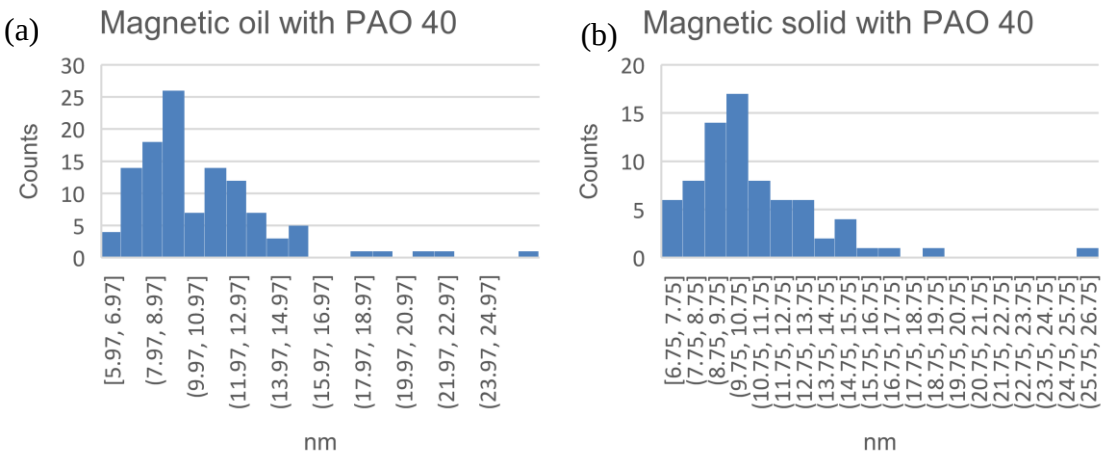

Figure 27. Particle size distribution diagrams of MNP in PAO 40. (a) The magnetic oil in PAO 40 showed 10.7 ± 3.3 nm diameter after 115 particles were counted. (b) The magnetic solid in PAO 40 showed 10.9 ± 3.0 nm diameter after 75 particles were counted.

We also extended this work and tried the grafting reactions under a biphasic condition. A mixture of 0.5 g of MNP and 0.5 g of PIB_{1000}-catechol in 15 mL of heptane and 15 mL of water was sonicated for 12 h. After the reaction, a biphasic mixture formed and the heptane layer became dark brown, indicating the successful solubilization of MNP in heptane. We found that this biphasic mixture allowed us to quickly isolate the soluble PIB-modified MNP because of the clear separation of two phases. After the aqueous layer was washed with heptane three times, it was found that the brown color in the heptane layer became substantially lighter. And the separation procedure was done within 1 h. The heptane layers were then combined and concentrated under reduced pressure using a rotary evaporator as a dark brown and magnetically susceptible oil. Although further quantification of the amounts of MNPs in this oil was not attempted, this result showed that the biphasic condition has the advantage of quickly isolating the PIB_{1000}-catechol modified MNP.

Conclusions

We successfully synthesized a series of terminally functionalized PIB oligomers that chemically bind to and solubilize iron oxide magnetic nanoparticles. We found that among the PIB ligands we tested, PIB oligomers functionalized with terminal catechol groups were the best ligands for solubilizing MNPs. Using this chemistry, we developed several methods to prepare solubilized MNPs. A method that uses a combination of magnetic separation and filtration was shown to yield soluble MNPs on a *ca.* 15 g scale. This separation method allowed us to solubilize as much as 56% of the starting MNPs as

oils with 10-30 wt% MNP content. These oils were soluble at concentrations of >50% by weight in organic solvents including alkanes. We also showed that the viscous PIB-modified MNP magnetic oil that is highly soluble in heptane dissolves in polyolefins. Poly(α-olefins) oils with M_n values of 687 and 1758 Da readily dissolve these modified MNPs. Similarly, a low melting point PE wax dissolved these same PIB-modified MNPs at 90 ºC leading to a magnetically susceptible PE powder on cooling and cryogenic grinding. Finally, other experiments showed that the PIB-bound magnetic oil at loadings as low as 1 wt% magnetically separated an excess of an alkane solvent from water. Further work to explore PIB oligomer modification of other types of nanoparticles and to study the uses of such modified nanoparticles is discussed in Chapter V.

CHAPTER V

POLYISOBUTYLENE OLIGOMERS AS TOOLS FOR NANOMATERIAL SOLUBILIZATION

Introduction

Silica nanoparticles have received great attention because of their wide range of applications in the electrical,[143] medical,[144] and mechanical fields.[145] However, while these nanoparticles have many applications, to use them effectively requires that these nanoparticles be appropriately accessible for use in modifying the materials involved in these applications. Tethering groups onto silica nanoparticles is a way to achieve this goal. Likewise, tethering organic groups onto silica nanoparticles is a method to improve the dispersibility of silica nanoparticles in organic solvents and to increase the stability of such dispersions.[146] Many different approaches have been studied to functionalize silica nanoparticles and to graft polymers onto these nanoparticles. One of the most common methods to functionalize silica nanoparticles uses triethoxysilane derivatives. For example, 3-aminopropyltriethoxysilane can be used to functionalize the surface of silica nanoparticles with amine groups. The resulting aminated silica nanoparticles have better dispersibility in organic solvents such as ethanol and toluene than unfunctionalized nanoparticles. However, these systems displayed poor stability and nanoparticles precipitated when the dispersion is left undisturbed for a short period of time.[147] This lack of stability is likely due to the short organic chains not being able to keep the silica nanoparticles solvated and dispersed in these organic solvents.

Polymers are an alternative to simple functional groups and have also been used to modify silica nanoparticles to alter their dispersbility and the stability of their dispersions. For example, polymers have been used as grafting reagents to improve the solubility of silica nanoparticles in organic solvents.[148] The dispersibility of these polymer supported-silica nanoparticles in organic solvents is usually dependent on the solubility of the polymer support in these solvents. For example, Fuji reported the synthesis of poly(ethyleneglycol)-supported silica nanoparticles.[14] These nanoparticles were well dispersed in *N*, *N*-dimethylacetamide. Benicewicz and coworkers also reported several syntheses of polymer-supported silica nanoparticles by radical addition-fragmentation chain-transfer (RAFT) polymerization on the surface of silica nanoparticles. For example, poly(methylmethacrylate)-attached silica nanoparticles[20] are soluble in dimethylsulfoxide (DMSO) and polyisoprene-attached silica nanoparticles[18] are soluble in tetrahydrofuran (THF).

Our success using polyisobutylene (PIB) to solubilize magnetic nanoparticles (MNPs) in heptane and nonpolar polymers[149] suggested to us that PIB could be another polymer used to solubilize silica nanoparticles in nonpolar solvents. Here, several approaches of functionalizing silica nanoparticles with PIB are discussed. This involves the treatment of silica nanoparticles with PIB derivatives as was done for MNPs as well as the use of PIB derivatives to functionalize amine terminated and thiol terminated silica nanoparticles. Several PIB derivatives were prepared and several PIB derivatives were used in my studies of silica nanoparticle solubilization in heptane. They include PIB terminated with trialkoxysilane groups, alkene-terminated PIB, thiol-terminated PIB,

carboxylic acid-terminated PIB, and carbonyl ethyl carbonate-terminated PIB. While studies of other aminated nanoparticles were not completed, I did also prepare aminated multiwalled carbon nanotubes (MWNTs) and the chemistry I used for modification of MWNTs with polyethylenimine is also reported.

Result and discussion

We started the work by functionalizing silica nanoparticles directly with commercially available lipophilic reagents to test the dispersibility and dispersion stability of the resulting silica nanoparticles in heptane. In accordance with a reported procedure,[96] octadecyldimethylchlorosilane **37** was allowed to react with the hydroxy groups on the surface of intrinsic silica nanoparticles to form a silyl ether linkage as shown in Scheme 25 (a). The resulting silica nanoparticles were well dispersed in heptane but the dispersions were not very stable. A precipitate formed after the mixture was left undisturbed for 30 min. The solution remained cloudy after precipitation which suggested that some silica nanoparticles were still dispersed in the heptane solution. The mixture of the solid and the cloudy solution was centrifuged to separate the precipitate from the supernatant. The heptane was then removed from the cloudy supernatant under reduced pressure using a rotary evaporator to give a waxy powder. Both the precipitate and the waxy powder were analyzed by thermal gravimetric analysis (TGA) and the results are summarized in Table 7. It was found that the white waxy powder had 85.4 wt% of mass loss and the precipitate sample had 24.3 wt% of mass loss. These mass losses were presumed to be due to the degradation of organic grafting on these nanoparticles during the temperature gradient.

These results showed that the grafting reaction was successful and some of the silica nanoparticles were solubilized. However, using this method 19 wt% of the original mass of silica nanoparticles was solubilized in heptane. Based on my experience in solubilizing MNPs, I ascribe the poor solubilization of silica nanoparticles was to the relatively short length of the lipophilic chain of octadecyldimethylsilyl ether and I presume that a 17-carbon chain is not long enough to solubilize silica nanoparticles in heptane. This suggests that using ligands with longer lipophilic chains would allow us to solubilize more silica nanoparticles in heptane.

Scheme 25. Grafting intrinsic silica nanoparticles with (a) octadecyldimethylchlorosilane 37 and (b) PIB-attached triethoxysilane 58

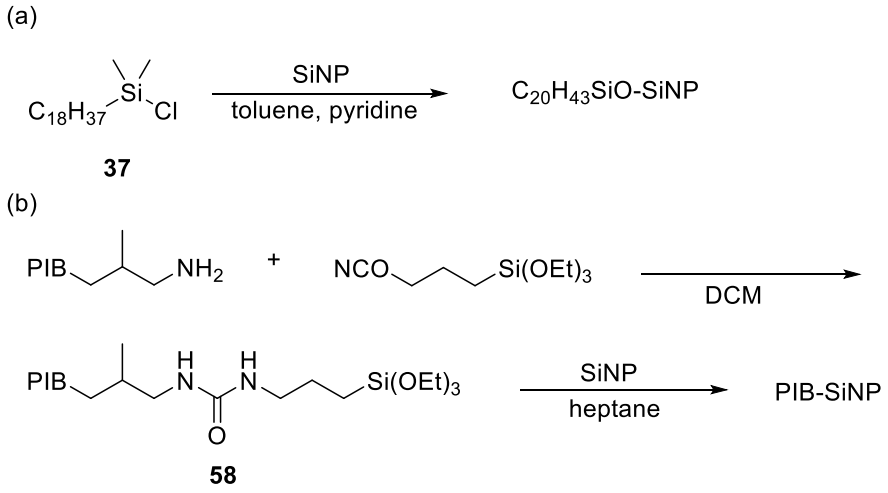

Next, we synthesized PIB-bound triethoxysilane **58** as shown in Scheme 25(b). PIB-bound amine, synthesized by following the literature procedure our group reported previously,[73] was allowed to react with 3-isocyanatopropytriethoxysilane to yield **58** by the formation of urido bond as evidenced by two peaks at 1636 and 1570 cm^{-1} in the IR

spectrum of the product. The triethoxysilyl terminated PIB **58** was then grafted to silica nanoparticles by allowing the hydroxy groups on the silica nanoparticles to react with the triethoxysiliyl group on **58**. 100 mg of silica nanoparticles and 0.5 mmol of **58** were mixed in 20 mL of heptane and the resulting mixture was sonicated at 40 ^{o}C for 12 h. After 12 h, the color of the heptane solution turned from transparent to opaque indicating silica nanoparticles were solubilized. The reaction mixture was then centrifuged to separate any insoluble silica nanoparticles from the cloudy supernatant dispersion of nanoparticles. Unlike the case with the octadecyldimethylsily modified silica nanoparticles, the precipitate isolated by centrifugation readily reformed as suspension on physical agitation. As a result, the centrifugation/decantation process was repeated three times to ensure complete separation of the insoluble precipitate and the supernatant. After each centrifugation, *ca*. 80 vol% of supernatant was removed and the same amount of fresh heptane was added to the residual mixture. The opaqueness of the resulting solution became less during each cycle. After three heptane treatments, the supernatant phases were combined and then concentrated under reduced pressure using a rotary evaporator to give a colorless viscous oil. Both the oil and the precipitate were then analyzed by TGA and the results are also summarized in Table 7. As shown in Table 7 entry 2, the colorless oil had 79.7 wt% of mass loss and the precipitate sample had 65.5% of mass loss. The high percentage of mass loss from the precipitate suggested the success of grafting PIB onto silica nanoparticles. 32 wt% of silica nanoparticles of the original mass of silica nanoparticles used for the grafting reaction were solubilized in heptane. If we compare the 32% of silica nanoparticles solubilized by **58** with the 19% solubilized by **37**, these results

indicate that PIB-grafting with triethoxysilyl groups is a better method to solubilize silica nanoparticles in heptane than the attachment of octadecyldimethylsilyl groups. However, if we compare the 32% of silica nanoparticles solubilized by **58** with the 56% of MNP solubilized by a catechol-terminated PIB, which was discussed in the last chapter, when 0.1 g of MNPs and 1.0 g of catechol-terminated PIB were used for the grafting reaction, this suggests that the amount of silica nanoparticles solubilized by a PIB-supported ligand can be still optimized. This optimization can be conducted by varying the ratios of silica nanoparticles with **58** to test whether the solubilization of silica nanoparticles can be improved. This might reasonably increase the amounts of silica nanoparticles solubilized since these silica nanoparticles are 20 nm in diameter. The MNPs previously used in the last chapter were 9 nm in diameter and the 56 wt% solubilization for those MNPs was achieved by using a 1/10 weight ratio of MNP/PIB-bound catechol so a similar 1/10 weight ratio of silica nanoparticles/PIB-bound ligand may well increase the extent of silica nanoparticles solubilization and labeling. We also noted that when unfunctionalized silica nanoparticles were used, the effectiveness of ligands in the solubilization of these nanoparticles was dependent on the reactivity of intrinsic hydroxy groups on the silica nanoparticles. This was seen when silica nanoparticles were treated with either a vinyl-terminated PIB or a hydroxy-terminated PIB. In either case, visually all of the silica nanoparticles precipitated after sonication and the solution was clear, indicating these two ligands were not able to solubilize silica nanoparticles. To expand the versatility of solubilizing silica nanoparticles with different ligands, we prepared silica nanoparticles

with different functionalities and then grafted the functionalized silica nanoparticles with a variety of PIB-supported ligands.

Table 7. TGA results of **37** and **58** functionalized silica nanoparticles

Entry	Ligand	SiNP/ligand (g/mmol)	Starting SiNP[a] Solubilized (%)	Organic Mass in the Soluble or Insoluble SiNP (%)	
				oil	solid
1	**37**	0.2 : 1.0	19	85.4	24.3
2	**58**	0.1 : 0.5	32	79.7	65.5

[a] It was calculated by dividing the weight of silica nanoparticles in the oil with the weight of original silica nanoparticles used for the grafting reaction. The weight of silica nanoparticles in the oil was obtained by multiplying the weight of oil, which is not listed here, by the weight percentage of silica nanoparticles in the oil obtained by TGA, 20.3% for example in entry 2.

We first chose to functionalize silica nanoparticles with amine groups. Aminated silica nanoparticles were prepared following a previous reported synthetic procedure.[45] According to this procedure, silica nanoparticles were allowed to react with 3-aminopropyltriethoxysilane to functionalize the surface of silica nanoparticles with amine groups. We determined the amounts of amine groups on silica nanoparticles by titration. To do this, 300 mg of these aminated silica nanoparticles were soaked in 30 mL of 0.02 M HCl solution and shaken for 1 h. A 15-mL sample of this HCl solution was then collected and titrated with 0.01 M NaOH. The amounts of amine groups on the silica nanoparticles was determined by calculating the amount of HCl consumed during shaking with aminated silica nanoparticles. It was found that the synthesized aminated silica nanoparticles contained 1.02 mmol/g of amine groups. These aminated silica nanoparticles

were analyzed by TGA and it was found that 19 wt% of organic materials on these aminated silica nanoparticles was lost by the point where temperature reached 500 ^{o}C. Another batch of aminated silica nanoparticles were synthesized using the same procedure and they contained 0.92 mmol/g of amine groups as determined by titration. For the following studies, only the first batch of silica nanoparticles was used and the second batch of silica nanoparticles was stored for future use.

Our previous experience of monitoring the solubilization of MNPs by UV-Visible spectroscopy as detailed in the last chapter suggested to us that the solubilization of silica nanoparticles too could be monitored by spectroscopy. Here we decided to monitor the solubilization of silica nanoparticles by fluorescence spectroscopy because our group had experience with functionalizing the surface of polymeric solids with fluorescent dyes.[150,151] If a small fraction of amine groups on aminated silica nanoparticles were labeled with fluorescent dyes, it would be possible to have the rest of amine groups available. These amine groups could then be allowed to react with PIB-supported ligands to solubilize these silica nanoparticles and to produce dispersions of fluorescent silica nanoparticles. As noted above, even a small amount of labeling led to an opaque phase, but because the fluorescent dye would be still detectable by its emission, we could monitor the degree of solubilization of these dye-labeled silica nanoparticles by analyzing the fluorescence intensity both in opaque suspensions or in solution. Although the exact amount of fluorescent dye labeling on silica nanoparticles is difficult to quantify, this fluorescence study would allow us to measure the relative solubilization of silica nanoparticles in solution because the relative fluorescence intensity represents the

amounts of silica nanoparticles solubilized in opaque suspensions or in solution. Initially, pyrene was chosen as the fluorophore to prepare these silica nanoparticles. Some initial results of solubilizing silica nanoparticles were obtained by allowing PIB-attached ligands such as carboxylic acid-terminated PIB **51** and ketone-terminated PIB **59** (Figure 28) to react with these pyrene-labeled silica nanoparticles in heptane. However, the fluorescence intensity of the resulting heptane solution was not as high as expected as shown in Figure 29. We also carried out experiments where oleic acid, a low molecular weight analog of the carboxylic acid-terminated PIB, was used as a ligand to graft onto aminated silica nanoparticles under the same conditions. In contrast to our prior experience comparing carboxylic acid-terminated PIB and oleic acid in MNP solubilization, a 10-fold higher fluorescence intensity was seen for the oleic acid-treated aminated silica nanoparticles versus that for a PIB-grafted sample in heptane. This result contradicted our assumption that PIB-attached ligands can solubilize more silica nanoparticles than their low molecular weight analogs. Further studies showed that pyrene-labeling was not suitable for this study because the fluorescence of pyrene was likely quenched by the free amines on these pyrene-labeled silica nanoparticles. The plausibility of this explanation was studied by conducting solubilization experiments of pyrene-labeled silica nanoparticles in THF in the presence of either oleic acid or HCl. As shown in Figure 29, hydrochloric acid-treated aminated silica nanoparticles in THF showed a 10-fold higher fluorescence intensity than untreated aminated silica nanoparticles in heptane and a *ca*. 30% lower fluorescence intensity than oleic acid treated silica nanoparticles in THF. However, oleic acid-treated silica nanoparticles showed a 20-fold higher fluorescence intensity than untreated

aminated silica nanoparticles in heptane. This unequal increase of fluorescence intensity suggested to us that the fluorescence intensity might be affected due to the presence of acid, which would decrease the amounts of free amines on the silica nanoparticles and reduce the fluorescence quenching effect from those free amines. In fact, our group's previous work also noted that the fluorescence of pyrene was quenched by using triethylamine.[150] Thus, the fluorescence seen in solutions or in stable suspensions reflects solubilization of nanoparticles and quenching of any pyrene fluorescence by unreacted amines. We were not able to design an experiment to separate these effects so we turned our attention to a different fluorescent label.

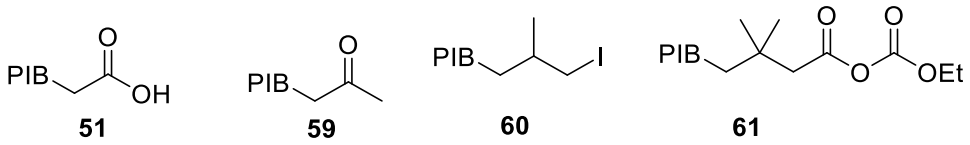

Figure 28. PIB-supported ligands that were used to graft to fluorescent dye-labeled silica nanoparticles to study the solubilization of aminated silica nanoparticles.

For this reason, we then functionalized aminated silica nanoparticles with a dansyl dye. Since the fluorescence of the dansyl dye is not affected by the presence of amines,[152,153] we can rule out the possibility that the fluorescence intensity will be affected by unreacted amine groups on silica nanoparticles after a solubilization experiment. Therefore, dansyl-labeling was a better option for determining the solubilization of silica nanoparticles in our study. Using a modified procedure, aminated silica nanoparticles were suspended in dichloromethane (DCM) by sonication in the presence of 10 mol% of dansyl

chloride and triethylamine. After the reaction, the resulting silica nanoparticles were filtered and washed with DCM until the filtrate did not show fluorescence under UV light. The success of functionalizing silica nanoparticles with dansyl groups was evident when these filtered silica nanoparticles showed blue fluorescence under UV light.

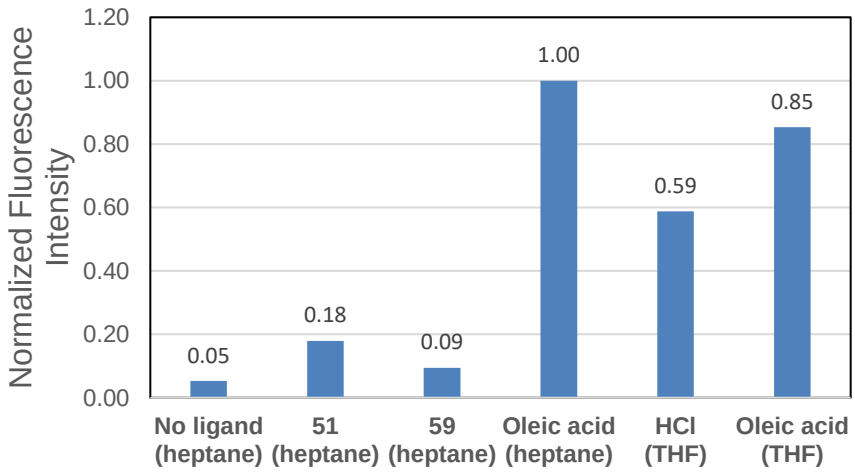

Figure 29. The comparison of fluorescence intensity of the supernatant of a mixture of pyrene-labeled silica nanoparticles and a ligand in either heptane or THF (noted in parentheses) that was sonicated for 4 h and then centrifuged at 3200 rpm for 10 min.

After preparation of the dansyl-labeled silica nanoparticles, the stability of the dye was tested by suspending these dye-labeled silica nanoparticles in heptane by sonication for 4 h. After the reaction mixture was centrifuged at 3200 rpm for 10 min, the fluorescence of the supernatant was measured by a fluorimeter. No fluorescence was observed in the supernatant which indicated that the dansyl dye on these silica nanoparticles was stable. We also tested the stability of dansyl-attached silica nanoparticles under basic conditions. When 10 mg of dansyl-labeled silica nanoparticles

were suspended in 10 mL of heptane in the presence of either 25 or 50 μL of triethylamine, no fluorescence intensity was observed in the supernatant solution after 4 h of sonication. However, when 100 μL of triethylamine was used, a fluorescence signal was observed at 450 nm as shown in Figure 30. We reasoned that this fluorescence signal was most likely due to the increased solubility of these silica nanoparticles in heptane because of the added triethylamine.

Next, we prepared three PIB-supported ligands **51**, **60**, and **61** (Figure 28) to test their binding ability to aminated silica nanoparticles. A mixture of 10 mg of aminated silica nanoparticles and 50 mg of a PIB-supported ligand in 10 mL of heptane was sonicated for 4 h. After 4 h, the mixture was then centrifuged at 3200 rpm for 10 min and the fluorescence of the supernatant was measured by a fluorimeter. As shown in Figure 29, iodide-terminated PIB ligand **60** poorly solubilized aminated silica nanoparticles in heptane. The solubilization of aminated silica nanoparticles by grafting the carboxylic acid-terminated PIB **51** was *ca.* 90-fold higher compared to that observed for **60**. Originally, we thought PIB-supported carbonyl ethyl carbonate **61** would have a greater ability than **60** to solubilize these silica nanoparticles. However, we found that **61** only solubilized *ca*. half of the silica nanoparticles solubilized by **60** based on fluorescence spectroscopic analysis.

We also determined the solubilizing ability of **51** and **61** by TGA. For this purpose, we prepared PIB-supported silica nanoparticles using an increased scale. A mixture of 200 mg of aminated silica nanoparticles and 500 mg of **51** or **61** in 20 mL of heptane were sonicated for 12 h. After the reaction, three cycles of centrifugation/decantation were

carried out using the same method previously described to separate the soluble and insoluble silica nanoparticles. After the separation, three supernatant solutions were combined and concentrated under reduced pressure using a rotary evaporator to give a clear oil. The oils and the solids collected from centrifugation were then analyzed by TGA. As shown in Table 8 entry 1, the oil obtained when **51** was used contained 11.6 wt% of silica nanoparticles but the oil obtained when **61** was used contained only 6.5 wt% of silica nanoparticles as shown in entry 2. The *ca*. 2-fold difference in the mass of silica nanoparticles in these oils is consistent with the result obtained in fluorescence studies as discussed in Figure 30. The amounts of silica nanoparticles solubilized in heptane are shown in Table 8.

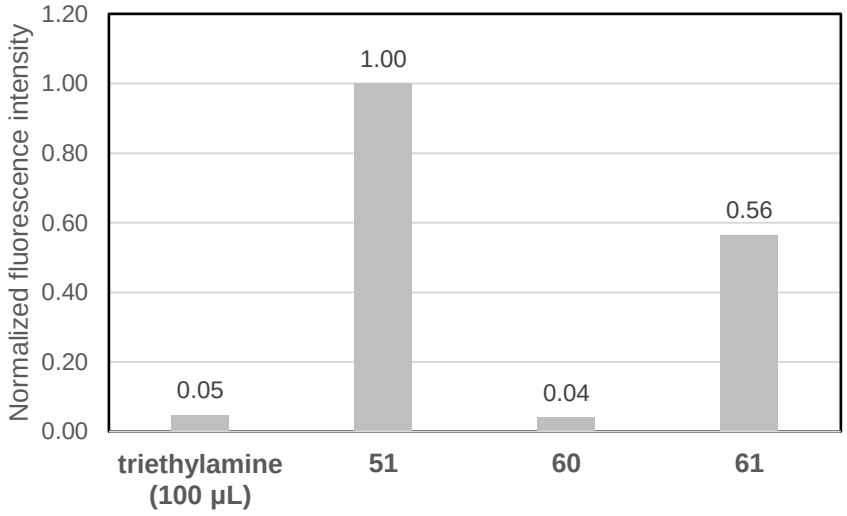

Figure 30. A comparison of fluorescence intensity at 450 nm ($\lambda_{excitation}$ of 340 nm) of the supernatant of a mixture of dansyl-labeled silica nanoparticles and a ligand in heptane after sonication for 4 h and then centrifugation at 3200 rpm for 10 min.

Table 8. TGA results of **51** and **61** functionalized silica nanoparticles.

Entry	Ligand	SiNP/ligand (g/g)	Starting SiNP[a] Solubilized (%)	PIB in the Oil or Insoluble Solids (%)	
				oil	solid
1	**51**	0.2 : 0.5	32	88.4	20.1
2	**61**	0.2 : 0.5	17	93.5	21.4

[a] This value was calculated by dividing the weight of silica nanoparticles in the oil by the weight of original silica nanoparticles used for the grafting reaction. The weight of silica nanoparticles in the oil was obtained by multiplying the weight of oil, which is not listed here, by the weight percentage of silica nanoparticles in the oil obtained by TGA, 6.5% for example in entry 2.

We also studied another approach for grafting PIB onto silica nanoparticles that were functionalized with thiol groups. We used 3-mercaptopropyltriethoxysilane to functionalize silica nanoparticles with thiol groups through a procedure that was similar to that employed to functionalize silica nanoparticles with amine groups as shown in Scheme 26a. The resulting silica nanoparticles were analyzed by TGA and the result showed that they contained 5.6 wt% of organic mass, which corresponds to *ca*. 0.28 mmol of thiols per gram of thiol-modified silica nanoparticles. The loading of thiol groups on these nanoparticles were lower than expected. Wang[154] reported the preparation of thiol-modified silica nanoparticles and showed that the resulting silica nanoparticles contained *ca*. 15 wt% of organic mass when 10 g of silica nanoparticles (average particle size of 20–50 nm and surface area of 640 m^2/g) were allowed to react with 75 mL of 3-mercaptopropyltrimethoxysilane in 150 mL of toluene, 10 mL of water, 10 mL of ethanol, and 2 mL of formic acid. This work showed that further optimization of the amounts of

thiol groups on silica nanoparticles can be carried out by varying the amounts of 3-mercaptopropyltriethoxysilane, using co-solvents, or adding acid.

Scheme 26. Synthesis of PIB-supported silica nanoparticles via thiol-ene reactions.

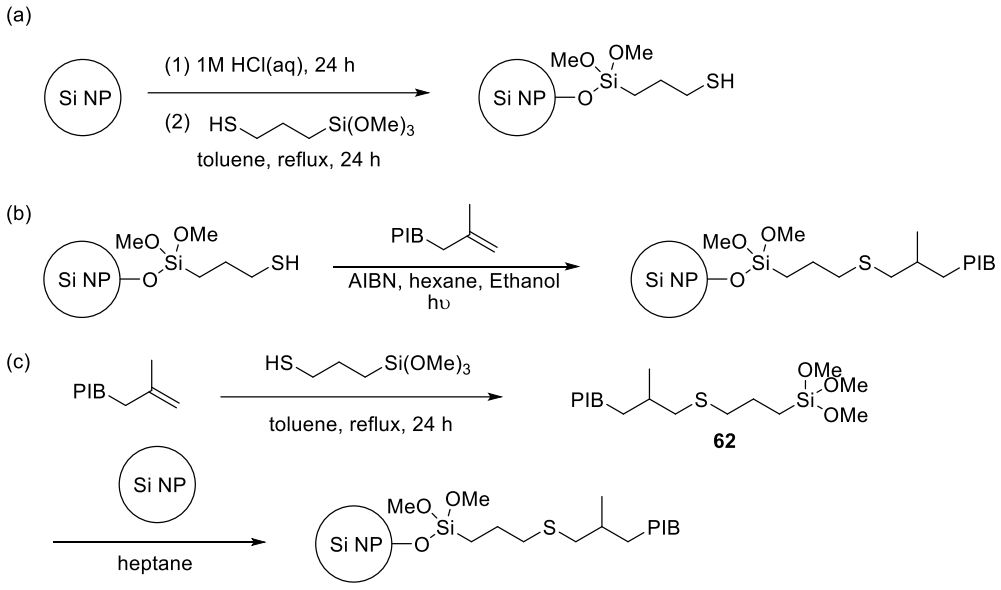

The thiol groups on these modified silica nanoparticles were then allowed to react with vinyl-terminated PIB **49** via a thiol-ene reaction to prepare PIB-grafted silica nanoparticles (Scheme 26b). After the reaction, the reaction solution became cloudy due to the silica nanoparticles being well dispersed. The solvent was removed under reduced pressure using a rotary evaporator and then heptane was added to redisperse the silica nanoparticles. The soluble silica nanoparticles were isolated as previously described by three cycles of the centrifugation/decantation method to give a clear oil. Both the oil and the precipitate from the centrifugation were analyzed by TGA and the results are summarized in Table 9. The amount of organic mass on the silica nanoparticles increased

from 5.6% to 11.1% indicating the success of grafting PIB on silica nanoparticles via a thiol-ene reaction. However, the collected oil only contained 1.6 wt% of silica nanoparticles. The above experiments were carried out only one time, and there could be experimental error leading to poor solubilization that could be reduced by further study and optimization. The poor solubilization was also likely due to limited amounts of thiol functionalities which allowed for fewer PIB groups to be grafted to the silica nanoparticles. As discussed previously, if the amounts of thiol groups on silica nanoparticles can be increased after optimization, the solubilization of silica nanoparticles can be improved by increasing the amounts of PIB-supported ligands that can be attached.

Table 9. TGA results of thermal degradation of **49** and **62** functionalized silica nanoparticles.

Entry	Ligand	SiNP/ligand (g/g)	Starting SiNP[a] Solubilized (%)	PIB in the Oil or Insoluble Solids (%)	
				oil	solid
1	**49**	0.2 : 0.5	3.5	98.5	11.1
2	**62**	0.2 : 0.5	14	96.5	5.3

[a] This value was calculated by dividing the weight of silica nanoparticles in the oil by the weight of original silica nanoparticles used for the grafting reaction. The weight of silica nanoparticles in the oil was obtained by multiplying the weight of oil, which is not listed here, by the weight percentage of silica nanoparticles in the oil obtained by TGA, 3.5% for example in entry 2.

A thiol-ene reaction was also used to synthesize a PIB-bound trimethoxysilane ligand as shown in Scheme 26c. For this synthesis, **49** was allowed to react with 3-mercaptopropyltrimethoxysilane to prepare PIB-bound trimethoxysilane **62** with a thioether linkage. This ligand **62** was then grafted to silica nanoparticles. However, the oil

obtained from this method only contained 3.5 wt% of silica nanoparticles as shown in Table 9 Entry 2. The reason of the poor grafting of trimethoxyalkylsilane to silica nanoparticles in this case is unclear. Further studies changing reaction conditions or the ratios of reagents in the grafting reactions should be carried out to optimize the solubilization of these silica nanoparticles in heptane.

The success of conducting radical catalyzed thiol-ene reactions to prepare PIB-supported silica nanoparticles suggested to us that radical polymerization could be used to prepare PIB-grafted silica nanoparticles with a higher molecular weight of PIB. This increase in molecular weight may improve the solubilization of silica nanoparticles in heptane. This idea was first tested by conducting a thiol-ene reaction using a 3 to 1 equivalent ratio of vinyl-terminated PIB to 3-mercaptopropytriethoxysilane to prepare a trimerized PIB-attached triethoxysilane as shown in Scheme 27. Unfortunately, only one equivalent of vinyl-terminated PIB reacted with one thiol group. The unsuccessful trimerization was most likely because the tertiary radical generated from the reaction had insufficient reactivity to react with a second equivalent of PIB alkene.

Scheme 27. Proposed synthesis of trimerized PIB-attached trimethoxysilane via a thiol-ene reaction.

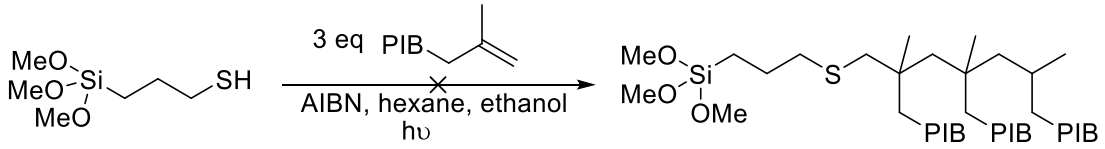

Because of this unsuccessful attempt, we turned our attention to controlled radical polymerization, specifically reversible addition-fragmentation chain-transfer (RAFT)

polymerization, as a method to graft polymers onto silica nanoparticles. 4-Cyano-4-(dodecylsulfanylthiocarbonyl)sulfanyl pentanoic acid (CDTPC), a commercially available RAFT reagent, was chosen to graft onto silica nanoparticles. Aminated silica nanoparticles were allowed to react with CDTPC in the presence of DCC to prepare CDTPC-grafted silica nanoparticles as shown in Scheme 28. We also synthesized a PIB oligomer with a pendant acrylate (**63**) as a monomer for RAFT polymerization. However, attempting RAFT polymerization of **63** using CDTPC as a RAFT reagent and AIBN as an initiator was not successful. To test whether there was any impurity in **63** causing this problem, a copolymerization of methylmethacrylate and **63** was carried out as shown in Scheme 29 and we found that only poly(methylmethacrylate) was obtained. This result indicated that even if there was any impurity in **63**, it did not affect the polymerization. Therefore, the unsuccessful polymerization was likely due to the low reactivity of reagents used in the reaction. The polymerization can be tried again with a more reactive RAFT reagent or with the use of a more reactive PIB-pendant acrylate.

Scheme 28. Synthesis of PIB-grafted silica nanoparticles for RAFT polymerization.

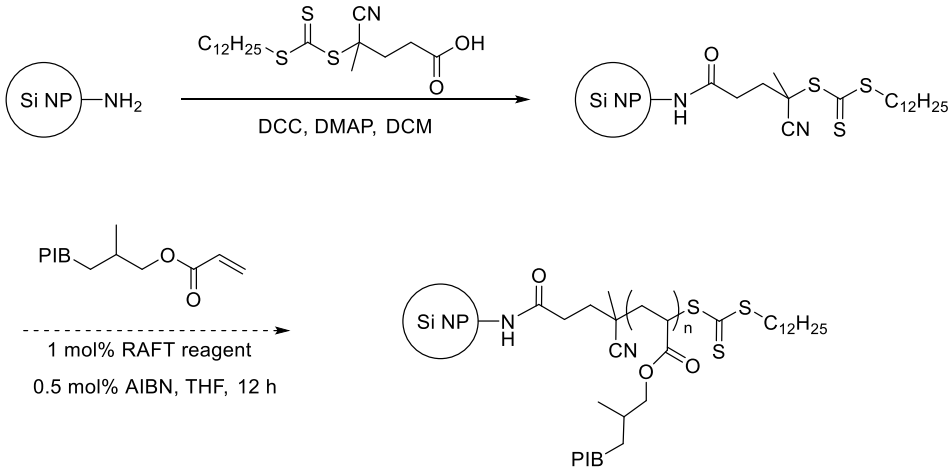

Scheme 29. Synthesis of 63 and copolymerization of 63 with methylmethacrylate.

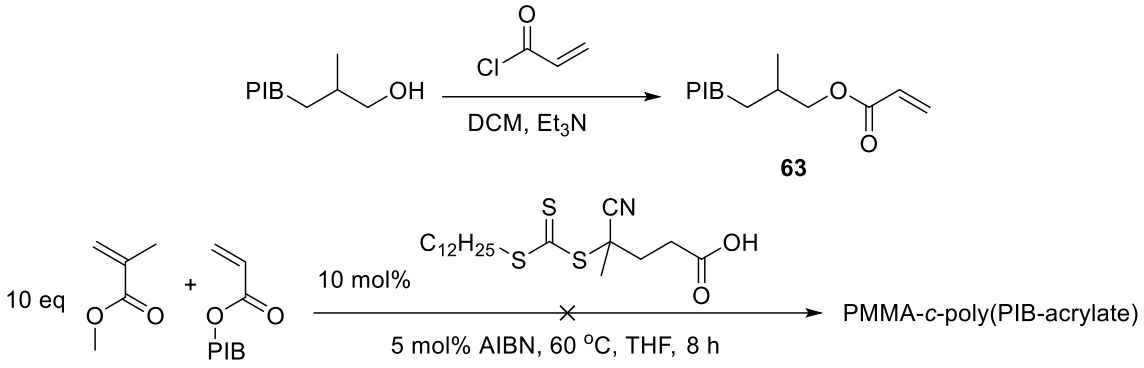

We also modified multiwalled carbon nanotubes (MWNTs) with polyethylenimine (PEI). Our group previously reported the modification of MWNTs with PEI and the resulting MWNTs were well dispersed in methanol and dimethylformamide (DMF).[43] We hypothesized that the amine groups on these MWNTs could be used to react with PIB-supported ligands to change the surface of these MWNTs from hydrophilic to hydrophobic and to solubilize them in nonpolar solvents. Using a modified procedure as shown in Scheme 30, a mixture of MWNTs and PEI in DMF was sonicated for 72 h and the resulting PEI-modified MWNTs were analyzed by TGA. The result showed that *ca*. 14 wt% of the organic materials on these MWNTs degraded when the temperature reached 500 ^{o}C. This result is consistent with the result reported previously from our group.[43] Further functionalization of these PEI-modified MWNTs with varying PIB-supported ligands and investigation of the solubility of the resulting PIB-modified MWNTs are currently being carried out by Dr. Manyam Praveen Kumar from Texas A&M University Qatar.

Scheme 30. Synthesis of PEI-modified MWNTs

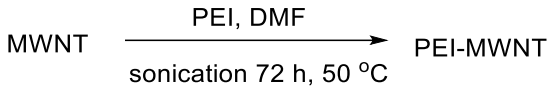

Conclusion

In this work, we studied several approaches of functionalizing silica nanoparticles with PIB. We successfully functionalized intrinsic silica nanoparticles with PIB-attached triethoxysilane and the resulting silica nanoparticles were highly dispersible in heptane. A separation method using three cycles of centrifugation and decantation yielded heptane soluble silica nanoparticles as oils. These oils contained *ca.* 20% of silica nanoparticles. We also functionalized intrinsic silica nanoparticles with 3-aminopropyltriethoxysilane or 3-mercaptopropyltrimethoxysilane to introduce either amine or thiol functionalities onto these silica nanoparticles. The amines or thiols were then allowed to react with a series of PIB-attached ligands to prepare PIB-supported silica nanoparticles. Aminated silica nanoparticles were successfully grafted with carboxylic acid-terminated PIB and *ca*. 32% of silica nanoparticles were solubilized in heptane when a 2 to 5 weight ratio of aminated silica nanoparticles to carboxylic acid-terminated PIB were used for the grafting reaction. However, when thiol-modified silica nanoparticles were used for the grafting reactions, the oils collected from these approaches contained lower amounts of silica nanoparticles compared to the grafting to intrinsic and aminated silica nanoparticles. Further optimization of the amounts of thiol groups on silica nanoparticles can be carried out to improve the solubilization of silica nanoparticles. Studies focused on preparing more soluble silica nanoparticles by synthesizing PIB-attached silica nanoparticles via a RAFT

polymerization can be carried out in the future. Studies of preparing heptane soluble PIB-supported multiwalled carbon nanotubes are currently being conducted by Dr. Manyam Praveen Kumar from Texas A&M University Qatar.

CHAPTER VI

EXPERIMENTAL SECTION

Materials and Instrumentation

Vinyl terminated polyisobutylene (PIB) with M_n of 1000 and 2300 was originally provided by BASF and later obtained from the TPC Group. Octadecyldimethylchlorosilane was purchased from Gelest. Silicon oxide nanoparticles (SiO_2, 10~20nm, 99.5%, non-porous) were purchased from SkySpring Nanomaterials. Multiwalled carbon nanotubes (MWNTs, 95%, 20-30 nm) were purchased from SkySpring Nanomaterials. Polyethylenimine (PEI, branched, M_w = 25,000 by LS, M_n = 10,000 by GPC) was purchased from SigmaAldrich. 0.20 μm nylon membranes were purchased from VWR. All other reagents and solvents were purchased from commercial sources and used without further purification unless otherwise stated. ^{1}H NMR spectra were recorded on Inova NMR spectrometers operating at 299.96 MHz and 499.59 MHz. Chemical shifts were reported in ppm with reference to $CDCl_3$ at 7.26 ppm. ^{13}C NMR spectra were recorded on Inova NMR spectrometers operating at 75.43 MHz and 125.72 MHz. Chemical shifts are reported in ppm with reference to $CDCl_3$ at 77.00 ppm. ^{31}P NMR spectra were recorded using an Inova NMR spectrometer operating at 121.42 MHz. Chemical shifts are reported in ppm with reference to 85% H_3PO_4 at 0.00 ppm. Coupling constants are given in Hz and rounded to the nearest 0.1 Hz, the spin multiplicities are indicated by the following symbols: s (singlet), d (doublet), t (triplet), dd (doublet of doublet), br (broad peak) and m (multiplet). UV–Visible spectra were recorded on a Shimadzu UV-2600 UV-Vis spectrophotometer. Fluorescence spectra were obtained by using a Horiba Scientific Fluoromax-4

spectrofluorometer. Infrared spectra (IR) were recorded on a Shimadzu IRAffinity-1S IR spectrophotometer. Thermogravimetric analysis (TGA) was performed under Ar atmosphere using a Mettler Toledo model TGA/DSC1 with a heating rate of 10 °C min^{-1}. Measurements were analyzed using Mettler Toledo STARe software v 10.00. Transmission electron microscopy (TEM) analysis was performed on a JEOL 1200 EX operating at 100 kV and micrographs were recorded at calibrated magnifications using a SLA-15C CCD camera. X-ray powder diffraction (XRD) analysis was performed on a Goniometer Ultima IV operating at 40 kV/20 mA. Elemental analyses were determined by Atlantic Microlab (Norcross, GA).

Synthesis and Experimental Procedures

Synthesis of PIB-SAc (25). Vinyl terminated PIB (20 g, 20 mmol, 1.0 equiv), thioacetic acid (4.56 g, 60 mmol, 3.0 equiv), and AIBN (0.33 g, 2 mmol, 0.1 equiv) were dissolved in 100 mL of heptane and 100 mL of absolute alcohol. The solution was stirred at ambient temperature with exposure to 365 nm light for 8 h. After the reaction was complete, water was added to the solution to perturb the system to form two layers. The heptane layer was washed by 90% aqueous ethanol for 3 times and dried by Na_2SO_4. The solvent was removed at reduced pressure using a rotary evaporator to give 19.5 g (91%) of **25**. ^{1}H NMR (500 MHz, $CDCl_3$) δ 2.93 (1 H, dd, *J* = 12.5 Hz, 7.5 Hz) , 2.72 (1 H, dd, *J* = 12.5 Hz, 7.5 Hz), 2.32 (3 H, s), 1.80-1.70 (1 H, m), 1.40-1.05 (140 H, m); ^{13}C NMR (125 MHz, $CDCl_3$) δ 195.71, 59.53,58.83, 58.21, 56.91, 52.24, 38.15, 37.87, 37.78, 35.95, 30.65, 29.27, 22.45.

Synthesis of PIB-SH (26). 25 (5.0 g, 5.0 mmol, 1.0 equiv) and KOH (280 mg, 5.0 mmol, 1.0 equiv) were dissolved in 50 mL of heptane and 50 mL of absolute alcohol. The solution was allowed to stir at 40 ^{o}C for 30 minutes. After the reaction was complete, HCl was added to neutralize the solution. The heptane layer was washed by 90% aqueous ethanol for 3 times and dried by Na_2SO_4. The solvent was removed under reduced pressure using a rotary evaporator to give 4.6 g (95%) of **26**. ^{1}H NMR (500 MHz, $CDCl_3$) δ 2.53 (1 H, dd, *J* = 12.5 Hz, 7.5 Hz), 2.38 (1 H, dd, *J* = 12.5 Hz, 7.5 Hz), 1.80-1.60 (1 H, m), 1.40-1.05 (140 H, m) ^{13}C NMR (125 MHz, $CDCl_3$) δ 59.51, 59.29, 58.81, 58.19, 56.84, 51.82, 38.13, 33.29, 32.41, 31.59, 30.77, 29.15, 21.68.

Synthesis of PIB-thiol-phthalonitrile (27). In a one-necked flask, **26** (10 g, 9.7 mmol, 1.0 equiv) and 4-nitrophthalonitrile (5.03 g, 29 mmol, 3.0 equiv) were dissolved in THF (1 g PIB thiol/10 mL THF). This flask was attached to a condenser and purged with nitrogen. Cesium carbonate (10 g, 29 mmol, 3.0 equiv) was added in three portions. The mixture was allowed to stir at 60 ^{o}C for 24 h. The mixture was allowed to cool to the ambient temperature and the THF was removed under reduced pressure using a rotary evaporator. The residue was dissolved in hexane and washed with three times of 150 mL 90% aqueous ethanol. The crude product was dried over magnesium sulfate and filtered. The solvent was removed under reduced pressure using a rotary evaporator to give 8.5 g (67%) of **27**. ^{1}H NMR (500 MHz, $CDCl_3$) δ 7.63 (1 H, d, *J* = 15 Hz), 7.55 (1 H, s), 7.49 (1 H, d, *J* = 15 Hz), 2.96 (1 H, dd, *J* = 17.5 Hz, 10 Hz), 2.86 (1 H, dd, *J* = 17.5 Hz, 10 Hz),

1.95-1.85 (1 H, m), 1.40-1.05 (140 H, m); ^{13}C NMR (125 MHz, $CDCl_3$) δ 147.78, 133.04, 129.99, 129.85, 116.19, 115.50, 115.11, 110.57, 59.48, 59.20, 58.79, 58.17, 56.97, 52.44, 41.49, 36.04, 31.22, 30.77, 28.58, 22.78.

Synthesis of PIB-sulfonyl-phthalonitrile (28). 27 (5.0 g, 4.2 mmol, 1.0 equiv) and *m*-CPBA (1.73g, 10 mmol, 2.2 equiv) were dissolved in 50 mL of $CHCl_3$. The solution was allowed to stir at 50^{o}C for 4 h under a N_2 atmosphere. The solution was allowed to cool to ambient temperature. Excess amount of saturated Na_2SO_3 solution was added to the flask to quench *m*-CPBA. The solvent was removed under reduced pressure using a rotary evaporator and 100 mL of hexane was added to dissolve the residue. The hexane solution was washed by 90% aqueous ethanol for 3 times and dried by Na_2SO_4. The solvent was removed under reduced pressure using a rotary evaporator to give the crude product which was purified by column chromatography using hexane/ethyl acetate = 9/1 as eluent to give 3.4 g (66%) of **28**: IR (neat): 2920, 2874, 2234, 1718 cm^{-1}; ^{1}H NMR (500 MHz, $CDCl_3$), δ 8.34 (1 H, s), 8.29 (1 H, d, *J* = 15 Hz), 8.07 (1 H, d, *J* = 15 Hz), 3.13 (1 H, dd, *J* = 25 Hz, 12.5 Hz), 2.99 (1 H, dd, *J* = 25 Hz, 12.5 Hz), 2.40-2.25 (1 H, m), 1.40-1.05 (140 H, m); ^{13}C NMR (125 MHz, $CDCl_3$) δ 147.78, 133.04, 129.99, 129.85, 116.19, 115.50, 115.11, 110.57, 59.48, 59.20, 58.79, 58.17, 56.97, 52.44, 41.49, 36.04, 31.22, 30.77, 28.58, 22.78.

Synthesis of PIB-SO_2-Co-Pc (29). 28 (3.0 g, 2.5 mmol, 4.0 equiv), DBU (192 mg, 1.3 mmol, 2.0 equiv) and $CoCl_2$ (90 mg, 0.25 mmol, 1 equiv) were added into a high-pressure

reaction vessel with a stir bar under N_2. The vessel was heated to 190 °C in a sand bath and the mixture was stirred for 12 h. The vessel was then allowed to cool to room temperature, 100 mL of hexane was added and the mixture was filtered through Celite. The hexane solution was washed with three times of 100 mL 90% aqueous ethanol. The remaining solution was dried over magnesium sulfate and filtered. The solvent was removed under reduced pressure using a rotary evaporator to give crude product which was purified by column chromatography using hexane as eluent to give 1.2 g (38%) of **29** which contained 1.02 g (85%) of metallated **29a** and 0.18 g (15%) of non-metallated **29b** based on ICP-MS analysis: IR (neat): 2920, 2881, 1723 cm^{-1}.

Synthesis of PIB-SO_2-Pc metal-free (29b). To a high-pressure reaction vessel, 0.50 g (0.437 mmol) of **28**, 1.31 mL of hexanol, and 6 mg of lithium metal were added. This reaction mixture was heated to 160 ^oC and stirred for 12 h in a sand bath and then cooled to room temperature before the product was extracted with hexane and then poured into 3.5 mL of concentrated H_2SO_4. The reaction mixture was allowed stirred for 15 minutes before being washed with acetonitrile, dried with $MgSO_4$, filtered, and the solvent was removed under reduced pressure using a rotary evaporator to give 0.23 g (46%) **29b** as blue-green viscous oil. UV–Vis (*n*-hexane) λ_{max} (ε) 696 nm (7.35×10^5) (a second peak at 659 nm was nearly the same intensity as the 696 nm peak). The ^1H NMR spectrum of **29b** had three broad peaks in the 8–10 ppm and one broad peak in 3.5–4.0 ppm regions for the aromatic and -CH_2SO_2- protons, respectively consistent with the formation of a mixture of regioisomers with PIB substituents on the aromatic periphery.

General procedure of nitro arenes reduction by hydrazine hydrate in the presence of catalyst. 1 mmol of nitroarene and 0.4 mol% of catalysts were dissolved by 5 mL of heptane and 5 mL anhydrous ethylene glycol in a Schlenk tube. 5 equivalent of hydrazine hydrate were added and the biphasic solution was stirred at 110 ^{o}C under a N_2 atmosphere for 24 h. The solution was cooled down to ambient temperature. The product was isolated by chromatography from the polar ethylene glycol-rich phase.

4-Chloroaniline. ^{1}H NMR (500 MHz, $CDCl_3$), δ 7.10 (2 H, d, *J* = 8.8 Hz), 6.60 (2 H, d, *J* = 8.8 Hz), 3.50-3.80 (2 H, br); ^{13}C NMR (125 MHz, $CDCl_3$) δ 144.90, 129.08, 123.12, 116.20.

4-Bromoaniline. ^{1}H NMR (300 MHz, $CDCl_3$), δ 7.23 (2 H, d, *J* = 8.4 Hz), 6.56 (2 H, d, *J* = 8.4 Hz), 3.60-3.70 (2 H, br); ^{13}C NMR (75 MHz, $CDCl_3$) δ 145.37, 131.97, 116.67, 110.15.

4-Aminobenzoic acid. ^{1}H NMR (500 MHz, DMSO-d_6), δ 7.59 (2 H, d, *J* = 8.5 Hz), 6.54 (2 H, d, *J* = 8.5 Hz), 5.70-5.84 (2 H, br); ^{13}C NMR (125 MHz, DMSO-d_6) δ 168.42, 153.64, 131.88, 117.41, 113.34.

4-Aminotoluene. ^{1}H NMR (500 MHz, $CDCl_3$), δ 7.02 (2 H, d, *J* = 8.5 Hz), 6.65 (2 H, d, *J* = 8.5 Hz), 3.50-3.60 (2 H, br), 2.30 (3 H, s); ^{13}C NMR (125 MHz, $CDCl_3$) δ 143.74, 129.63, 127.59, 115.13, 20.34.

4-Tert-butylaniline. ^{1}H NMR (500 MHz, $CDCl_3$), δ 7.19 (2 H, d, *J* = 9.0 Hz), 6.65 (2 H, d, *J* = 9.0 Hz), 3.50-3.60 (2 H, br), 1.28 (9 H, s); ^{13}C NMR (125 MHz, $CDCl_3$) δ 143.70, 141.32, 125.97, 114.87, 33.83, 31.46.

4-Aminophenol. ^{1}H NMR (500 MHz, DMSO-d_6), δ 8.50-8.55 (1 H, br), 6.46 (2 H, d, *J* = 9.0 Hz), 6.42 (2 H, d, *J* = 9.0 Hz); ^{13}C NMR (125 MHz, DMSO-d_6) δ 148.79, 140.89, 116.19, 116.111.

1,4-Diaminobenzene. ^{1}H NMR (500 MHz, DMSO-d_6), δ 6.57 (4 H, s), 3.25-3.40 (4 H, br); ^{13}C NMR (125 MHz, DMSO-d_6) δ 138.56, 116.70.

1-Aminonaphthalene. ^{1}H NMR (500 MHz, $CDCl_3$), δ 7.82-7.89 (2 H, m), 7.48-7.55(2 H, m), 7.34-7.41(2 H, m), 6.79-6.82(1 H, m), 4.10-4.20 (2 H, br); ^{13}C NMR (125 MHz, CDCl3) δ 142.00, 134.28, 128.44, 126.26, 125.75, 124.74, 123.53, 120.72, 118.83, 109.57.

General procedure for octadecyldimethylsilyl ether synthesis (38a-38e). To a mixture of alcohol (10 mmol) and triethylamine (1.5 g, 15 mmol) in 15 mL of dichloromethane, was added 10 mL of octadecyldimethylchlorosilane (**37)** (10 mmol, 1.0 M in DCM). The mixture was stirred for 18 h at 40 °C. After the solvent was removed under reduced pressure using a rotary evaporator, the residue was dissolved in 30 mL of hexane and washed by 10 mL of 90% aqueous ethanol three times. The hexane phase was dried over Na_2SO_4 and the solvent was removed under reduced pressure using a rotary evaporator to give the product.

Methoxy(octadecyldimethyl)silane (38a). 3.0 g (89%). Clear liquid; ^{1}H NMR (500 MHz, $CDCl_3$) δ 3.42 (s, 3 H), 1.28-1.22 (br, 32 H), 0.85 (t, *J* = 6.9 Hz, 3 H), 0.60 (t, *J* = 7.0 Hz, 2 H), 0.09 (s, 6 H); ^{13}C NMR (125 MHz, $CDCl_3$) δ 50.1, 32.0, 29.7, 29.5, 29.4, 22.9, 16.0, 14.1, -2.73. IR (neat, cm^{-1}) 2920, 2853, 1466, 1250, 1188, 1092, 837, 781, 721. HRMS (ESI+) calculated for $C_{21}H_{46}OSi$ [M+H]+ : 343.3396, found: 343.3380.

Ethoxy(octadecyldimethyl)silane (38b). 3.3 g (93%). Clear liquid; ^{1}H NMR (500 MHz, $CDCl_3$) δ 3.66 (q, *J* = 6.9 Hz, 2 H), 1.28-1.22 (br, 32 H), 1.19 (t, *J* = 7.2 Hz, 3 H), 0.88 (t, *J* = 6.9 Hz, 3 H), 0.59 (t, *J* = 8.0 Hz, 2 H), 0.09 (s, 6 H); ^{13}C NMR (125 MHz, $CDCl_3$) δ 58.2, 32.0, 29.7, 29.6, 29.4, 22.7, 18.5, 16.4, 14.1, -2.12. IR (neat, cm^{-1}) 2920, 2853, 1466, 1250, 1107, 1080, 945, 837, 779, 721. HRMS (ESI+) calculated for $C_{22}H_{48}OSi$ [M+H]+ : 357.3553, found: 357.3539.

Butoxy(octadecyldimethyl)silane (38c). 3.5 g (94%). Clear liquid; ^{1}H NMR (500 MHz, $CDCl_3$) δ 3.57 (t, *J* = 6.9 Hz, 2 H), 1.5 (m, 2 H), 1.40-1.20 (br, 34 H), 0.91 (t, *J* = 7.3 Hz, 3 H), 0.88 (t, *J* = 7.0 Hz, 3 H), 0.58 (t, *J* = 7.8 Hz, 2 H), 0.08 (s, 6 H); ^{13}C NMR (125 MHz, $CDCl_3$) δ 62.2, 46.2, 29.8, 29.7, 29.6, 29.5, 22.6, 18.7, 16.4, 14.1, -2.14. IR (neat, cm^{-1}) 2920, 2853, 1466, 1250, 1094, 1038, 980, 889, 837, 779, 719. HRMS (ESI+) calculated for $C_{24}H_{52}OSi$ [M+H]+ : 385.3866, found: 385.3868.

Hexyloxy(octadecyldimethyl)silane (38d). 3.7 g (90%). Clear liquid; ^{1}H NMR (500 MHz, $CDCl_3$) δ 3.56 (t, *J* = 6.6 Hz, 2 H), 1.51 (m, 2 H), 1.35-1.20 (br, 38 H), 0.90-0.87 (m, 6 H), 0.58 (t, *J* = 8.0 Hz, 2 H), 0.08 (s, 6 H); ^{13}C NMR (125 MHz, $CDCl_3$) δ 62.8, 31.9, 29.7, 29.6, 29.4, 22.7, 16.4, 14.1, -2.10. IR (neat, cm^{-1}) 2920, 2853, 1466, 1248,

1096, 1041, 951, 837, 781, 719. HRMS (ESI+) calculated for $C_{26}H_{56}OSi$ [M+H]+ : 413.4179, found: 413.4242.

Decyloxy(octadecyldimethyl)silane (38e). 4.2 g (89%). Clear liquid; ^{1}H NMR (500 MHz, $CDCl_3$) δ 3.56 (t, *J* = 6.9 Hz, 2 H), 1.48 (m, 2 H), 1.30-1.20 (br, 46 H), 0.88 (m, 6 H), 0.60 (t, *J* = 7.2 Hz, 2 H), 0.08 (s, 6 H); ^{13}C NMR (125 MHz, $CDCl_3$) δ 62.8, 29.8, 29.5, 29.4, 29.1, 25.9, 23.2, 22.7, 16.4, -2.14. IR (neat, cm^{-1}) 2920, 2853, 1466, 1248, 1098, 837, 779, 719. HRMS (ESI+) calculated for $C_{26}H_{56}OSi$ [M+H]+ : 469.4805, found: 469.4945.

Cleavage of decyloxy(octadecyldimethyl)silane (38e). To 2.0 g of **38e** (4.4 mmol) and 10 mL of heptane, 10 mL of TBAF was added (10 mmol, 1 M in THF). The mixture was stirred for 6 h at 40 °C. After the solution was cooled down to ambient temperature, the solvent was removed at reduced pressure using a rotary evaporator and 20 mL of heptane was added. The mixture was washed by 10 mL of water three times to remove TBAF. The heptane solution was then extracted with 90% aqueous ethanol. The ethanol phase was concentrated under reduced pressure using a rotary evaporator to give 493 mg (73%) of decanol (**40**). Clear liquid. ^{1}H NMR (300 MHz, $CDCl_3$) δ 3.62 (t, *J* = 7.2 Hz, 2 H), 1.63 (m, *J* = 6.9 Hz, 2 H), 1.44 (m, *J* = 7.2 Hz, 2 H), 1.25 (br, 12 H), 0.85 (t, *J* = 6.9 Hz, 3 H). IR (neat, cm^{-1}) 3320, 2956, 2864, 1466, 1378, 1120, 1065, 877. The heptane phase was concentrated under reduced pressure using a rotary evaporator to give 1.32 g (94%) of octadecyldimethylsilanol (**39**). White solid. This compound has no signal in ^{19}F NMR. ^{1}H NMR (300 MHz, $CDCl_3$) δ 1.25 (br, 32 H), 0.88 (t, *J* = 6.6 Hz, 3 H), 0.49 (t, *J* = 6.6 Hz,

2 H), 0.03 (s, 6 H); ^{13}C NMR (75 MHz, $CDCl_3$) δ 33.5, 31.9, 29.8, 29.7, 29.6, 29.5, 29.4, 29.3, 22.7, 18.4, 14.1, 0.39. IR (neat, cm^{-1}) 3500, 2914, 2848, 1469, 1249, 1066, 840, 810, 788, 775, 717, 709; mp 35-40 °C This product was further purified by a recrystallization from pentane at -20 °C to give bis(octadecyldimethylsilyl)disiloxane (**39b**). White solid. ^{1}H NMR (300 MHz, $CDCl_3$) δ 1.25 (br, 32 H), 0.88 (t, *J* = 6.6 Hz, 3 H), 0.49 (t, *J* = 6.6 Hz, 2 H), 0.03 (s, 6 H); ^{13}C NMR (125 MHz, $CDCl_3$) δ 33.5, 32.0, 30.4, 30.1, 29.7, 29.6, 29.5, 29.4, 29.1, 23.3, 22.7, 18.4, 0.43, 0.35. IR (neat, cm^{-1}) 2914, 2848, 1469, 1249, 1066, 840, 810, 788, 775, 717, 709; mp 41-42 °C. Elemental analysis (%): calcd C 75.15, H 13.56; found: C 75.28, H 13.65.

Regeneration of 37 from 39. To 1.4 g of **39** (3.6 mmol) and 20 mL of DCM, 3 drops of dry DMF and 3 mL of thionyl chloride were added. The mixture was stirred under nitrogen for 2 days at 40 °C. The solution was concentrated under reduced pressure using a rotary evaporator to give 1.48 g (98%) of **37**. ^{1}H NMR (300 MHz, $CDCl_3$) δ 1.25 (m, 32 H), 0.88 (t, *J* = 6.8 Hz, 3 H), 0.81 (t, *J* = 8.0 Hz, 2 H), 0.39 (s, 6 H); ^{13}C NMR (75 MHz, $CDCl_3$) δ 50.3, 33.7, 32.1, 29.9, 23.3, 22.9, 16.0, 14.2, 6.0.

Synthesis of (dodec-11-en-2-yloxy)(octadecyldimethyl)silane (**41**). To one two-necked 100 mL round-bottomed flask, 1.08 g of 10-undecenal (10.1 mmol) was added in 10 mL of heptane and 20 mL freshly dried THF under N_2 atmosphere. 3.6 mL of CH_3MgBr (10 mmol, in 1.4 M THF/toluene solution) was added dropwise through addition funnel and this mixture was stirred for 1 h. 1.76 g of **37** (10.1 mmol) in 5 mL of heptane was added

dropwise through addition funnel and the mixture was stirred at 40 ^{o}C for 18 h then 10 mL of water was added to quench the reaction. The heptane layer was washed by water (10 mL × 2) and the water layer was washed by heptane (10 mL × 2). The combined organic phases were dried over Na_2SO_4 and the solvent was removed under reduced pressure using a rotary evaporator to give 2.17 g (91%) of **41**. The ^{1}H NMR (300 MHz, $CDCl_3$) δ 5.82 (m, 1 H), 5.13 (d, *J* = 17 Hz, 1 H), 4.88 (d, *J* = 10 Hz, 1 H), 3.60 (m, 1 H), 2.13 (m, 2 H), 1.40-1.10 (br, 48 H), 0.88 (t, *J* = 6.6 Hz, 3 H), 0.49 (t, *J* = 6.6 Hz, 2 H), 0.17 (s, 6 H). IR (neat, cm^{-1}) 3098, 2914, 2849, 1462, 1250, 1061, 866, 837, 814, 789, 770, 729, 719. ^{13}C NMR (125 MHz, $CDCl_3$) δ 139.2, 114.1, 68.6, 68.2, 33.8, 33.4, 31.9, 29.7, 29.4, 28.9, 22.7, 17.8, 16.9, 0.29, -1.48. HRMS (ESI+) calculated for $C_{26}H_{56}OSi$ [M+Ag]+ : 601.3934, found: 601.3915.

Synthesis of dodec-10-en-2-ol (42). To 2.0 g of **41** (4.0 mmol) and 25 mL of heptane and 20 mL of THF, 4.1 mL of TBAF (4.1 mmol, 1 M in THF) was added. The mixture was stirred for 6 h at 40 °C then 25 mL of NH_4Cl aqueous solution was added. The heptane phase was washed with water (25 mL × 2). The product is extracted by 90% aqueous ethanol and the ethanol phase was concentrated under reduced pressure using a rotary evaporator to give 0.55 g (75%) of **42**. ^{1}H NMR (300 MHz, $CDCl_3$) δ 5.80 (m, 1 H), 4.99 (d, *J* = 17.0 Hz, 1 H), 4.93 (d, *J* = 10.0 Hz, 1 H), 3.78 (m, 1 H), 2.03 (m, 2 H), 1.40-1.20 (br, 16 H), 1.18 (d, *J* = 6.0 Hz, 3 H). ^{13}C NMR (125 MHz, $CDCl_3$) δ 139.2, 114.1, 68.2, 39.5, 33.8, 29.4, 28.9, 25.7. The heptane phase was concentrated under reduced pressure using a rotary evaporator to give 1.23 g (94%) of **39**.

(1-(4-Methoxyphenyl)ethoxy)(octadecyl dimethyl)silane (43). To one two-necked 50 mL round-bottomed flask, 303 mg of 4-methoxybenzaldehyde (2.23 mmol) was added in 10 mL freshly dried THF under N_2 atmosphere. 2.0 mL of CH_3MgBr (2.40 mmol, THF/toluene solution was titrated by 1-menthol and phenanthroline as indicator) was added through air-tight syringe and this mixture was stirred at ambient temperature for 14 h. 776 mg of **37** (2.24 mmol) in 10 mL of dried THF was added through air-tight syringe and this mixture was stirred for 24 h. The solvent was removed under reduced pressure using a rotary evaporator then 30 mL of heptane was added. The heptane layer was washed by water (10 mL × 2) then 90% aqueous ethanol (15 mL × 2). The heptane phase was dried over Na_2SO_4 and the solvent was removed under reduced pressure using a rotary evaporator to give 858 mg (83%) of **43**. Clear liquid. The ^{1}H NMR (500 MHz, $CDCl_3$) δ 7.24 (d, 2 H, *J* = 14.5 Hz), 6.85 (d, 2 H, *J* = 14.5 Hz), 4.80 (q, 1 H, *J* = 6.5 Hz), 3.80 (s, 3 H), 1.40 (d, 3 H, *J* = 6.5 Hz), 1.30-1.10 (br, 32 H), 0.89 (t, *J* = 7.0 Hz, 3 H), 0.53 (m, 2 H), 0.03 (s, 6 H); ^{13}C NMR (125 MHz, $CDCl_3$) δ 158.5, 138.8, 126.5, 113.4, 70.18, 55.2, 33.5, 31.9, 29.71, 29.66, 29.59, 29.36, 29.35, 26.96, 23.19, 22.69, 16.79, 14.12, -1.54. IR (neat, cm^{-1}) 2914, 2849, 1462, 1250, 1165, 1067, 866, 837, 814, 789, 770, 756, 729, 719. HRMS (ESI+) calculated for $C_{29}H_{54}O_2Si$ [M+Na]+ : 485.3791, found: 485.3803.

Synthesis of octadecyldimethylsilylacetylene (44). To a flame-dried 100-mL three-necked round-bottomed flask, 4.16 g of **37** (11.9 mmol) in 25 mL of heptane was added. 0.58 g of sodium acetylide (11.9 mmol in 18% of xylene slurry) in 25 mL of freshly dried THF was added to the mixture via syringe. The mixture was stirred at rt under N_2

atmosphere for 24 h then 50 mL of water was added. The heptane phase was washed with water (25 mL × 2) and 90% aqueous ethanol (25 mL × 3). The heptane phase was dried over Na_2SO_4 and concentrated under reduced pressure using a rotary evaporator to give 3.2 g (80%) of **44**. White solid. ^{1}H NMR (500 MHz, $CDCl_3$) δ 2.38 (s, 1 H), 1.25 (br, 32 H), 0.88 (t, *J* = 6.6 Hz, 3 H), 0.63 (t, *J* = 7.8 Hz, 2 H), 0.17 (s, 6 H); ^{13}C NMR (125 MHz, $CDCl_3$) δ 93.3, 89.5, 33.3, 31.9, 30.1, 29.7, 29.6, 29.4, 29.3, 29.0, 22.71, 15.87, -1.96. IR (neat, cm^{-1}) 3271, 2916, 2847, 2035, 1464, 1250, 866, 842, 824, 787, 772, 716, 694, 683; mp: 24-25 ^{o}C. Elemental analysis (%): calcd C 78.48, H 13.17; found: C 78.69, H 13.20.

Synthesis of 4-((Dimethyl(octadecyl)silyl)ethynylacetophenone (45). To a flame-dried 50 mL two-necked round-bottomed flask, 246 mg of 4-iodoacetophenone (1.0 mmol), 404 mg of **44** (1.2 mmol), 23 mg of $Pd(PPh_3)_4$ (0.02 mmol), and 7.6 mg of CuI (0.04 mmol) in 10 mL of freshly dried THF were added. 0.21 mL of Et_3N was added to the mixture then it was stirred at rt under N_2 atmosphere 24 h. The solvent was removed under reduced pressure using a rotary evaporator then 30 mL of heptane was added. The heptane phase was washed by water (25 mL × 2) and 90% aqueous ethanol (25 mL × 3). The heptane phase was dried over Na_2SO_4 and concentrated under reduced pressure using a rotary evaporator to give 417 mg of mixture which contains 85% of **45** (The yield is 82%) and 15% of acetylene dimers. Brown solid. ^{1}H NMR (500 MHz, $CDCl_3$) δ 7.89 (d, *J* = 8 Hz, 2 H), 7.53 (d, *J* = 8 Hz, 2 H), 2.60 (s, 3 H), 1.28-1.24 (br, 32 H), 0.88 (t, *J* = 6.6 Hz, 3 H), 0.59 (m, 2 H), 0.09 (s, 6 H); ^{13}C NMR (75 MHz, $CDCl_3$) δ 196.8, 136.2, 132.0, 128.0, 127.9, 104.4, 97.61, 33.21, 31.90, 30.04, 29.69, 29.65, 29.59, 29.35, 29.32, 28.99, 26.42,

23.75, 22.66, 15.95, -1.89. IR (neat, cm^{-1}) 2914, 2849, 2160, 2066, 1682, 1601, 1470, 1265, 844, 831, 818, 808, 785, 773, 718, 586. HRMS (ESI+) calculated for $C_{30}H_{50}OSi$ [M+H]+ : 455.3709, found: 455.3728.

Synthesis of 4-ethynylacetophenone (46). To 417 mg of the mixture **45** obtained from previous procedure and 10 mL of heptane and 10 mL of THF, 1.0 mL of TBAF (1.0 mmol, 1 M in THF) was added. The mixture was stirred at rt for 2 h then 20 mL of heptane and 20 mL of NH_4Cl aqueous solution was added. The heptane phase was washed with water (20 mL × 2). The product is extracted by 90% aqueous ethanol and the ethanol phase was concentrated under reduced pressure using a rotary evaporator to give 126 mg (95%) of **46**. ^{1}H NMR (300 MHz, $CDCl_3$) δ 7.92 (d, *J* = 9 Hz, 2 H), 7.61 (d, *J* = 9 Hz, 2 H), 2.60 (s, 3 H). IR (neat, cm^{-1}) 3350, 2961, 2916, 2874, 2212, 1674, 1599, 1400, 1288, 1261, 1221, 1177, 817. The heptane phase was concentrated under reduced pressure using a rotary evaporator to give 303 mg (90%) of **39**.

4-*(N,N*-Dibutyl-4-aminophenyl) azophenylmethoxy(octadecyl)dimethylsilane (47). 255 mg (0.74 mmol) of **37** in 10 mL of DCM was added to a mixture of 250 mg (0.74 mmol) of 4-(*N,N*-dibutyl-4-aminophenyl) azophenylmethanol and 0.15 mL of triethylamine in 15 mL of dichloromethane. The mixture was stirred for 18 h at 40 °C. After the mixture was cooled to the ambient temperature, the solvent was removed under reduced pressure using a rotary evaporator. The residue was dissolved in 30 mL of DCM and washed by two times of 10 mL of water. The dichloromethane was removed under

reduced pressure using a rotary evaporator to give the crude product. The crude was purified by silica gel column chromatography (eluent: ethyl acetate/dichloromethane = 1/9, R_f = 0.8) to give the 270 mg (53%) of **47**. Red solid. ^{1}H NMR (500 MHz, $CDCl_3$) δ 7.83 (d, *J* = 10 Hz, 2 H), 7.79 (d, *J* = 10 Hz, 2 H), 7.41 (d, *J* = 10 Hz, 2 H), 6.68 (d, *J* = 10 Hz, 2 H), 4.75 (s, 2 H), 3.36 (t, *J* = 7.5 Hz, 4 H), 1.62, (m, 4 H), 1.39 (m, 4 H), 1.29-1.23 (br, 32 H), 0.98 (t, *J* = 7.5 Hz, 6 H), 0.88 (t, *J* = 5.0 Hz, 3 H), 0.64 (t, *J* = 7.5 Hz, 1 H), 0.60 (t, *J* = 7.5 Hz, 1 H), 0.14 (s, 3 H), 0.13 (s, 3 H); ^{13}C NMR (125 MHz, $CDCl_3$) δ 152.4, 150.3, 143.0, 142.1, 127.3, 126.8, 125.1, 122.0, 110.96, 50.87, 33.42, 31.90, 29.69, 29.35, 23.13, 22.67, 20.25, 17.80, 16.35, 13.90, 0.39, -2.03. IR (neat, cm^{-1}) 3300, 2916, 2849, 1599, 1514, 1396, 1365, 1250, 1153, 1138, 1109, 1086, 1061, 868, 837. HRMS (ESI+) calculated for $C_{41}H_{71}N_3OSi$ [M+H]+ : 650.5445, found: 650.5487.

Synthesis of PIB-dimethylchlorosilane. 3 g (3 mmol) of PIB_{1000}-alkene and 3 drops of chloroplatinic acid were placed into a flame-dried 50-mL pressure vessel with a stir bar with a septum. 10 mL of freshly distilled toluene was added via syringe and the mixture was allowed to stir for 10 min at room temperature under nitrogen to dissolve the PIB-alkene. Then 0.6 mL of dimethylchlorosilane was added via syringe. The septum was removed while flushing with nitrogen and the screw cap was put on to seal the apparatus. After the mixture was stirred at 80 ^{o}C for 48 h, the mixture was cooled to ambient temperature. The toluene and the unreacted dimethylchlorosilane were removed under reduced pressure using a rotary evaporator to give as 3.0 g of PIB-dimethylchlorosilane

as an oil. This oil contained 90% hydrosilylated product and 10% of unreacted PIB-alkene. ^{1}H NMR (300 MHz, $CDCl_3$) δ 1.40-0.90 (m, 146 H), 0.44 (s, 6H).

General procedures of phase selectivity studies of octadecyldimethylsilyl ethers. The octadecyldimethylsilyl ether that was to be analyzed (1 mmol) was placed in a vial and dissolved in 10 mL of cyclohexane, hexane, heptane or cyclooctane. Then 10 mL of DMF or 90% ethanol was added to this hydrocarbon solution. The mixture was sealed and heated to 80 °C to generate a homogeneous solution. The solution was cooled to room temperature to produce a biphasic solution. An aliquot of the polar solution was then analyzed by ^{1}H NMR spectroscopy. When the polar solvent is DMF, we integrated the α-C-H next to the ether linkage and divided the integral by the numbers of the α-C-H. We then compared this number with the integration of the satellite peak of the aldehyde proton in the DMF solvent to determine the leaching of the silyl ethers into the polar solvent. These satellite peaks are due to the coupling of the aldehyde proton to the adjacent ^{13}C isotope, which is present in 1% of all molecules naturally. Thus, each of these satellite peaks represents 0.5% of the concentration of DMF. Thus, the concentration of silyl ethers in DMF solution can be calculated by using integral ratio of the α-C-H versus aldehyde proton. Then used the concentration to calculate the amounts of silyl ethers leaching into DMF solution to compare to the original amounts of silyl ethers, thus, the leaching percentage can be obtained. When the polar solvent is 90% aqueous ethanol, we integrated the CH_3 attached on Si and divided the integral by the numbers of the C-H. We then

compared this number with the integration of CH_2 in the ethanol solvent to determine the leaching of the silyl ethers into the polar solvent.

Synthesis of Fe_3O_4 nanoparticles. 3.51 g of ferric chloride hexahydrate ($FeCl_3 \cdot 6H_2O$) and 1.81 g of ferrous sulphate heptahydrate ($FeSO_4 \cdot 7H_2O$) (molar ratio 2:1, respectively) were dissolved in 150 mL of deionized water and stirred vigorously under a N_2 atmosphere at 70 °C. After 1 h, 15 mL ammonium hydroxide (35%) was rapidly added to the mixture and the reaction mixture was stirred for another 1 h and finally cooled to room temperature. The black precipitate that formed was trapped by a magnet and the particles were washed five times with hot water and finally dried in an oven under vacuum at 50 °C overnight. Usually around 2 g of Fe_3O_4 was obtained.

Synthesis of PIB-attached ligands for magnetic nanoparticles. PIB-OH (**31**),[34] PIB-2,6-dimethylaniline (**49**),[73] PIB-carboxylic acid (**50**),[142] and PIB-phenol (**55**)[34] were synthesized by following synthesis procedure in the literature.

Synthesis of PIB_{1000}-bound phosphonic acid (51). 10 g (10 mmol) of PIB_{1000}-iodide **59** was mixed with triethyl phosphite (50 mL) in a 250-mL, one-necked, round-bottomed flask and stirred under reflux (150 ^oC) for 8 h under nitrogen. After completion of the reaction, excess triethylphosphite was removed under reduced pressure using a rotary evaporator. The crude was purified by silica gel column chromatography. It was flushed first with hexane to remove inactive PIB and then flushed with ethyl acetate/hexane (1/19)

to yield the product. The solution was dried over anhydrous sodium sulfate and removed under reduced pressure using a rotary evaporator to give 7.5 g (75% yield) of PIB_{1000}-CH_2-$PO(OC_2H_5)_2$. ^{1}H NMR (500 MHz, $CDCl_3$) δ 4.12-4.06 (m, 4 H), 1.7 (m, 1 H), 1.53 (m, 1 H), 1.4-0.8 (m, 140 H), ^{13}C NMR (125 MHz, $CDCl_3$) δ multiple peaks at 60-58.1, 38.1-37.7, and 32.5-30.8. ^{31}P NMR (121 MHz, $CDCl_3$) 32.2. IR (neat, cm^{-1}): 2949, 2893, 1470, 1389, 1366, 1229, 1028, 953. 1 g (1.0 mmol) of PIB_{1000}-CH_2-$PO(OC_2H_5)_2$ was dissolved in 5 mL of dichloromethane in a 25-mL, one-necked, round-bottomed flask. 0.46 g (3 mmol) of bromotrimethylsilane was added and the mixture was allowed to stir under nitrogen for 12 h at room temperature. After removing volatile species under reduced pressure using a rotary evaporator, 5 mL of heptane and 5 mL of methanol were added and the mixture was allowed to stir vigorously for 2 h at room temperature. The heptane layer was washed by methanol (5 mL × 3) and dried over anhydrous sodium sulfate and the solvent was removed under reduced pressure using a rotary evaporator to give 0.7 g (74% yield) of **51**. ^{1}H NMR (500 MHz, $CDCl_3$) δ 1.7 (m, 2 H), 1.4-0.8 (m, 140 H), ^{13}C NMR (125 MHz, $CDCl_3$) δ multiple peaks at 60-58.2, 38.5-33.4, and 31.2-30.8. ^{31}P NMR (121 MHz, $CDCl_3$) 35.3. IR (neat, cm^{-1}): 2976, 2949, 2893, 1734, 1653, 1474, 1389, 1366, 1231, 908.

Synthesis of PIB_{2300}-bound hydroxamic acid (**52**). PIB_{2300}-carboxylic acid (**50**) (1.5 g, 0.65 mmol) was allowed to react with 1.95 mmol of l,l'-carbonyldiimidazole in 15 mL of CH_2Cl_2 for 12 h at room temperature. At this point, an aliquot of solution was analyzed by ^{1}H-NMR to determine the complete consumption of **50**. DCM solution was washed

with 5 mL of 1M HCl aqueous solution 2 times, 5 mL of saturated $NaHCO_3$ aqueous solution 2 times, and then 5 mL of brine once. The solution was dried over anhydrous sodium sulfate and the solvent was removed under reduced pressure using a rotary evaporator to give 1.45 g (95% yield) of PIB_{2300}-bound carbonylimidazole. ^{1}H NMR (500 MHz, $CDCl_3$) δ 8.30 (s, 1 H), 7.57 (s, 1 H), 7.06 (s, 1 H), 1.40-0.90 (m, 360 H). 20 mL DCM solution dissolving 1.45 g of previous synthesized PIB_{2300}-bound carbonylimidazole was added to 10 mL of methanol solution containing freshly prepared *o*-benzylhydroxylamine (To prepare this solution, 600 mg of *o*-benzylhydroxylamine hydrochloride was added to methanol solution containing 1 equivalent of KOH to form KCl precipitate immediately. The filtrate was ready for use, after filtering the mixture through a pipet with cotton plug). The solution was allowed to magnetically stir under N_2 atmosphere for 24 h at room temperature. After the reaction, the solvent was removed under reduced pressure using a rotary evaporator. The residue was dissolved in 30 mL of hexane and washed with 10 mL of 1M HCl aqueous solution twice, 10 mL of saturated $NaHCO_3$ aqueous solution twice, and then 10 mL of 9/1 ethanol/water three times. The solution was dried over anhydrous sodium sulfate and the solvent was removed under reduced pressure using a rotary evaporator to provide 1.25 g (86% yield) of product PIB_{2300}-bound *o*-benzylhydroxamic acid. ^{1}H NMR (500 MHz, $CDCl_3$) δ 8.09 (br, 1 H), 7.40-7.36 (m, 5 H), 4.90 (d, J = 9.5 Hz, 2 H), 1.40-0.90 (m, 360 H). ^{13}C NMR (125 MHz, $CDCl_3$) δ 175.9, 135.3, 129.3,128.6, 77.9, multiple peaks at 60-58.1, 38.5-37.5, and 33-30.8. IR (neat, cm^{-1}): 2972, 2949, 2891, 1668, 1487, 1472, 1456, 1389, 1366, 1231, 907. 0.4 g of PIB_{2300}-bound *o*-benzylhydroxamic acid and 15 mg of palladium on carbon (10%

Pd on carbon) was mixed with 5 mL of THF and 2 mL of MeOH. This mixture was allowed to stir under 1 atm of H_2 overnight at room temperature. The catalyst was removed by filtration and the solvent was removed under reduced pressure using a rotary evaporator to yield 0.37 g (95%) product **52**. ^{1}H NMR (500 MHz, $CDCl_3$) δ 8.29 (br, 1 H), 1.40-0.90 (m, 360 H). ^{13}C NMR (125 MHz, $CDCl_3$) δ 176.2, multiple peaks at 60-58, 38.5-37.5, and 33-30.8. IR (neat, cm^{-1}): 3387, 2974, 2949, 2891, 2358, 2341, 1653, 1474, 1389, 1366, 1231, 1072.

Syntheses of PIB_{1000}- and PIB_{2300}-bound catechol (53). 10 g (10 mmol) of PIB_{1000}-alkene was dissolved in 100 mL of dichloromethane in a round-bottomed flask, then 11 g (100 mmol) of catechol and 3 mL of sulfuric acid were added and the mixture was allowed to stir for 12 h at room temperature. After the reaction, the reaction mixture was filtered and the solvent was removed under reduced pressure using a rotary evaporator. The residue was dissolved in 150 mL of hexane, first washed with 30 mL DMF once and then with 50 mL of 9/1 ethanol/water three times. The hexane layer was dried over anhydrous sodium sulfate and concentrated to give crude product. The crude product was further purified by silica-gel column chromatography (hexane was used as eluent to flush out unreacted and saturated PIB first and then hexane/ethyl acetate (19/1) was used to flush out the product) to furnish 7.3 g (67% yield) of PIB_{1000}-catechol **53**. ^{1}H NMR (500 MHz, $CDCl_3$) δ 6.88 (br, 1 H), 6.77 (br, 2 H), and 1.40-1.00 (m, 140 H). ^{13}C NMR (125 MHz, $CDCl_3$) δ 143.5, 142.9, 140.7, 118.4, 114.9, 113.5, 44.7, 37.2, 31.9, 30.4, 29.7, 29.6, 29.4, 29.1, 24.7, 22.7, 14.1. IR (neat, cm^{-1}): 3374, 2951, 2893, 1707, 1605, 1468, 1389, 1366,

1228. PIB_{2300}-catechol was synthesized using the same procedure as PIB_{1000}-catechol but using 23 g of (10 mmol) of PIB_{2300}-alkene instead. After the reaction and purification, 18.2 g (75% yield) of PIB_{2300}-catechol **53** was obtained. ^{1}H NMR (500 MHz, $CDCl_3$) δ 6.88 (d, *J* = 2 Hz, 1 H), 6.77 (d, *J* = 2 Hz, 1 H), 6.77 (s, 1 H), and 1.40-0.90 (m, 360 H). ^{13}C NMR (125 MHz, $CDCl_3$) δ 143.5, 142.9, 140.7, 118.4, 114.9, 113.5, 44.7, 37.2, 31.9, 30.4, 29.7, 29.6, 29.4, 29.1, 24.7, 22.7, 14.1. IR (neat, cm^{-1}): 3375, 2949, 2891, 1472, 1389, 1366, 1229, 949, 924.

Synthesis of PIB_{2300}-bound veratrole (54). A solution of PIB_{2300}-alkene (5 g, 2.2 mmol) in 10 mL of veratrole was carefully combined with 3 mL of concentrated H_2SO_4 at room temperature and this reaction mixture was stirred at room temperature for 24 h. The solvent was removed under reduced pressure using a rotary evaporator. The resulting organic residue/product was dissolved in 50 mL of hexane and washed with 20 mL of 9/1 ethanol/water five times, and dried over anhydrous Na_2SO_4. The crude product was obtained after the removal of solvent. The crude was further purified by silica-gel column chromatography (hexane was used as eluent to flush out unreacted and saturated PIB first and then hexane/ethyl acetate (19/1) was used to flush out the product) to give 3.7 g (70% yield) of **54**. ^{1}H NMR (500 MHz, $CDCl_3$) δ 6.89 (s, 1 H), 6.87 (d, *J* = 8 Hz, 1 H), 6.78 (d, *J* = 8 Hz, 1 H), 3.89 (s, 3 H), 3.86 (s, 3 H), 1.60-0.80 (m, 380 H); ^{13}C NMR (125 MHz, $CDCl_3$) δ 148.1, 146.6, 143.0, 118.1, 110.4, 110.2, 59.5-58.2 (multiple peaks), 55.9, 55.8, 38.4-37.8 (multiple peaks), 32.5-30.6 (multiple peaks). IR (neat, cm^{-1}): 2949, 2893, 1589, 1516, 1468, 1389, 1366, 1256, 1229, 1150, 1032, 949, 922.

Synthesis of 4-(2-Methylnonadecan-2-yl)benzene-1,2-diol (56). A mixture containing 55% of 2-methyl-1-octadecene and 45% of 2-methyl-2-octadecene was prepared by following the procedure reported in the literature.[155] 840 mg (3 mmol) of this mixture and 1.65 g (15 mmol) of catechol were dissolved in 20 mL of DCM, 3 mL of H_2SO_4 was added and the mixture was allowed to stir for 4 h under N_2 atmosphere at room temperature. After the reaction, the solvent was removed at reduced pressure using a rotary evaporator and the residue was added with 30 mL of hexane. After the hexane solution was washed with 15 mL of 9/1 of ethanol/water three times, the solvent was removed under reduced pressure using a rotary evaporator to give crude product. The desired product was recrystallized in pentane to give 400 mg (35% yield) of **56**. ^{1}H NMR (500 MHz, $CDCl_3$) δ 6.85-6.68 (m, 3 H), 1.77-1.73 (m, 1 H), 1.51 (m, 2 H) 1.40-1.20 (m, 35 H), 0.88 (t, *J* = 11 Hz, 3 H). ^{13}C NMR (125 MHz, $CDCl_3$) δ 143.5, 142.9, 140.7, 118.3, 114.8, 113.4, 44.6, 37.2, 31.9, 30.4, 29.6, 29.4, 29.1, 24.7, 22.6, 14.1. IR (neat, cm^{-1}): 3466, 3352, 2918, 2849, 1607, 1521, 1508, 1471, 1464, 1366, 1306, 1292, 1283, 806, 783; mp: 56-58 ºC.

Synthesis of PIB_{1000}- and PIB_{2300}-bound iodide (**59**). In a 250-mL round-bottomed flask charged with a stir bar, 25.0 g (25 mmol) of PIB_{1000}-bound alcohol **31** was dissolved in 100 mL of DCM. To this solution, 8.1 g (32.5 mmol) of iodine, 8.5 g of (32.5 mmol) triphenylphosphine, and 2.2 g of (32.5 mmol) imidazole were added and the solution was stirred overnight at room temperature under N_2. The orange solution was filtered, and solvent was removed under reduced pressure using a rotary evaporator. The product was purified by silica gel column chromatography (hexane as eluent) to afford 22.1 g (88%

yield) of PIB_{1000}-bound iodide **59** as a colorless viscous oil. ^{1}H NMR (500 MHz, $CDCl_3$) δ 3.19 (dd, *J* = 11.8, 5.3 Hz, 1 H), 3.05 (dd, *J* = 11.8, 8.3 Hz, 1 H), 0.87-1.47 (m, 140 H). ^{13}C NMR (125 MHz, $CDCl_3$) δ multiple poorly resolved peaks between 60-58, 38-37, and 32-29. PIB_{2300}-iodide was synthesized by a similar procedure. 46.0 g (20 mmol) of PIB_{2300}-bound alcohol was dissolved in 200 mL of DCM. To this solution, 3.2 g (12.6 mmol) of iodine, 6.0 g of (22.9 mmol) triphenylphosphine, and 1.6 g of (23.5 mmol) imidazole were added and the solution was stirred for 12 h at room temperature under N_2. After the completion of the reaction, solvent was removed under reduced pressure using a rotary evaporator and the viscous mass was dissolved in 200 mL of hexane and washed with 150 mL of DMF (50 mL x 3) and then 9/1 ethanol/water (50 mL x 5). The alkane phase was dried over anhydrous sodium sulfate and the solvent was removed under reduced pressure using a rotary evaporator to give 41.4 g (90% yield) of PIB_{2300}-bound iodide **59** as a colorless viscous oil. ^{1}H NMR (500 MHz, $CDCl_3$) δ 3.25 (dd, *J* = 9.3, 4.2 Hz, 1 H), 3.12 (dd, *J* = 9.3, 6.8 Hz, 1 H), 1.8 (s, 2 H), 1.6-0.8 (m, 320 H). ^{13}C NMR (75 MHz, $CDCl_3$) δ multiple peaks between 60-58, 38.5-38, and 33-30.1.

Studies of comparative solubilization of MNPs with ligands 25, 26, 31, 48-56 and stearic acid. 4.0 mg of Fe_3O_4 nanoparticles were mixed with 4 mL of cyclohexane in a 20-mL test tube. The test tube was sonicated at 40 ^{o}C for 75 min. Then 0.1 mL of 3% ammonium hydroxide aqueous solution and 0.04 mmol of a PIB_{1000}- or PIB_{2300}-functionalized ligand, stearic acid, or **56** in 6 mL of cyclohexane was added to the test tube. The reaction mixture was then sonicated for 1 h at 40 °C. At this point, the sonication

was stopped and the reaction mixture was centrifuged at 3200 rpm for 15 min. A small portion (0.3 mL) of the supernatant was removed and diluted with 2.4 mL of cyclohexane. The diluted solution was analyzed by UV-Visible spectrometer to record the absorbance at 380 nm. The remainder of the reaction mixture was placed back in the sonication bath at 40 °C and the sonication was continued for an additional 3 h. At this point, the sonication was stopped and the reaction mixture was centrifuged at 3200 rpm for 15 min. A small portion (0.3 mL) of the supernatant was removed and diluted with 2.4 mL of cyclohexane. The diluted solution was analyzed by UV-Visible spectrometer to record the absorbance at 380 nm.

General procedures for optimization of the concentration of soluble modified MNPs using different PIB-catechol/MNP weight ratios with either PIB_{1000} or PIB_{2300} ligands. A sample of Fe_3O_4 nanoparticles (the weight of the Fe_3O_4 nanoparticles to PIB-catechol used is shown in Table 5) was mixed with 10 mL of cyclohexane in a 50 mL, two-necked, round-bottomed flask. The mixture was sonicated at 40 ^oC for 75 min, at which point 0.1 mL of 30% ammonium hydroxide aqueous solution and PIB_{1000}-catechol or PIB_{2300}-catechol in 15 mL of cyclohexane were added to the flask. The reaction mixture was sonicated for another 75 min, at this point, the flask was transferred to a heating bath and the reaction mixture was magnetically stirred at 40 ^oC for an additional 12 h. The solvent was removed at reduced pressure using a rotary evaporator and the residue was suspended in 30 mL of heptane. The magnetic solid and the magnetic oil were isolated

from this suspension by two different methods – magnetic decantation (Method A) and centrifugation (Method B) as described in Scheme 22 and the text in Chapter IV.

Multigram scale preparation of PIB-catechol grafted MNPs. A 10 g portion of Fe_3O_4 nanoparticles were mixed with 100 mL of cyclohexane in a 500-mL two-necked round-bottomed flask. The mixture was sonicated at 40 ^oC for 75 min at which point 1 mL of 3% ammonium hydroxide aqueous solution and 10 g of PIB_{1000}-catechol in 150 mL of cyclohexane were added. Sonication of the mixture was continued at 40 ^oC for 24 h. Then the magnetic solid and the magnetic oil were separated by Method C as described in Scheme 22. During the reaction, the kinetics of the reactions were monitored by UV-Visible spectrometer as described above by taking aliquots of the reaction mixture. Reactions with the PIB_{2300}-catechol used the same procedure except that reactions with PIB_{2300}-catechol used 5 g of the MNPs and 11.5 g of the PIB_{2300}-catechol.

General procedures for stability tests of PIB_{2300}-catechol modified magnetic oil stability of a biphasic mixture of a 50 wt% PIB_{2300}-catechol modified MNP/cyclohexane solution and water. 3 mg of the PIB_{2300}-catechol modified magnetic oil was dissolved in 10 mL of cyclohexane in a 50-mL sample vial. Then 10 mL of DI water and a magnetic stir bar were added and the resulting mixture was stirred at room temperature in a sealed vial. The optical density of the cyclohexane phase was monitored periodically (as shown in Figure 23).

Stability of a biphasic mixture of a 50 wt% PIB_{2300}-catechol modified MNP/cyclohexane solution and a 1 M aqueous NaOH solution. 3 mg of the PIB_{2300}-catechol modified magnetic oil was dissolved in 10 mL of cyclohexane in a 50-mL sample vial. Then 10 mL of 1 M NaOH aqueous solution and a magnetic stir bar were added and the resulting mixture was allowed to stir at room temperature in a sealed vial. The optical density of the cyclohexane phase was monitored periodically.

Stability of a biphasic mixture of a 50 wt% PIB_{2300}-catechol modified MNP/cyclohexane solution and a 1 M aqueous NaOH solution. 3 mg of the PIB_{2300}-catechol modified magnetic oil was dissolved in 10 mL of cyclohexane in a 50-mL sample vial. Then 0.5 mmol of catechol was dissolved in 10 mL of a 1.0 M NaOH aqueous solution. This basic solution was added to the cyclohexane solution and the resulting mixture was allowed to stir at room temperature in a sealed vial. The optical density of the cyclohexane phase was monitored periodically as shown in Figure 23.

Stability of a biphasic mixture of a 50 wt% PIB_{2300}-catechol modified MNP/cyclohexane solution and a 1 M aqueous HCl solution. 3 mg of the PIB_{2300}-catechol modified magnetic oil was dissolved in 10 mL of cyclohexane in a 50-mL sample vial. Then 10 mL of a 1 M HCl aqueous solution and a magnetic stir bar were added and the resulting mixture was allowed to stir at room temperature in a sealed vial. The optical density of the cyclohexane phase was monitored periodically as shown in Figure 23.

General procedure for testing PIB_{1000}-catechol modified magnetic oil in organic solvents. 500 mg of PIB_{1000}-catechol modified magnetic oil was dissolved in 5 mL of various solvents in 20 mL sample vials to visually test the magnetic oil's solubility. Pictures of these vials are shown in Figure 24.

General procedure of mixing PIB-catechol modified magnetic nanoparticles with Polywax and PAOs. (a) Preparation of magnetic Polywax. 0.5 g of the magnetic oil was added to a 20-mL test tube and placed in an oil bath. 5 g of polyethylene oligomer (Polywax from Baker Hughes, M_n = 400 Da) was then added and the test tube was heated in the oil bath at 90 ^oC with occasional swirling for 15 min. The Polywax melted and mixed with the magnetic oil to form a homogeneous solution. After cooling a solid brownish wax formed. Cryogenic grinding then produced a magnetically susceptible dark brown polyethylene powder. **(b) Preparation of magnetic PAOs.** 0.2 g of the magnetic oil was put in a 20-mL vial and placed in an oil bath. 2 g of PAO 10 or PAO 40 was added to the vial and the vial was heated in the oil bath at 100 ^oC with occasional swirling for 10 min. The heated PAOs mixed with the magnetic oil to form homogeneous solutions. After cooling, magnetically susceptible a dark brown viscous oil formed.

General procedure of acquiring TEM images of PIB-catechol modified magnetic nanoparticles in PAO 40. An aliquot of the mixture of the magnetic oil in PAO 40 was dissolved in 10 mL of heptane. The heptane solution was sonicated for 1 min and then deposited on the cupper grid via a pipet. After the heptane was evaporated, the sample was

ready for analysis by TEM. An aliquot of the mixture of the magnetic solid in PAO 40 was dissolved in 10 mL of heptane. The heptane solution was sonicated for 1 min and then deposited on the cupper grid via a pipet. After the heptane was evaporated, the sample was ready for analysis by TEM.

Synthesis of octadecyldimethylsilated silica nanoparticles. 200 mg of silica nanoparticles, 0.12 mL of pyridine, 5.0 mL of toluene, and 0.35 g of octadecyldimethylchlorosilane were placed into a 25-mL round-bottomed flask. The mixture was stirred at 110 ^{o}C for 24 h. After the reaction, the solvent was removed under a reduced pressure using a rotary evaporator and the residue was suspended in 10 mL of heptane. The suspension was then centrifuged at 3200 rpm for 10 min. 80 vol% of the supernatant was removed and heptane was refilled to the original amount. The mixture was sonicated for 1 min then the resulting suspension was centrifuged at 3200 rpm for 10 min. 80 vol% of the supernatant was removed and heptane was refilled to the original amount. The mixture was sonicated for 1 min then the resulting suspension was centrifuged at 3200 rpm for 10 min. 80 vol% of the supernatant was then removed. All three supernatants were then combined and concentrated under vacuum at room temperature for 12 h to give a waxy solid. 2907, 2814, 1482, 1076, 802, 781. The precipitate from the centrifugation was dried under vacuum at room temperature for 12 h as a white solid. IR (neat, cm^{-1}): 2905, 2813, 1482, 1074, 802, 781.

Synthesis of aminated silica nanoparticles. 5 g of silica nanoparticles (SiO_2, 10~20nm, 99.5%, non-porous from SkySpring Nanomaterials) were first cleaned by placing them in 100 mL of 5% hydrochloric acid at room temperature overnight. The silica nanoparticles were then recovered by filtration, washed with water, and dried under vacuum at room temperature for 12 h. The dried silica nanoparticles were then added to a 10 wt% solution of 3-aminopropyltriethoxysilane in 100 mL of toluene. This mixture was heated to reflux overnight. The product aminated silica nanoparticles were isolated by filtration, washed with THF and MeOH then dried under vacuum at room temperature for 12 h. 5.5 g of product was obtained. Titrimetric analysis of the aminated silica nanoparticles was carried out by first suspending 300 mg of aminated silica nanoparticles in a 30 mL of 0.02 M HCl solution and shaking the mixture for 1 h. 15 mL of the resulting HCl solution was taken out and separated into three portions with equal volume. A known volume of this HCl solution was then titrated with a 0.01 M NaOH solution to a pH 9 endpoint using phenolphthalein as a pH indicator. In this way, the amount of HCl consumed by basic groups on the aminated silica nanoparticles could then be determined by using the equation shown below. These aminated silica nanoparticles had amine loadings of 1.02 mmol of amines/g. IR (neat, cm^{-1}): 1074, 802.

$$amine\ density\ = \frac{V_{\mathrm{HCl}} \times M_{\mathrm{HCl}} - V_{\mathrm{NaOH}} \times M_{\mathrm{NaOH}}}{Weight\ of\ aminated\ silica\ nanoparticle}$$

As an example, 394 mg aminated silica nanoparticles were weight and soaked in 30 mL of 0.02 M HCl.10 mL of this HCl solution was then titrated with 6.6 mL of 0.01 M NaOH solution. So the amine density of the silica nanoparticles equals to ((10 (mL) × 0.02 (M))-(6.6 (mL) × 0.01 (M))) × 3 / 394 (mg) = 1.02 mmol/g

Synthesis of thiol-modified silica nanoparticles. 5 g of silica nanoparticles (20 nm in diameter) were first cleaned by placing them in 100 mL of 5% hydrochloric acid at room temperature overnight. The silica nanoparticles were then recovered by filtration, washed with water, and dried under vacuum at room temperature for 12 h. The dried silica nanoparticles were then added to a 10 wt% solution of 3-mercaptopropyltrimethoxysilane in 100 mL of toluene. This mixture was heated to reflux overnight. The product thiol modified silica nanoparticles were isolated by filtration, washed with THF and MeOH then dried under vacuum. 5.2 g of product was obtained. IR (neat, cm^{-1}): 1074, 802.

Synthesis of PIB-modified silica nanoparticles via a thiol-ene reaction. 420 mg of thiol-modified silica nanoparticles, 1.07 g of PIB_{1000}-alkene, and 16 mg of AIBN were mixed in 15 mL of hexane and 15 mL of ethanol. The mixture was sonicated for 10 min and then allowed to stir for 8 h with the exposure of 365 nm UV light. After the reaction, the solvent was removed at reduced pressure using a rotary evaporator and the residue was suspended in 10 mL of heptane. The suspension was then centrifuged at 3200 rpm for 10 min. 80 vol% of the supernatant was removed and heptane was refilled to the original amount. The mixture was sonicated for 1 min then the resulting suspension was centrifuged at 3200 rpm for 10 min. 80 vol% of the supernatant was removed again and heptane was refilled to the original amount. The mixture was sonicated for 1 min then the resulting suspension was centrifuged at 3200 rpm for 10 min. 80 vol% of the supernatant was then removed. All three supernatants were then combined and concentrated under

reduced pressure using a rotary evaporator at room temperature for 12 h to give an oil. IR (neat, cm^{-1}): 2949, 2893, 1471, 1389, 1366, 1229, 1089, 951, 812. The precipitate from the centrifugation was dried under vacuum at room temperature for 12 h as a white solid. IR (neat, cm^{-1}): 1080, 799.

Synthesis of PIB-uridopropyltriethoxysilane (57). 3.3 g of 3-(triethoxysilyl)propyl isocyanate in 50 mL of DCM was added dropwise to 11 g of PIB_{1000}-NH_2 in 150 mL of DCM via an addition funnel. The solution was allowed to stir at room temperature under N_2 for 24 h. After the reaction, the solvent was removed under reduced pressure by a rotary evaporator. The residue was dissolved in 150 mL of hexane and washed with 50 mL of 90% aqueous ethanol three times. The hexane phase was dried over Na_2SO_4 and the solvent was removed under reduced pressure using a rotary evaporator to yield 11.3 g of product. ^{1}H NMR (300 MHz, $CDCl_3$) 4.38 (t, *J* = 5.7 Hz, 1 H), 4.25 (t, *J* = 5.7 Hz, 1 H), 3.82 (q, *J* = 7.0 Hz, 6 H), 3.17 (q, *J* = 6.6 Hz, 2 H), 3.07 (m, 1 H), 2.89 (m, 1 H) 1.40-1.00 (m, 142 H), 0.64 (t, *J* = 8.1 Hz, 2H). ^{13}C NMR (125 MHz, $CDCl_3$) δ 158.5, multiple peaks at 60-58.2, 38.5-33.4, and 31.2-30.8. IR (neat, cm^{-1}): 2924, 1636, 1570, 1468, 1389, 1366, 1252, 1231, 1076, 1049.

Synthesis of PIB-uridopropyltriethoxysiliane modified silica nanoparticles for TGA. 100 mg of silica nanoparticles and 500 mg of **57** were mixed with 10 mL of heptane and 10 mL of absolute ethanol in a 50 mL, two-necked, round-bottomed flask. The mixture was sonicated at 40 ^{o}C for 30 min, at this point, the flask was transferred to a heating bath

and the reaction mixture was magnetically stirred at 40 ^{o}C for an additional 12 h. The solvent was removed at reduced pressure using a rotary evaporator and the residue was suspended in 10 mL of heptane. The suspension was then centrifuged at 3200 rpm for 10 min. 80 vol% of the supernatant was removed and heptane was refilled to the original amount. The mixture was sonicated for 1 min then the resulting suspension was centrifuged at 3200 rpm for 10 min. 80 vol% of the supernatant was removed and heptane was refilled to the original amount. The mixture was sonicated for 1 min then the resulting suspension was centrifuged at 3200 rpm for 10 min. 80 vol% of the supernatant was then removed. All three supernatants were then combined and concentrated under reduced pressure using a rotary evaporator at room temperature for 12 h to give an oil. The precipitate from the centrifugation was dried under vacuum at room temperature for 12 h as a white solid.

Synthesis of PIB carbonyl ethylcarbonate (61). To a solution of PIB_{1000} acid (500 mg, 0.5 mmol) and pyridine (261 mg, 3.3 mmol) in DCM (15 ml) at 0 ^{o}C was added ethyl chloroformate (60 mg, 0.55 mmol). After 5 min of stirring, catalytic amount of DMAP was added into the reaction mixture. The resulting solution was stirred at 0 ^{o}C for 0.5 h, diluted with DCM (20 mL), and washed with saturated $NaHCO_3$ (10 mL), 0.1 M HCl (l0 mL), and saturated NaCl(10 mL). The DCM solution was dried over anhydrous Na_2SO_4, and evaporated under reduced pressure using a rotary evaporator to give 400 mg of **61**. ^{1}H NMR (300 MHz, $CDCl_3$) 4.31 (q, J = 7.2 Hz, 2 H), 2.42 (s, 1 H), 1.77 (s, 1 H), 1.40-1.00 (m, 143 H). ^{13}C NMR (75 MHz, $CDCl_3$) δ 173.5, 166.4, 65.3, 65.4, multiple peaks at 60-

58.2, 38.5-33.4, and 31.2-30.8. IR (neat, cm^{-1}): 2949, 2891, 1809, 1734, 1472, 1389,1366, 1339, 1227, 951, 812.

Synthesis of PIB_{1000}-trimethoxysilylpropylthioether (62). Vinyl terminated PIB_{1000} (5 g, 5 mmol, 1 equiv), 3-mercaptopropyltriethoxysilane (3.57 g, 15 mmol, 3 equiv), and AIBN (0.08g, 0.5 mmol, 0.1 equiv) were dissolved in 40 mL of hexane and 25 mL of absolute alcohol. The solution was stirred at ambient temperature with exposure of 365 nm light for 8 h. After the reaction was complete, water was added to the solution to perturb the system to form two layers. The hexane layer was washed by 90% aqueous ethanol for 3 times and dried by Na_2SO_4. The solvent was removed under reduced pressure using a rotary evaporator to give 4.5 g of the product. ^{1}H NMR (500 MHz, $CDCl_3$) 3.57 (s, 9 H), 2.49 (dd, *J* = 12.5, 8.5, 1 H), 2.33 (s, *J* = 12.5, 8.5, 1 H), 1.40-1.00 (m, 140 H). ^{13}C NMR (75 MHz, $CDCl_3$) δ 173.5, 166.4, 65.3, 65.4, multiple peaks at 60-58.2, 38.5-33.4, and 31.2-30.8. IR (neat, cm^{-1}): 2949, 2891, 1389, 1365, 1229, 1107, 1067, 951, 922.

Synthesis of dansyl dye-grafted silica nanoparticle. 1.0 g of aminated silica nanoparticles were dispersed in 30 mL of DCM. 40 mg (0.15 mmol) of dansyl chloride in 10 mL of DCM was added to the DCM suspension, and then 1 mL of triethylamine was added. The mixture was allowed to sonicate at 40 ^{o}C for 12 h. After the reaction, the mixture was filtered and washed with DCM until the filtrate does not show fluorescence to give a white solid. The filtered solid was recovered and dried under vacuum to give 0.9

g of dansyl dye-grafted silica nanoparticles as yellowish solid. IR (neat, cm^{-1}): 1620, 1541, 1037, 787, 694.

Studies of comparative solubilization of silica nanoparticles with ligands 50, 60, and 61. 10 mg of silica nanoparticles were weighed and put in a 20-mL test tube. 0.05 mmol of a PIB_{1000}-functionalized ligand in 10 mL of heptane was added to the test tube. The test tube was sonicated at 40 ^{o}C for 1 h. At this point, the sonication was stopped and the reaction mixture was centrifuged at 3200 rpm for 10 min. The supernatant was analyzed by fluorescence spectrometer to record the fluorescence intensity at 450 nm with excitation wavelength at 340 nm. After the measurement, the supernatant was added back to the test tube and the reaction mixture was placed back in the sonication bath at 40 °C and the sonication was continued for an additional 3 h. At this point, the sonication was stopped and the reaction mixture was centrifuged at 3200 rpm for 10 min. The supernatant was analyzed by fluorescence spectrometer to record the fluorescence intensity at 450 nm with excitation wavelength at 340 nm.

General procedures for preparing PIB-modified silica nanoparticles using different PIB_{1000}-ligands for TGA. A sample of silica nanoparticles and a PIB-ligand (the weight of the silica nanoparticles to PIB-ligand used is shown in Table 8 and 9) was mixed with 20 mL of heptane in a 50 mL, two-necked, round-bottomed flask. The mixture was sonicated at 40 ^{o}C for 12 h. The solvent was removed at reduced pressure using a rotary evaporator and the residue was suspended in 10 mL of heptane. The suspension was then

centrifuged at 3200 rpm for 10 min. 80 vol% of the supernatant was removed and heptane was refilled to the original amount. The mixture was sonicated for 1 min then the resulting suspension was centrifuged at 3200 rpm for 10 min. 80 vol% of the supernatant was removed and heptane was refilled to the original amount. The mixture was sonicated for 1 min then the resulting suspension was centrifuged at 3200 rpm for 10 min. 80 vol% of the supernatant was then removed. All three supernatants were then combined and concentrated under reduced pressure using a rotary evaporator at room temperature for 12 h to give an oil. The precipitate from the centrifugation was dried under vacuum at room temperature for 12 h as a white solid.

Stability of dansyl dye-grafted silica nanoparticles in heptane. 10 mg of the dansyl dye-grafted silica nanoparticles were mixed with 10 mL of heptane in a 20-mL test tube. The test tube was sonicated at 40 ^{o}C for 1 h. At this point, the sonication was stopped and the reaction mixture was centrifuged at 3200 rpm for 10 min. The supernatant was analyzed by fluorescence spectrometer to record the fluorescence intensity at 450 nm with excitation wavelength at 340 nm. After the measurement, the supernatant was added back to the test tube and the reaction mixture was placed back in the sonication bath at 40 °C and the sonication was continued for an additional 3 h. At this point, the sonication was stopped and the reaction mixture was centrifuged at 3200 rpm for 10 min. The supernatant was analyzed by fluorescence spectrometer to record the fluorescence intensity at 450 nm with excitation wavelength at 340 nm.

Stability of dansyl dye-grafted silica nanoparticles in heptane in the presence of triethylamine. 10 mg of the dansyl dye-grafted silica nanoparticles were mixed with 10 mL of heptane in the presence of 25, 50, or 100 μL of triethylamine a 20-mL test tube. The test tube was sonicated at 40 ºC for 1 h. At this point, the sonication was stopped and the reaction mixture was centrifuged at 3200 rpm for 10 min. The supernatant was analyzed by fluorescence spectrometer to record the fluorescence intensity at 450 nm with excitation wavelength at 340 nm. After the measurement, the supernatant was added back to the test tube and the reaction mixture was placed back in the sonication bath at 40 °C and the sonication was continued for an additional 1 h. At this point, the sonication was stopped and the reaction mixture was centrifuged at 3200 rpm for 10 min. The supernatant was analyzed by fluorescence spectrometer to record the fluorescence intensity at 450 nm with excitation wavelength at 340 nm. After the measurement, the supernatant was added back to the test tube and the reaction mixture was placed back in the sonication bath at 40 °C and the sonication was continued for an additional 2 h. At this point, the sonication was stopped and the reaction mixture was centrifuged at 3200 rpm for 10 min. The supernatant was analyzed by fluorescence spectrometer to record the fluorescence intensity at 450 nm with excitation wavelength at 340 nm.

Synthesis of PEI-modified MWNTs. 2 g of MWNTs (95%, 20-30 nm, purchased from SkySpring) and 10 g of polyethylenimine (branched, M_w = 25,000 by LS, M_n = 10,000 by GPC, purchased from SigmaAldrich) were mixed in 100 mL of DMF. The mixture was sonicated for at 50 ˚C for 72 h. The resulting suspension was filtered by a 0.20 μm nylon

membrane, and the precipitate was washed with 1 M HCl, 1 M NaOH, water, and methanol to remove any excess PEI. After the solid was dried under vacuum at room temperature for 12 h, 1.9 g of the product was obtained. Titrimetric analysis of the PEI-modified MWNTs was carried out by first suspending 300 mg of PEI-modified MWNTs in a 20 mL of 0.01 M HCl solution and shaking the mixture for 1 h. 15 mL of the resulting HCl solution was taken out and separated into three portions with equal volume. A known volume of this HCl solution was then titrated with a 0.01 M NaOH solution to a pH 9 endpoint using phenolphthalein as a pH indicator. In this way, the amount of HCl consumed by basic groups on the PEI-modified MWNTs could then be determined by using the equation shown below. These PEI-modified MWNTs had amine loadings of 0.88 mmol of amines/g. IR (neat, cm^{-1}): 1080, 689.

$$amine\ density\ = \frac{V_{\mathrm{HCl}} \times M_{\mathrm{HCl}} - V_{\mathrm{NaOH}} \times M_{\mathrm{NaOH}}}{Weight\ of\ PEI - modified\ MWNTs}$$

CHAPTER VII

CONCLUSIONS

In conclusion, the work reported in this dissertation demonstrates several new strategies to manipulate the solubility of molecules. We used two lipophilic molecules, PIB and octadecyldimethylchlorosilane, as solubility promoters for developing recyclable catalysts, facilitating efficient purification in organic synthesis, and preparing highly nonpolar phase soluble nanoparticles. Chapter II reported the syntheses of several PIB-supported MPcs as phase selective catalysts. A PIB-sulfonyl-supported CoMPc was shown to be an effective and recyclable catalyst for nitroarene reduction using hydrazine hydrate as the reducing agent and an equal volume of heptane and ethylene glycol as the solvent system. Eight nitroarenes were tested in the reduction reaction and were successfully converted to corresponding aminoarenes. The high stability and phase selectivity of this PIB-sulfonyl-supported CoMPc allowed this catalyst to be recycled 10 times and the reactivity of the catalyst did not change as evidenced by kinetic studies. We also synthesized PIB-sulfonyl-supported FeMPc as a catalyst for the oxidation of ethyl phenylhydrazinecarboxylate to ethyl phenylazocarboxylate and PIB-bound Cr(OTf)MPc as a catalyst for the rearrangement reaction of an epoxide to the corresponding aldehyde. These two catalysts were effective for these catalytic reactions but they were not recyclable.

We also demonstrated the use of octadecyldimethylchlorosilane as a recyclable silylation reagent and a purification auxiliary. A procedure using heptane phase selectively

soluble octadecyldimethylsilyl groups to facilitate separations and a procedure for silyl reagent regeneration were developed. The results showed that alcohols and alkynes protected by these groups are phase-selectively soluble in hydrocarbon solvents. In a thermomorphic cyclohexane/DMF system, >96% of the silylated alcohols were in the cyclohexane phase, allowing these compounds to be purified by a simple liquid/liquid extraction. Applications of this silylating agent were extended in a Grignard synthesis and Sonogashira reaction. Octadecyldimethylchlorosilane was utilized in the protection of an alkoxide generated from a Grignard reaction. It was also used to synthesize octadecyldimethylsilylethyne as a reagent and a purification auxiliary in a Pd-catalyzed cross-coupling reaction with an aryl halide.

We also showed that we can utilize the high phase selective solubility of PIB in nonpolar solvent to prepare nanoparticles that are highly soluble in nonpolar solvents. We synthesized a series of PIB-attached ligands to bind to Fe_3O_4 magnetic nanoparticles and studied the varying ability of these ligands to successfully solvate the resulting nanoparrticles. We also developed a separation method to isolate heptane soluble PIB-grafted magnetic nanoparticles as oils. These oils were soluble at concentrations of >50% by weight in organic solvents including alkanes. A heptane solution containing soluble magnetic nanoparticles as low as 1 wt% was found to be separable from water by a magnet. We also showed that the viscous PIB-modified MNP magnetic oil dissolved in poly(α-olefin)s. Similarly, a low melting point PE wax dissolved these same PIB-modified MNPs at 90 ºC giveing a magnetically susceptible PE powder after cooling and cryogenic grinding.

The strategy we used for preparing highly soluble magnetic nanoparticles was extended to prepare highly soluble silica nanoparticles. Silica nanoparticles were directly modified with a PIB-uridotriethoxysilane to prepare the resulting soluble silica nanoparticles. Aminated silica nanoparticles were also prepared and the amine groups were used to react with selected PIB-supported ligands to prepare PIB-supported supported silica nanoparticles. Thiol-modified silica nanoparticles were also synthesized and these thiols were used to react with alkene-terminated PIB via a thiol-ene reaction to prepare PIB-modified silica nanoparticles.

REFERENCES

(1) Narita, A.; Wang, X.-Y.; Feng, X.; Müllen, K. *Chem. Soc. Rev.* **2015**, *44*, 6616.

(2) Wu, J.; Pisula, W.; Müllen, K. *Chem. Rev.* **2007**, *107*, 718.

(3) Lee, J.; Kalin, A. J.; Yuan, T.; Al-Hashimi, M.; Fang, L. *Chem. Sci.* **2017**, *8*, 2503.

(4) Chmil, K.; Scherf, U. *Acta Polym.* **1997**, *48*, 208.

(5) Matsuno, Y.; Shoji, T.; Kim, S.; Chiba, K. *Org. Lett.* **2016**, *18*, 800.

(6) Okada, Y.; Wakamatsu, H.; Sugai, M.; Kauppinen, E. I.; Chiba, K. *Org. Lett.* **2015**, *17*, 4264.

(7) Maity, S. K.; Mann, G.; Jbara, M.; Laps, S.; Kamnesky, G.; Brik, A. *Org. Lett.* **2016**, *18*, 3026.

(8) Paradís-Bas, M.; Tulla-Puche, J.; Albericio, F. *Org. Lett.* **2015**, *17*, 294.

(9) Wooding, A.; Kilner, M.; Lambrick, D. B. *J. Colloid Interface Sci.* **1991**, *144*, 236.

(10) Sahoo, Y.; Pizem, H.; Fried, T.; Golodnitsky, D.; Burstein, L.; Sukenik, C. N.; Markovich, G. *Langmuir* **2001**, *17*, 7907.

(11) Boyer, C.; Whittaker, M. R.; Bulmus, V.; Liu, J.; Davis, T. P. *NPG Asia Mater.* **2010**, *2*, 23.

(12) Otsuka, H.; Nagasaki, Y.; Kataoka, K. *Adv. Drug Deliv. Rev.* **2003**, *55*, 403.

(13) Goulet, P. J. G.; Bourret, G. R.; Lennox, R. B. *Langmuir* **2012**, *28*, 2909.

(14) Liu, L.; Watanabe, H.; Shirai, T.; Fuji, M.; Takahashi, M. *J. Appl. Polym. Sci.* **2012**, *126*, E522.

(15) Honold, T.; Skrybeck, D.; Wagner, K. G.; Karg, M. *Langmuir* **2017**, *33*, 253.

(16) Zubarev, E. R.; Xu, J.; Sayyad, A.; Gibson, J. D. *J. Am. Chem. Soc.* **2006**, *128*, 4958.

(17) Jia, Z.; Yuan, W.; Zhao, H.; Hu, H.; Baker, G. L. *RSC Adv.* **2014**, *4*, 41087.

(18) Khani, M. M.; Abbas, Z. M.; Benicewicz, B. C. *J. Polym. Sci., Part A: Polym. Chem.* **2017**, *55*, 1493.

(19) Zhao, D.; Di Nicola, M.; Khani, M. M.; Jestin, J.; Benicewicz, B. C.; Kumar, S. K. *ACS Macro Lett.* **2016**, *5*, 790.

(20) Li, C.; Han, J.; Ryu, C. Y.; Benicewicz, B. C. *Macromolecules* **2006**, *39*, 3175.

(21) Wang, L.; Cole, M.; Li, J.; Zheng, Y.; Chen, Y. P.; Miller, K. P.; Decho, A. W.; Benicewicz, B. C. *Polym. Chem.* **2015**, *6*, 248.

(22) Kainz, Q. M.; Linhardt, R.; Maity, P. K.; Hanson, P. R.; Reiser, O. *ChemSusChem* **2013**, *6*, 721.

(23) Sha, S.-C.; Zhu, R.; Herbert, M. B.; Kalow, J. A.; Swager, T. M. *J. Polym. Sci., Part A: Polym. Chem.* **2017**.

(24) Sun, W.; Mignani, S.; Shen, M.; Shi, X. *Drug Discov. Today* **2016**, *21*, 1873.

(25) Kainz, Q. M.; Reiser, O. *Acc. Chem. Res.* **2014**, *47*, 667.

(26) Yang, Y.; Achazi, K.; Jia, Y.; Wei, Q.; Haag, R.; Li, J. *Langmuir* **2016**, *32*, 12453.

(27) Abu-Reziq, R.; Alper, H.; Wang, D.; Post, M. L. *J. Am. Chem. Soc.* **2006**, *128*, 5279.

(28) Wang, Y.; Su, P.; Wang, S.; Wu, J.; Huang, J.; Yang, Y. *J. Mater. Chem. B* **2013**, *1*, 5028.

(29) Copéret, C.; Chabanas, M.; Petroff Saint-Arroman, R.; Basset, J.-M. *Angew. Chem. Int. Ed.* **2003**, *42*, 156.

(30) Nishimura, S. *Handbook of heterogeneous catalytic hydrogenation for organic synthesis*; J. Wiley: New York, 2001.

(31) McNamara, C. A.; Dixon, M. J.; Bradley, M. *Chem. Rev.* **2002**, *102*, 3275.

(32) Simison, K. L.; Stokes, C. D.; Harrison, J. J.; Storey, R. F. *Macromolecules* **2006**, *39*, 2481.

(33) Bergbreiter, D. E.; Tian, J.; Hongfa, C. *Chem. Rev.* **2009**, *109*, 530.

(34) Li, J.; Sung, S.; Tian, J.; Bergbreiter, D. E. *Tetrahedron* **2005**, *61*, 12081.

(35) Hongfa, C.; Tian, J.; Bazzi, H. S.; Bergbreiter, D. E. *Org. Lett.* **2007**, *9*, 3259.

(36) Hongfa, C.; Su, H.-L.; Bazzi, H. S.; Bergbreiter, D. E. *Org. Lett.* **2009**, *11*, 665.

(37) Priyadarshani, N.; Liang, Y.; Suriboot, J.; Bazzi, H. S.; Bergbreiter, D. E. *ACS Macro Lett.* **2013**, *2*, 571.

(38) Shaw, M. H.; Twilton, J.; MacMillan, D. W. C. *J. Org. Chem.* **2016**, *81*, 6898.

(39) Prier, C. K.; Rankic, D. A.; MacMillan, D. W. C. *Chem. Rev.* **2013**, *113*, 5322.

(40) Skubi, K. L.; Blum, T. R.; Yoon, T. P. *Chem. Rev.* **2016**, *116*, 10035.

(41) Liang, Y.; Bergbreiter, D. E. *Catal. Sci. Technol.* **2016**, *6*, 215.

(42) Liang, Y.; Bergbreiter, D. E. *Polym. Chem.* **2016**, *7*, 2161.

(43) Liao, K.-S.; Wan, A.; Batteas, J. D.; Bergbreiter, D. E. *Langmuir* **2008**, *24*, 4245.

(44) Allen, A. L.; Tan, K. J.; Fu, H.; Batteas, J. D.; Bergbreiter, D. E. *Langmuir* **2012**, *28*, 5237.

(45) Liao, K.-S.; Fu, H.; Wan, A.; Batteas, J. D.; Bergbreiter, D. E. *Langmuir* **2009**, *25*, 26.

(46) Zhang, Y.; Furyk, S.; Bergbreiter, D. E.; Cremer, P. S. *J. Am. Chem. Soc.* **2005**, *127*, 14505.

(47) Sorokin, A. B. *Chem. Rev.* **2013**, *113*, 8152.

(48) Young, J. G.; Onyebuagu, W. *J. Org. Chem.* **1990**, *55*, 2155.

(49) Villemin, D.; Hammadi, M.; Hachemi, M.; Bar, N. *Molecules* **2001**, *6*, 831.

(50) Xia, Q.-H.; Ge, H.-Q.; Ye, C.-P.; Liu, Z.-M.; Su, K.-X. *Chem. Rev.* **2005**, *105*, 1603.

(51) Esswein, A. J.; Nocera, D. G. *Chem. Rev.* **2007**, *107*, 4022.

(52) Che, C.-M.; Lo, V. K.-Y.; Zhou, C.-Y.; Huang, J.-S. *Chem. Soc. Rev.* **2011**, *40*, 1950.

(53) Ghani, F.; Kristen, J.; Riegler, H. *J. Chem. Eng. Data* **2012**, *57*, 439.

(54) Verma, P. K.; Bala, M.; Thakur, K.; Sharma, U.; Kumar, N.; Singh, B. *Catal. Lett.* **2014**, *144*, 1258.

(55) Sharma, U.; Kumar, N.; Verma, P. K.; Kumar, V.; Singh, B. *Green Chem.* **2012**, *14*, 2289.

(56) Merino, E. *Chem. Soc. Rev.* **2011**, *40*, 3835.

(57) Ferraz, E. R. A. *Front. Biosci.* **2012**, *E4*, 914.

(58) Breuer, M.; Ditrich, K.; Habicher, T.; Hauer, B.; Keßeler, M.; Stürmer, R.; Zelinski, T. *Angew. Chem. Int. Ed.* **2004**, *43*, 788.

(59) Henkel, T.; Brunne, R. M.; Müller, H.; Reichel, F. *Angew. Chem. Int. Ed.* **1999**, *38*, 643.

(60) Li, X.-G.; Huang, M.-R.; Duan, W.; Yang, Y.-L. *Chem. Rev.* **2002**, *102*, 2925.

(61) Jagadeesh, R. V.; Wienhöfer, G.; Westerhaus, F. A.; Surkus, A.-E.; Pohl, M.-M.; Junge, H.; Junge, K.; Beller, M. *Chem. Commun.* **2011**, *47*, 10972.

(62) Dai, X.; Cui, X.; Yuan, H.; Deng, Y.; Shi, F. *RSC Adv.* **2015**, *5*, 7970.

(63) Bauer, I.; Knölker, H.-J. *Chem. Rev.* **2015**, *115*, 3170.

(64) Shokouhimehr, M.; Kim, T.; Jun, S. W.; Shin, K.; Jang, Y.; Kim, B. H.; Kim, J.; Hyeon, T. *Appl. Catal. Gen.* **2014**, *476*, 133.

(65) Islam, S. M.; Ghosh, K.; Roy, A. S.; Molla, R. A.; Salam, N.; Chatterjee, T.; Iqubal, M. A. *J. Organomet. Chem.* **2014**, *772–773*, 152.

(66) Zeynizadeh, B.; Setamdideh, D. *Synth. Commun.* **2006**, *36*, 2699.

(67) Schabel, T.; Belger, C.; Plietker, B. *Org. Lett.* **2013**, *15*, 2858.

(68) Bhaumik, K.; Akamanchi, K. G. *Can. J. Chem.* **2003**, *81*, 197.

(69) Periasamy, M.; Thirumalaikumar, M. *J. Organomet. Chem.* **2000**, *609*, 137.

(70) Swamy, K. C. K.; Kumar, N. N. B.; Balaraman, E.; Kumar, K. V. P. P. *Chem. Rev.* **2009**, *109*, 2551.

(71) Hirose, D.; Taniguchi, T.; Ishibashi, H. *Angew. Chem. Int. Ed.* **2013**, *52*, 4613.

(72) Sharma, U.; Kumar, P.; Kumar, N.; Kumar, V.; Singh, B. *Adv. Synth. Catal.* **2010**, *352*, 1834.

(73) Priyadarshani, N.; Benzine, C. W.; Cassidy, B.; Suriboot, J.; Liu, P.; Sue, H.-J.; Bergbreiter, D. E. *J. Polym. Sci., Part A: Polym. Chem.* **2014**, *52*, 545.

(74) Lowe, A. B. *Polym. Chem.* **2014**, *5*, 4820.

(75) Hoyle, C. E.; Bowman, C. N. *Angew. Chem. Int. Ed.* **2010**, *49*, 1540.

(76) Roskamp, M.; Enders, S.; Pfrengle, F.; Yekta, S.; Dekaris, V.; Dernedde, J.; Reissig, H.-U.; Schlecht, S. *Org. Biomol. Chem.* **2011**, *9*, 7448.

(77) Leznoff, C. C.; Marcuccio, S. M.; Greenberg, S.; Lever, A. B. P.; Tomer, K. B. *Can. J. Chem.* **1985**, *63*, 623.

(78) del Rey, B.; Keller, U.; Torres, T.; Rojo, G.; Agulló-López, F.; Nonell, S.; Martí, C.; Brasselet, S.; Ledoux, I.; Zyss, J. *J. Am. Chem. Soc.* **1998**, *120*, 12808.

(79) Grady, M.; Kristjansdottir, S.; Tam, W.; Older, C.; Ritter, J. In *Catalysis of Organic Reactions*; Prunier, M., Ed.; CRC Press, 2008; Vol. 123, pp 319–328.

(80) Wuts, P. G. M.; Greene, T. W. *Greene's Protective Groups in Organic Synthesis*; John Wiley & Sons, Inc.: Hoboken, NJ, USA, 2006.

(81) Zhang, W. *Tetrahedron* **2003**, *59*, 4475.

(82) Liu, Y.-S.; Zhao, C.; Bergbreiter, D. E.; Romo, D. *J. Org. Chem.* **1998**, *63*, 3471.

(83) Lickiss, P. D.; Stubbs, K. M. *J. Organomet. Chem.* **1991**, *421*, 171.

(84) Stranix, B. R.; Liu, H. Q.; Darling, G. D. *J. Org. Chem.* **1997**, *62*, 6183.

(85) Encinas, L.; Chiara, J. L. *Eur. J. Org. Chem.* **2009**, *2009*, 2163.

(86) Guo, J.; Lu, Y.-J.; Zhang, L.; Ye, X.-S. *Synlett* **2012**, *23*, 1696.

(87) Fujita, Y.; Fujita, S.; Okada, Y.; Chiba, K. *Org. Lett.* **2013**, *15*, 1155.

(88) Aihara, K.; Komiya, C.; Shigenaga, A.; Inokuma, T.; Takahashi, D.; Otaka, A. *Org. Lett.* **2015**, *17*, 696.

(89) McBride, K.; Gaide, T.; Vorholt, A.; Behr, A.; Sundmacher, K. *Chem. Eng. Process.* **2016**, *99*, 97.

(90) Bergbreiter, D. E.; Yang, Y.-C. *J. Org. Chem.* **2010**, *75*, 873.

(91) Yang, Y.-C.; Bergbreiter, D. E. *Pure Appl. Chem.* **2013**, *85*, 493.

(92) Behr, A.; Turkowski, B.; Roll, R.; Schöbel, R.; Henze, G. In *Regulated Systems for Multiphase Catalysis*; Leitner, W., Hölscher, M., Eds.; Springer Berlin Heidelberg: Berlin, Heidelberg, 2006; Vol. 23, pp 19–52.

(93) Rackl, D.; Kreitmeier, P.; Reiser, O. *Green Chem.* **2016**, *18*, 214.

(94) Hobbs, C.; Yang, Y.-C.; Ling, J.; Nicola, S.; Su, H.-L.; Bazzi, H. S.; Bergbreiter, D. E. *Org. Lett.* **2011**, *13*, 3904.

(95) n-OCTADECYLDIMETHYLCHLOROSILANE https://www.gelest.com/product/n-octadecyldimethylchlorosilane/ (accessed Jun 25, 2017).

(96) Han, K. M.; Cheong, W. J. *Bull. Korean Chem. Soc.* **2008**, *29*, 2281.

(97) Sommer, L. H.; Frye, C. L.; Parker, G. A.; Michael, K. W. *J. Am. Chem. Soc.* **1964**, *86*, 3271.

(98) Naka, A.; Matsumoto, Y.; Itano, T.; Hasegawa, K.; Shimamura, T.; Ohshita, J.; Kunai, A.; Takeuchi, T.; Ishikawa, M. *J. Organomet. Chem.* **2009**, *694*, 346.

(99) Daudt, W. H.; Hyde, J. F. *J. Am. Chem. Soc.* **1952**, *74*, 386.

(100) Savela, R.; Zawartka, W.; Leino, R. *Organometallics* **2012**, *31*, 3199.

(101) Tacke, R.; Kornek, T.; Heinrich, T.; Burschka, C.; Penka, M.; Pülm, M.; Keim, C.; Mutschler, E.; Lambrecht, G. *J. Organomet. Chem.* **2001**, *640*, 140.

(102) Metz, S.; Nätscher, J. B.; Burschka, C.; Götz, K.; Kaupp, M.; Kraft, P.; Tacke, R. *Organometallics* **2009**, *28*, 4700.

(103) Hoffmann, F.; Wagler, J.; Roewer, G. *Eur. J. Inorg. Chem.* **2010**, *2010*, 1133.

(104) Masaoka, S.; Banno, T.; Ishikawa, M. *J. Organomet. Chem.* **2006**, *691*, 174.

(105) Chinchilla, R.; Nájera, C. *Chem. Rev.* **2007**, *107*, 874.

(106) Handa, S.; Fennewald, J. C.; Lipshutz, B. H. *Angew. Chem. Int. Ed.* **2014**, *53*, 3432.

(107) Xu, C.; Du, W.; Zeng, Y.; Dai, B.; Guo, H. *Org. Lett.* **2014**, *16*, 948.

(108) Plater, M. J.; Aiken, S.; Bourhill, G. *Tetrahedron* **2002**, *58*, 2405.

(109) Ishikawa, M.; Sakamoto, H.; Tabuchi, T. *Organometallics* **1991**, *10*, 3173.

(110) Thorand, S.; Krause, N. *J. Org. Chem.* **1998**, *63*, 8551.

(111) Bracher, F.; Krauß, J. *Eur. J. Org. Chem.* **2001**, *2001*, 4701.

(112) Lu, A.-H.; Salabas, E. L.; Schueth, F. *Angew. Chem. Int. Ed.* **2007**, *46*, 1222.

(113) Saha, K.; Agasti, S. S.; Kim, C.; Li, X.; Rotello, V. M. *Chem. Rev.* **2012**, *112*, 2739.

(114) Liu, P. *Ind. Eng. Chem. Res.* **2013**, *52*, 13517.

(115) Lang, X.; Chen, X.; Zhao, J. *Chem. Soc. Rev.* **2014**, *43*, 473.

(116) Laurent, S.; Forge, D.; Port, M.; Roch, A.; Robic, C.; Vander Elst, L.; Muller, R. N. *Chem. Rev.* **2008**, *108*, 2064.

(117) Kharisov, B. I.; Dias, H. V. R.; Kharissova, O. V.; Vazquez, A.; Pena, Y.; Gomez, I. *RSC Adv.* **2014**, *4*, 45354.

(118) Wu, L.; Mendoza-Garcia, A.; Li, Q.; Sun, S. *Chem. Rev.* **2016**, *116*, 10473.

(119) Kainz, Q. M.; Fernandes, S.; Eichenseer, C. M.; Besostri, F.; Koerner, H.; Mueller, R.; Reiser, O. *Faraday Discuss.* **2014**, *175*, 27.

(120) Jiao, Y.; Chou, T.; Akcora, P. *Macromolecules* **2015**, *48*, 4910.

(121) Arslan, M.; Gevrek, T. N.; Lyskawa, J.; Szunerits, S.; Boukherroub, R.; Sanyal, R.; Woisel, P.; Sanyal, A. *Macromolecules* **2014**, *47*, 5124.

(122) Avdeev, M. V.; Bica, D.; Vekas, L.; Aksenov, V. L.; Feoktystov, A. V.; Marinica, O.; Rosta, L.; Garamus, V. M.; Willumeit, R. *J. Colloid Interface Sci.* **2009**, *334*, 37.

(123) Viali, W. R.; Alcantara, G. B.; Sartoratto, P. P. C.; Soler, M. A. G.; Mosiniewicz-Szablewska, E.; Andrzejewski, B.; Morais, P. C. *J. Phys. Chem. C* **2010**, *114*, 179.

(124) Zaharescu, T.; Borbath, I.; Vekas, L. *Radiat. Phys. Chem.* **2014**, *105*, 22.

(125) Joseph, A.; Mathew, S. *ChemPlusChem* **2014**, *79*, 1382.

(126) Liang, Y.; Harrell, M. L.; Bergbreiter, D. E. *Angew. Chem. Int. Ed.* **2014**, *53*, 8084.

(127) Chao, C.-G.; Bergbreiter, D. E. *Catal. Commun.* **2016**, *77*, 89.

(128) Lee, N.; Yoo, D.; Ling, D.; Cho, M. H.; Hyeon, T.; Cheon, J. *Chem. Rev.* **2015**, *115*, 10637.

(129) Mitcova, L.; Rahma, H.; Buffeteau, T.; Clerac, R.; Vellutini, L.; Heuze, K. *RSC Adv.* **2015**, *5*, 88574.

(130) Perrault, S. D.; Walkey, C.; Jennings, T.; Fischer, H. C.; Chan, W. C. W. *Nano Lett.* **2009**, *9*, 1909.

(131) Bulte, J. W.; Douglas, T.; Witwer, B.; Zhang, S. C.; Strable, E.; Lewis, B. K.; Zywicke, H.; Miller, B.; van Gelderen, P.; Moskowitz, B. M.; Duncan, I. D.; Frank, J. A. *Nat. Biotechnol.* **2001**, *19*, 1141.

(132) Zhu, J.; Wei, S.; Ryu, J.; Sun, L.; Luo, Z.; Guo, Z. *ACS Appl. Mater. Interfaces* **2010**, *2*, 2100.

(133) He, Q.; Yuan, T.; Zhang, X.; Luo, Z.; Haldolaarachchige, N.; Sun, L.; Young, D. P.; Wei, S.; Guo, Z. *Macromolecules* **2013**, *46*, 2357.

(134) Gawande, M. B.; Branco, P. S.; Varma, R. S. *Chem. Soc. Rev.* **2013**, *42*, 3371.

(135) Lopez-Lopez, M. T.; Duran, J. D. G.; Delgado, A. V.; Gonzalez-Caballero, F. *J. Colloid Interface Sci.* **2005**, *291*, 144.

(136) Tadmor, R.; Rosensweig, R. E.; Frey, J.; Klein, J. *Langmuir* **2000**, *16*, 9117.

(137) Mahdavi, M.; Bin Ahmad, M.; Haron, M. J.; Namvar, F.; Nadi, B.; Ab Rahman, M. Z.; Amin, J. *Molecules* **2013**, *18*, 7533.

(138) Mirshahghassemi, S.; Lead, J. R. *Environ. Sci. Technol.* **2015**, *49*, 11729.

(139) POLYWAX Polyethylenes http://www.bakerhughes.com/news-and-media/resources/technical-data-sheet/polywax-polyethylenes (accessed Jun 12, 2017).

(140) SpectraSyn^{TM} Hi Vis PAO http://www.exxonmobilchemical.com/Chem-English/brands/spectrasyn-hi-vis-pao.aspx?ln=productsservices (accessed Jun 12, 2017).

(141) INEOS Products http://www.ineos.com/products/?Grade=Diisobutylene+HP&BU=INEOS+Oligomers&DocumentType=SSS (accessed Jun 12, 2017).

(142) Harrell, M. L.; Malinski, T.; Torres-Lopez, C.; Gonzalez, K.; Suriboot, J.; Bergbreiter, D. E. *J. Am. Chem. Soc.* **2016**, *138*, 14650.

(143) Grabowski, C. A.; Koerner, H.; Meth, J. S.; Dang, A.; Hui, C. M.; Matyjaszewski, K.; Bockstaller, M. R.; Durstock, M. F.; Vaia, R. A. *ACS Appl. Mater. Interfaces* **2014**, *6*, 21500.

(144) Li, Z.; Barnes, J. C.; Bosoy, A.; Stoddart, J. F.; Zink, J. I. *Chem. Soc. Rev.* **2012**, *41*, 2590.

(145) Kumar, S. K.; Jouault, N.; Benicewicz, B.; Neely, T. *Macromolecules* **2013**, *46*, 3199.

(146) Kango, S.; Kalia, S.; Celli, A.; Njuguna, J.; Habibi, Y.; Kumar, R. *Prog. Polym. Sci.* **2013**, *38*, 1232.

(147) Sui, T.; Song, B.; Zhang, F.; Yang, Q. *RSC Adv* **2016**, *6*, 393.

(148) Wu, S.-H.; Mou, C.-Y.; Lin, H.-P. *Chem. Soc. Rev.* **2013**, *42*, 3862.

(149) Chao, C.-G.; Kumar, M. P.; Riaz, N.; Khanoyan, R. T.; Madrahimov, S. T.; Bergbreiter, D. E. *Macromolecules* **2017**, *50*, 1494.

(150) Bergbreiter, D. E.; Gray, H. N.; Srinivas, B. *Macromolecules* **1994**, *27*, 7294.

(151) Bergbreiter, D. E.; Walchuk, B.; Holtzman, B.; Gray, H. N. *Macromolecules* **1998**, *31*, 3417.

(152) Holmes-Farley, S. R.; Whitesides, G. M. *Langmuir* **1986**, *2*, 266.

(153) *Chemosensors: Principles, Strategies, and Applications*; Wang, B., Anslyn, E. V., Eds.; John Wiley & Sons, Inc.: Hoboken, NJ, USA, 2011.

(154) Wu, J.; Xie, J.; Ling, L.; Ma, G.; Wang, B. *J. Coat. Technol. Res.* **2013**, *10*, 849.

(155) Posner, G. H.; Shulman-Roskes, E. M.; Oh, C. H.; Carry, J.-C.; Green, J. V.; Clark, A. B.; Dai, H.; Anjeh, T. E. N. *Tetrahedron Lett.* **1991**, *32*, 6489.